

Copy
10-11-11-84K01

CL
44

Copy
RM SL54D30

~~CONFIDENTIAL~~

NACA

Unavailable Report
EC 12958 dtd 7-27-98
Shon

RESEARCH MEMORANDUM

for the

U. S. Army Chemical Corps

WIND-TUNNEL INVESTIGATION OF THE EFFECTS ON THE AERODYNAMIC

CHARACTERISTICS OF MODIFICATIONS TO A MODEL OF A

BOMB MOUNTED ON A WING-FUSELAGE MODEL

AND TO A MODEL OF THE BOMB ALONE

By Thomas J. King, Jr.

Langley Aeronautical Laboratory
Langley Field, Va.

CLASSIFIED DOCUMENT

This material contains information affecting the National Defense of the United States within the meaning of the espionage laws, Title 18, U.S.C., Secs. 793 and 794, the transmission or revelation of which in any manner to an unauthorized person is prohibited by law.

NATIONAL ADVISORY COMMITTEE
FOR AERONAUTICS
WASHINGTON

~~CONFIDENTIAL~~

NACA Bu. whd
Collection
of
Shon
10-11-11-84K01
at 7-27-98



NATIONAL ADVISORY COMMITTEE FOR AERONAUTICS

RESEARCH MEMORANDUM

for the

U. S. Army Chemical Corps

WIND-TUNNEL INVESTIGATION OF THE EFFECTS ON THE AERODYNAMIC

CHARACTERISTICS OF MODIFICATIONS TO A MODEL OF A

BOMB MOUNTED ON A WING-FUSELAGE MODEL

AND TO A MODEL OF THE BOMB ALONE

By Thomas J. King, Jr.

SUMMARY

An investigation was conducted in the Langley high-speed 7- by 10-foot tunnel to determine effects of modifications to a bomb model (particularly with regard to drag) when mounted on a wing-fuselage model and tested at Mach numbers from 0.70 to 1.10. In addition, the static longitudinal stability characteristics of several configurations of a larger scale model of the bomb alone were obtained over a Mach number range from 0.50 to 0.95.

The results obtained for the wing-fuselage-bomb model indicate that large reductions in installation drag were obtained for the wing-fuselage-bomb model when the flat nose of the basic bomb was replaced by rounded or pointed noses of various calibers. Shortening the mounting pylon gave further decreases in the installation drag.

The tests of the bomb alone indicated that only the flat-nose configurations were stable over the greater part of the Mach number range. Nose-shape modifications which improved the drag also caused the bombs to become unstable at low angles of attack. The stability of the low-drag bomb configurations could be improved by lengthening the cylindrical portion of the body behind the center of gravity.

INTRODUCTION

An investigation was conducted in the Langley high-speed 7- by 10-foot tunnel at the request of the U. S. Army Chemical Corps to determine

~~CONFIDENTIAL~~

the aerodynamic effects of modifications to a bomb designed to house a cluster of smaller bombs. Primarily, the investigation was to determine a configuration of the bomb which would give low installation drag when mounted from an airplane wing. Some tests previously had been made of the basic bomb shape at the Cornell Aeronautical Laboratory and are reported in reference 1. In the present investigation, various configurations of a 0.0298-scale model of the bomb were tested in combination with a swept-wing--fuselage model mounted on a reflection plane in the Langley high-speed 7- by 10-foot tunnel.

Additional tests were made to determine the effects of some of the modifications on the stability of the isolated bomb. In these tests, aerodynamic characteristics in pitch were determined for a sting-mounted 0.1517-scale bomb model over a range of angle of attack from -3° to about 16° and Mach numbers from 0.50 to 0.95.

SYMBOLS

The following symbols apply to the semispan-wing-fuselage--bomb model:

C_L	lift coefficient, $\frac{\text{Twice semispan lift}}{qS_w}$
C_D	drag coefficient, $\frac{\text{Twice semispan drag}}{qS_w}$
C_m	pitching-moment coefficient referred to $0.15\bar{c}$ of wing, $\frac{\text{Twice semispan pitching moment}}{qS_w\bar{c}}$
C_{D_s}	bomb-plus-interference drag coefficient, $(C_{D_{\text{model} + \text{bomb}}} - C_{D_{\text{model}}}) \frac{S_w}{2S_s}$
q	free-stream dynamic pressure, $\frac{1}{2} \rho V^2$, lb/sq ft
S_w	twice wing area of semispan model, 0.291 sq ft
S_s	maximum frontal area of 0.0298-scale bomb, 0.00132 sq ft

- \bar{c} mean aerodynamic chord of wing, $\frac{2}{S_w} \int_0^{b/2} c^2 dy$
(using theoretical tip), 0.299 ft
- c local wing chord parallel to free stream, ft
- b twice span of semispan model, 1.000 ft
- M effective Mach number, $\frac{2}{S_w} \int_0^{b/2} cM_a dy$
- M_γ local Mach number obtained from calibration made without a model in place on reflection-plane plate
- M_a average chordwise Mach number
- ρ mass density of air, slugs/cu ft
- α angle of attack, deg
- R_w Reynolds number based on wing \bar{c}

Subscript:

- E denotes bomb configurations with extended fins

The following symbols apply to the bomb-alone model:

- C_{L_F} lift coefficient, $\frac{\text{Lift}}{qS_F}$
- C_{D_F} drag coefficient, $\frac{\text{Drag}}{qS_F}$
- C_{m_F} pitching-moment coefficient referred to $0.378l_b$,
 $\frac{\text{Pitching moment}}{qS_F l_b}$
- S_F maximum frontal area of body, 0.0336 sq ft
- l_b overall length of basic bomb configuration (configuration 1, fig. 6), 1.138 ft
- R_b Reynolds number of bomb based on l_b

MODELS AND APPARATUS

Semispan Wing-Fuselage-Bomb Model

This investigation was conducted in the Langley high-speed 7- by 10-foot tunnel with a small semispan wing and a wing-fuselage model mounted on a reflection-plane plate (fig. 1). The plate was mounted on the tunnel wall and was located about three inches from the wall so that it would be out of the tunnel boundary layer. The 0.0298-scale semispan model was attached to a strain-gage balance by an extension of the wing root which passed through the reflection-plane plate. A gap of about $1/16$ inch was maintained between the wing root and the turntable cutout and between the inner surface of the half fuselage and the reflection-plane plate to prevent fouling. The balance, located outside the tunnel wall, was enclosed by a can to minimize air leakage into the model flow field.

The wing was made of steel and had a quarter-chord sweepback angle of 40° , aspect ratio of 3.43, taper ratio of 0.479, and NACA 65A010 airfoil sections normal to the quarter-chord line. The wing had $1\frac{1}{2}^\circ$ incidence relative to fuselage reference line and $3\frac{1}{2}^\circ$ negative dihedral relative to the fuselage plane of symmetry.

The fuselage was made of a steel beam covered with bismuth-tin alloy.

The bombs were suspended beneath the wing (with the bomb axis parallel to the fuselage reference line) by constant-chord pylons with 33° sweepback. Sketches of the pylon-bomb configurations are shown in figure 2. The pylons were constructed of steel and had NACA 64A007 airfoil sections parallel to the airstream. Ordinates of the various bomb noses are given in figure 3. The bomb noses, cylindrical midsections, tail, and fins (fig. 4) were made of brass. Photographs of a bomb suspended beneath the wing-fuselage combination and beneath the wing alone are presented in figures 5(a) and 5(b).

Bomb-Alone Model

Eight configurations of a 0.1517-scale model of the bomb (fig. 6) were tested on a sting-support system in the Langley high-speed 7- by 10-foot tunnel. The noses are defined in figure 7 and details of the bomb tail section and fins are shown in figure 8. The noses and cylindrical midsection were made of aluminum whereas the tail section and fins were made of steel. The model contained an internal strain-gage balance and was pitched through the angle-of-attack range at constant Mach number.

TESTS

Semispan-Wing-Fuselage—Bomb Model

The semispan-wing-fuselage—bomb model was tested on a reflection plane mounted on the wall of the Langley high-speed 7- by 10-foot tunnel, which induces over the reflection-plane surface a region of local velocities higher than the midstream tunnel velocities and permits testing of small semispan models up to Mach numbers of 1.10. Local Mach number variations in the test region for average test Mach numbers are shown in figure 9. The change in local Mach number over the model is greatest at the high effective Mach numbers and decreases with decreasing speed. The effective Mach number, which is used as the basis for data presentation, is obtained from the following relationship:

$$M = \frac{2}{S_w} \int_0^{b/2} cM_a dy$$

Lift, drag, and pitching-moment coefficients were obtained over an angle-of-attack range that generally extended from -3° to 12° at Mach numbers from 0.70 to 1.10. The variation of Reynolds number (based on wing mean aerodynamic chord) with Mach number is shown in figure 10. The jet-boundary corrections to the data were considered to be negligible.

The results presented in the present paper are believed to be accurate within the following limits for each Mach number:

M	ΔM	ΔC_D	ΔC_{D_s}
0.70	± 0.003	± 0.0005	± 0.056
.90	± 0.003	± 0.0004	± 0.041
1.10	± 0.003	± 0.0003	± 0.035

Bomb-Alone Model

Lift, drag, and pitching-moment measurements were obtained on the 0.1517-scale model of the bomb. The pitching moments were measured about an axis 5.15 inches from the forward end of bomb configuration 1 (fig. 6). The models were tested over an angle-of-attack range that generally extended from -3° to 16° at Mach numbers from 0.50 to 0.95.

The Mach numbers and dynamic pressures were corrected for blocking by the method of reference 2. No jet-boundary corrections were applied as they are considered to be extremely small. The drag data have been corrected to correspond to a pressure at the base of the model equal to free-stream static pressure. For this correction, the pressure inside the models was measured at a point just forward of the base of the model.

The angle of attack has been corrected for deflection of the sting-support system under load.

The variation of Reynolds number (based on length of configuration 1) with Mach number is presented in figure 10.

RESULTS

The results of the investigation are presented in the following figures:

Figure

Semispan-wing-fuselage—bomb model:

Basic data:

Wing-fuselage	11
Wing alone	12
Wing-fuselage—bomb combinations	13
Wing-bomb combinations	14
Drag characteristics	15 to 18
Summary of aerodynamic characteristics	19 to 20

Bomb-alone model:

Basic data	21
Summary of pitching-moment-curve slopes	22
Comparison of pitching-moment characteristics	23
Minimum drag characteristics	24

The lift-curve slopes were averaged between zero and 0.10 lift coefficient, and the pitching-moment-curve slopes were measured at zero lift for the reflection-plane model. The pitching-moment-curve slopes were measured at zero angle of attack for the bomb-alone results.

Semispan-Wing-Fuselage—Bomb Model

Drag characteristics.— The increments in drag coefficient (including interference) based on bomb maximum frontal area are presented in figures 17 and 18 for the zero-lift condition.

Large reductions in the bomb-plus-interference drag were obtained when the original flat nose was replaced by rounded or pointed noses of various calibers (fig. 17). The largest reduction in drag due to nose shape was obtained by using the nose of configuration 5 (a 1.9 caliber long, spherical-tipped parabolic nose). The drag of configuration 5 at a Mach number of 0.70 was only 30 percent of the drag of configuration 1. Below a Mach number of 0.94, the lowest bomb-plus-interference drag was obtained with three pylon-bomb arrangements (long pylon and bomb configuration 5, long pylon and bomb configuration 3_E, and short pylon and bomb configuration 3_E).

The effect of extending the fins on bomb configuration 3 was to reduce the bomb-plus-interference drag slightly, except at $M = 1.10$.

Extending the bomb cylindrical midsection of configuration 4 (yielding configuration 9) reduced the bomb-plus-interference drag over the Mach number range. Comparison of the drag results of configurations 3 and 9 to determine the effect of lengthening the cylindrical midsection while keeping the overall length constant shows that configuration 9 with the lengthened midsection had slightly lower bomb-plus-interference drag, except between $M = 0.80$ and $M = 0.95$. The opposite effect of extending the bomb cylindrical midsection is shown for the wing-alone case (fig. 18). Configuration 3 had lower bomb-plus-interference drag than configuration 9 except near a Mach number of 1.0.

Shortening the pylon length substantially reduced the bomb-plus-interference drag of configuration 3_E (bomb with nose 3, original midsection and extended fins). This short-eylon arrangement had the lowest bomb-plus-interference drag of any pylon-bomb combination above Mach number 0.94 and only slightly higher drag than the better configurations at lower Mach numbers (fig. 17).

Lift and pitch characteristics.- The lift-curve slopes and pitching-moment-curve slopes are summarized in figures 19 and 20. The cross-hatched areas of figure 19 define the boundaries of the parameters with the pylons and bombs mounted from the wing. In general, the addition of a bomb-eylon arrangement to the wing decreased the lift-curve slope, the largest decrements occurring between Mach numbers of 0.90 and 1.05. The bomb-eylon arrangements caused small changes in $\partial C_m / \partial C_L$ at Mach numbers below 0.90; however, at higher Mach numbers, changes in the aerodynamic-center location of the order of 5 percent were caused by the addition of the bomb-eylon arrangements. Near a Mach number of 1.0 all bomb-eylon configurations produced forward movements of the aerodynamic center.

Bomb-Alone Model

Pitch characteristics.- The basic bomb (configuration 1, flat nose, original midsection and tail) was stable for the Mach numbers investigated, except for an unstable trend at $M = 0.95$ (fig. 22). The configurations having other nose shapes all showed varying degrees of instability near zero angle of attack. The most unstable arrangements were bomb configurations 3 and 3_E (1.9 caliber noses). Lengthening (behind the center of gravity) the cylindrical portions of bomb configurations 4 and 4_E decreased the bombs' instability to near neutral values. The fin extensions had little effect on the stability of the bombs.

A comparison of the pitching-moment curves of the various bomb configurations with the original fins is shown in figure 23 for two Mach numbers. All configurations exhibited stable pitching-moment variations at angles of attack above about 6° . There was no large effect of Mach number on the pitching-moment-coefficient variation above angles of attack for which $\partial C_m / \partial \alpha$ became negative.

Drag characteristics.- The drag coefficients of the bomb models at zero angle of attack are summarized in figure 24. The drag of the basic bomb (configuration 1) was from 5 to 13 times the drag of the modified bombs with sharp noses. Bomb configurations 3 and 3_E (1.9 caliber noses) did not show a drag rise until a Mach number of 0.88. The drag rises for configurations 4, 4_E, 9, and 9_E occurred around a Mach number of 0.75. The fin extensions reduced the drag of configurations 1 and 3 but had little effect on the drag of the other configurations. The bombs having the lengthened midsections (configurations 9 and 9_E) had higher drag than the same bomb with the original midsection (configurations 4 and 4_E) at Mach numbers below about 0.85.

CONCLUSIONS

The results of a wind-tunnel investigation of a 0.0298-scale-model bomb mounted from a semispan-wing-fuselage and wing-alone model indicate that large reductions in drag at low lift coefficients are obtained when the flat nose of the bomb is replaced by rounded or pointed noses of various calibers. The bomb-plus-interference drag is further reduced by using fin extensions, bomb midsection extension, or shorter mounting pylon. The installation of the bombs reduces the lift-curve slope and generally causes forward movements in the aerodynamic center.

Results of an investigation of a sting-mounted 0.1517-scale model of the bomb alone indicate that only the flat-nose configurations were stable over the greater part of the Mach number range. All nose-shape modifications improved the drag but caused the bombs to become unstable

at low angles of attack. The instability of the low-drag bomb configurations could be decreased by lengthening (behind the center of gravity) the cylindrical portion of the body.

Langley Aeronautical Laboratory,
National Advisory Committee for Aeronautics,
Langley Field, Va., April 16, 1954.

Thomas J. King, Jr.

Thomas J. King, Jr.
Aeronautical Research Scientist

Approved: *Thomas A. Harris*
Thomas A. Harris
Chief of Stability Research Division

pwg

REFERENCES

1. Keslo, R. S.: Tests of a 0.179-Scale, 500-Pound, General Purpose Bomb Model in the Cornell Aeronautical Laboratory 12-foot Variable-Density Wind Tunnel, for Office, Chief of Ordnance. Rep. No. AK-452-W6, Cornell Aero. Lab., Inc., 1950
2. Herriot, John G.: Blockage Corrections for Three-Dimensional-Flow Closed-Throat Wind Tunnels, With Consideration of the Effect of Compressibility. NACA Rep. 995, 1950. (Supersedes NACA RM A7B28.)

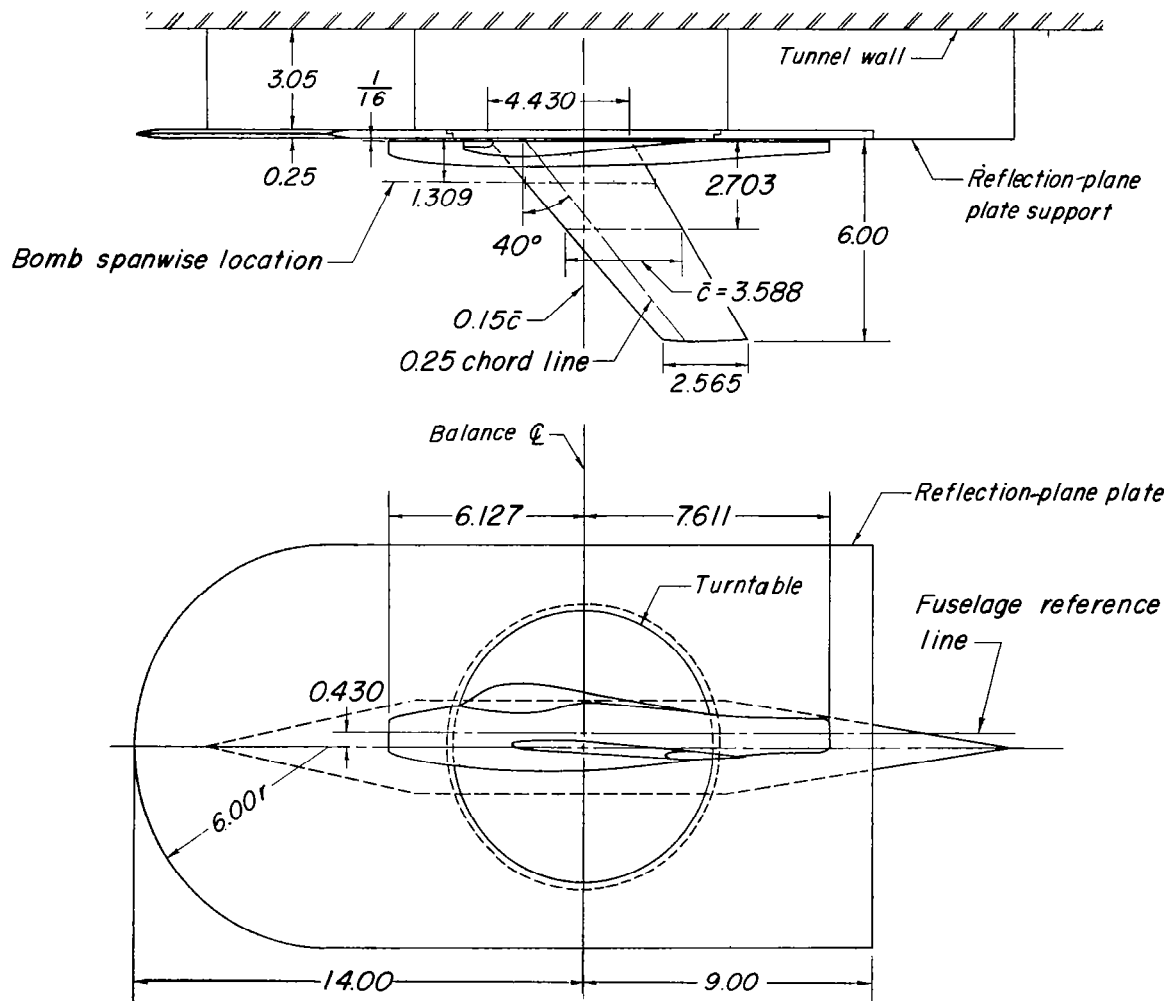


Figure 1.- Drawing of test setup and 40° sweptback-wing-fuselage combination. Wing incidence, 1.5° ; wing dihedral, -3.5° . All dimensions are in inches.

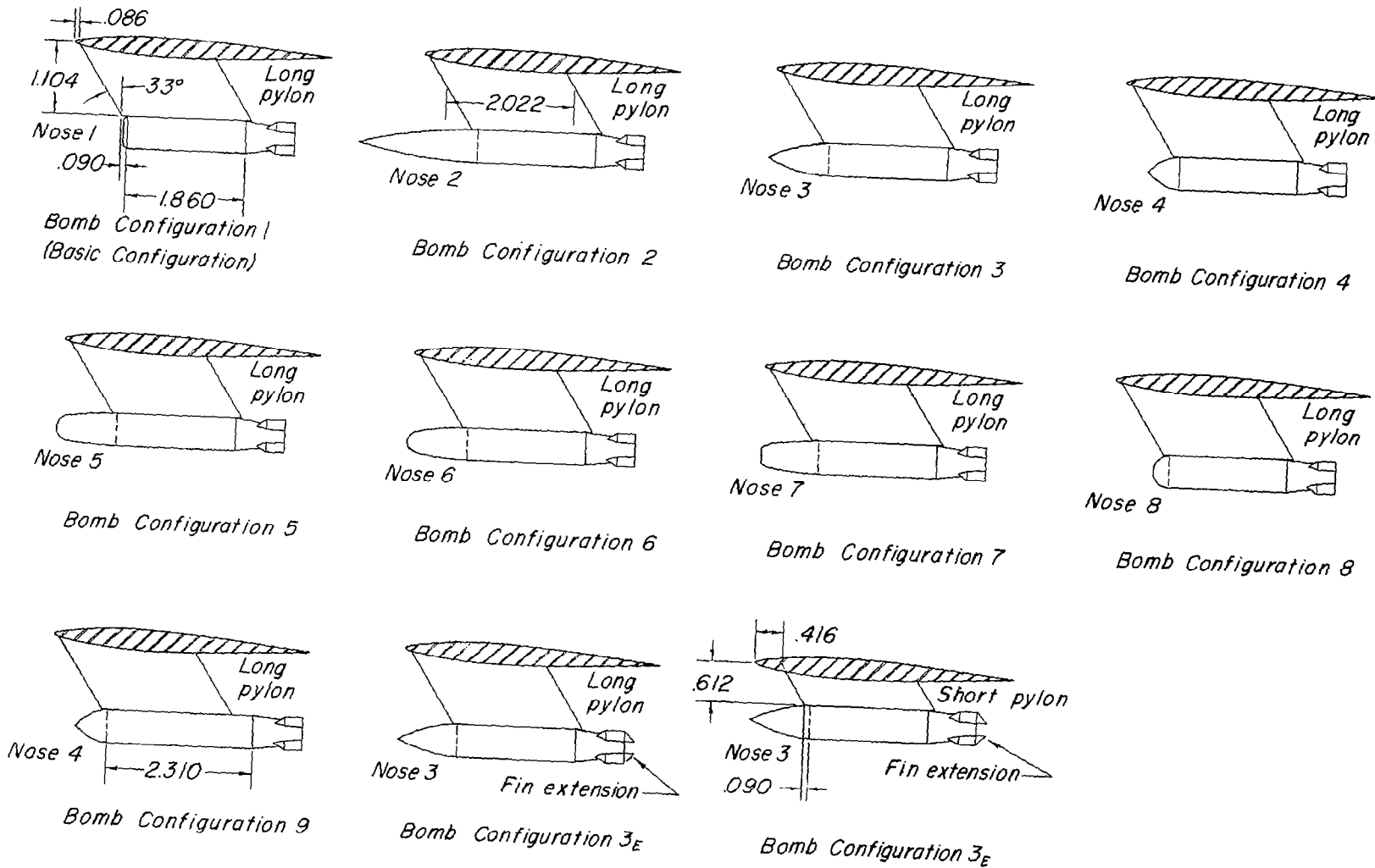
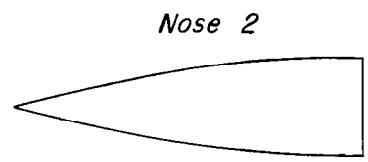
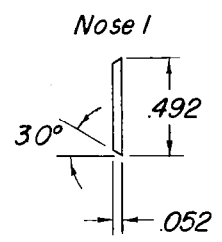
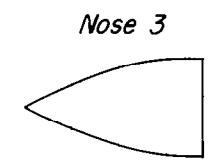


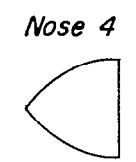
Figure 2.- Pylon-bomb arrangements tested on 0.0298-scale wing and wing-fuselage model. All dimensions are in inches.



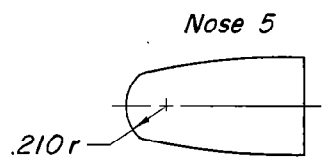
Ordinates, inches	
Station	Radius
0	0
.100	.027
.200	.052
.400	.098
.600	.137
.800	.171
1.000	.198
1.200	.219
1.400	.234
1.600	.243
1.790	.246
1.840	.246



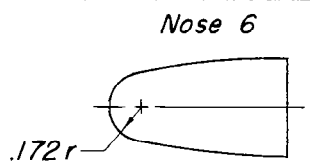
Ordinates, inches	
Station	Radius
0	0
.100	.052
.200	.098
.400	.171
.600	.219
.800	.243
.895	.246
.945	.246



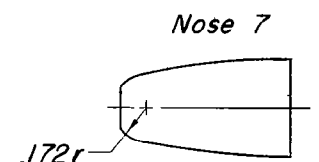
Ordinates, inches	
Station	Radius
0	0
.050	.052
.100	.098
.150	.137
.200	.171
.300	.219
.400	.243
.448	.246
.498	.246



Ordinates, inches	
Station	Radius
0	0
.199	.209
.305	.219
.505	.234
.705	.243
.895	.246
.945	.246



Ordinates, inches	
Station	Radius
0	0
.135	.168
.150	.171
.350	.206
.550	.230
.750	.243
.890	.246
.940	.246



Ordinates, inches	
Station	Radius
0	.120
.104	.168
.119	.171
.319	.206
.519	.230
.719	.243
.859	.246
.909	.246

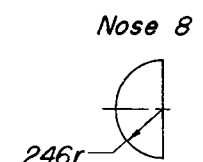


Figure 3.- Profiles of noses tested on the 0.0298-scale bomb.

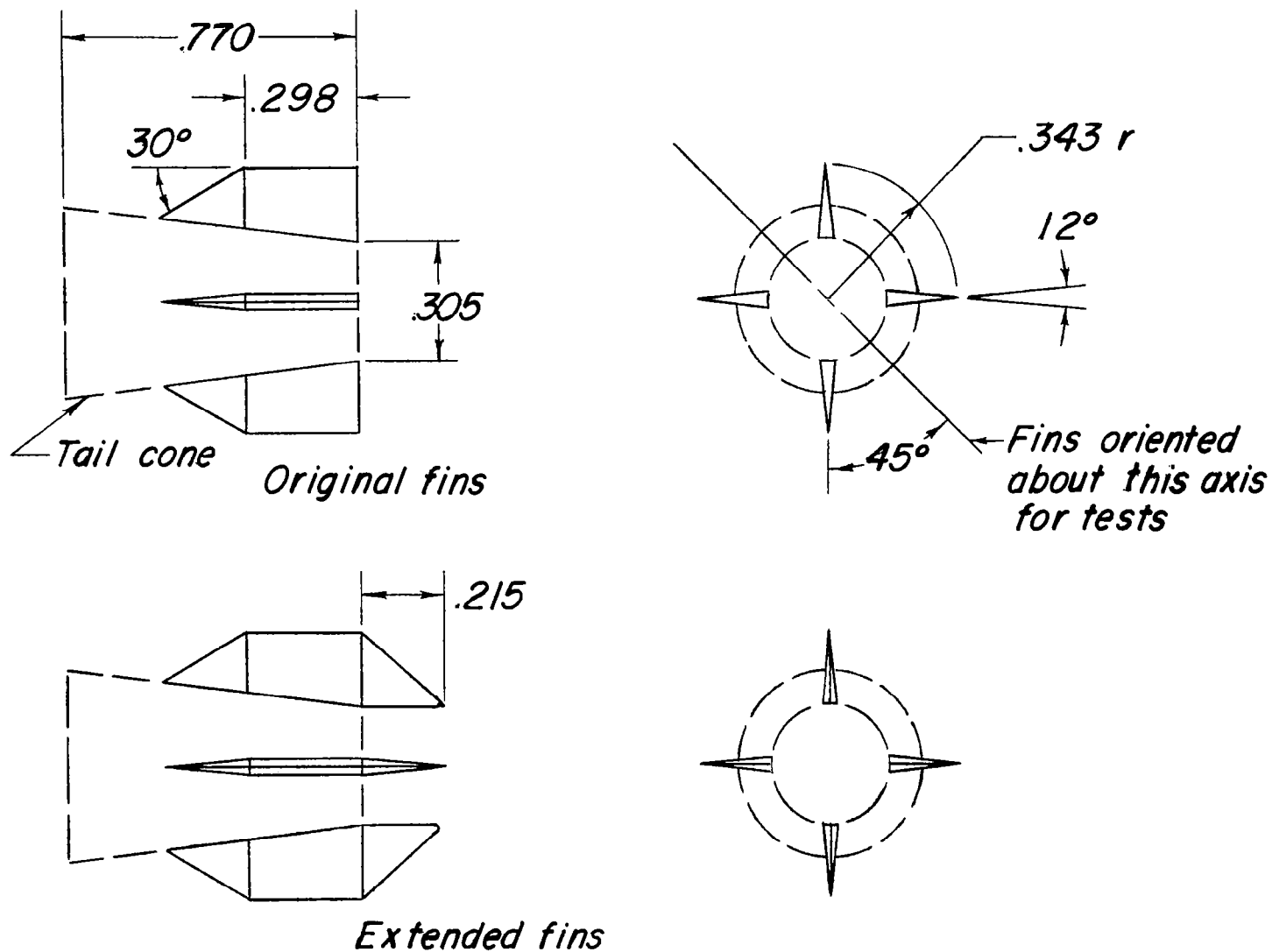
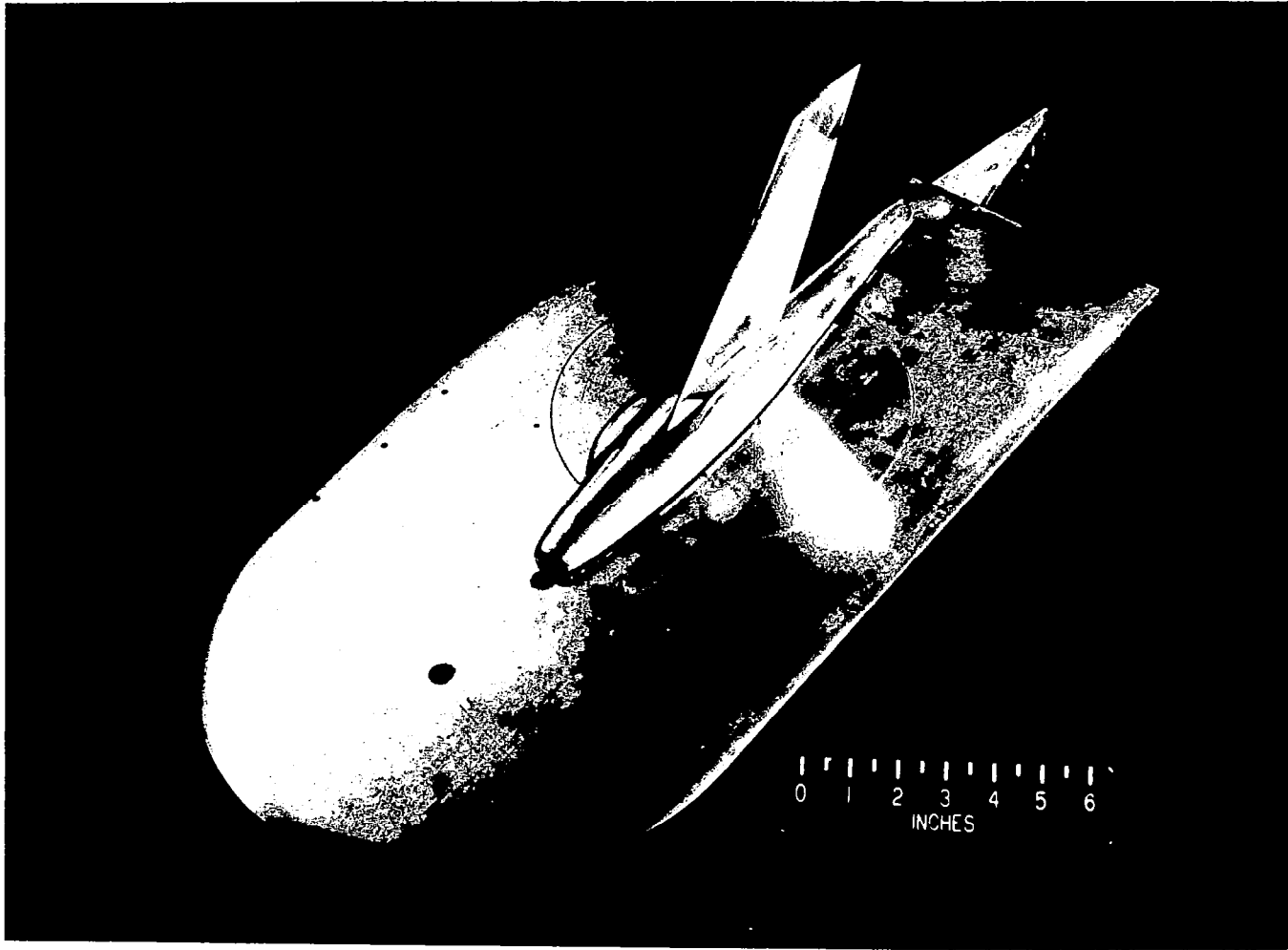


Figure 4.- Details of fins of 0.0298-scale bomb. All dimensions are in inches.



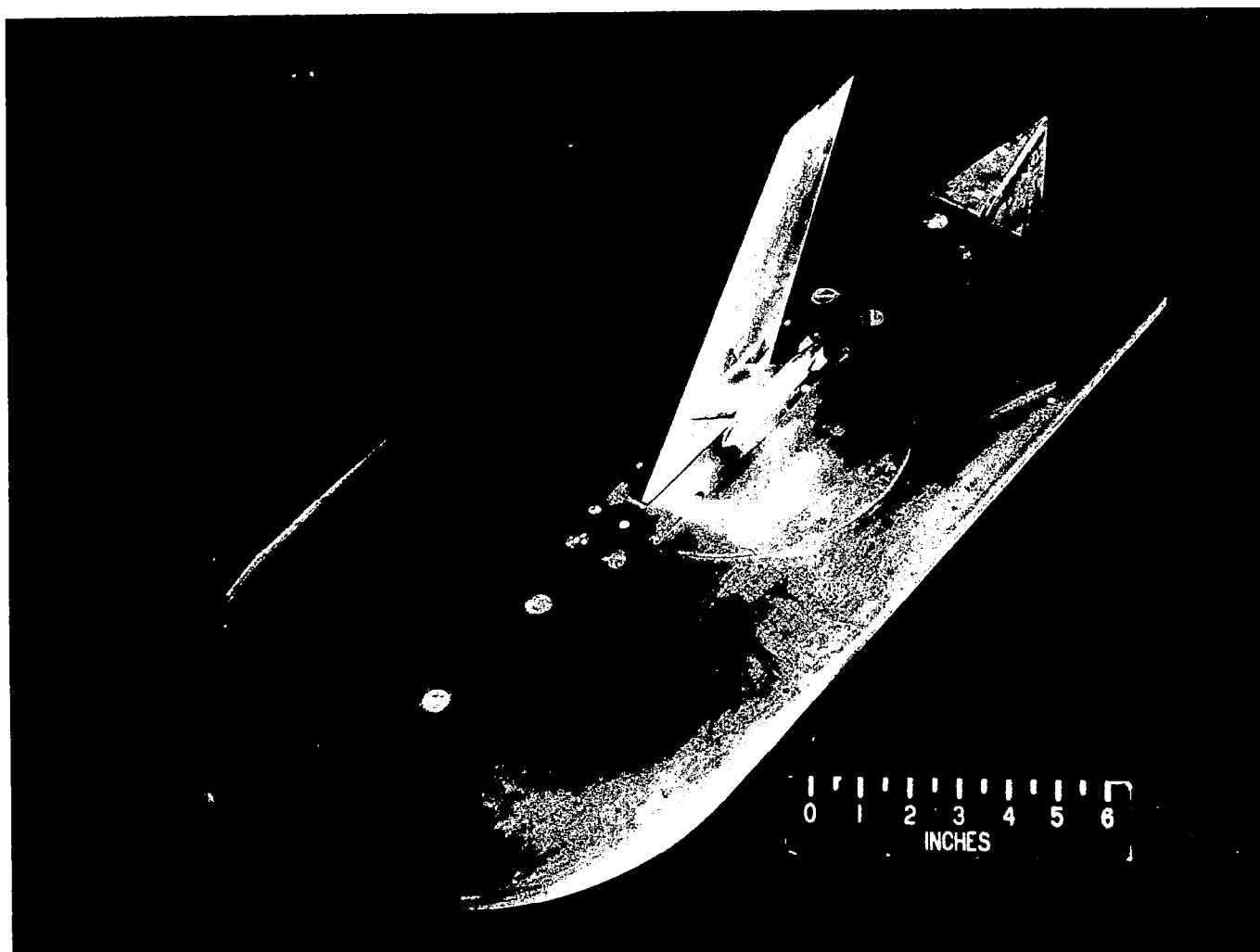
L-75967

(a) Wing-fuselage—bomb model.

Figure 5.- Photographs of reflection-plane model.

GOVERNMENT PRINTING OFFICE

GOVERNMENT PRINTING OFFICE



L-75970

(b) Wing-bomb model.

Figure 5.- Concluded.

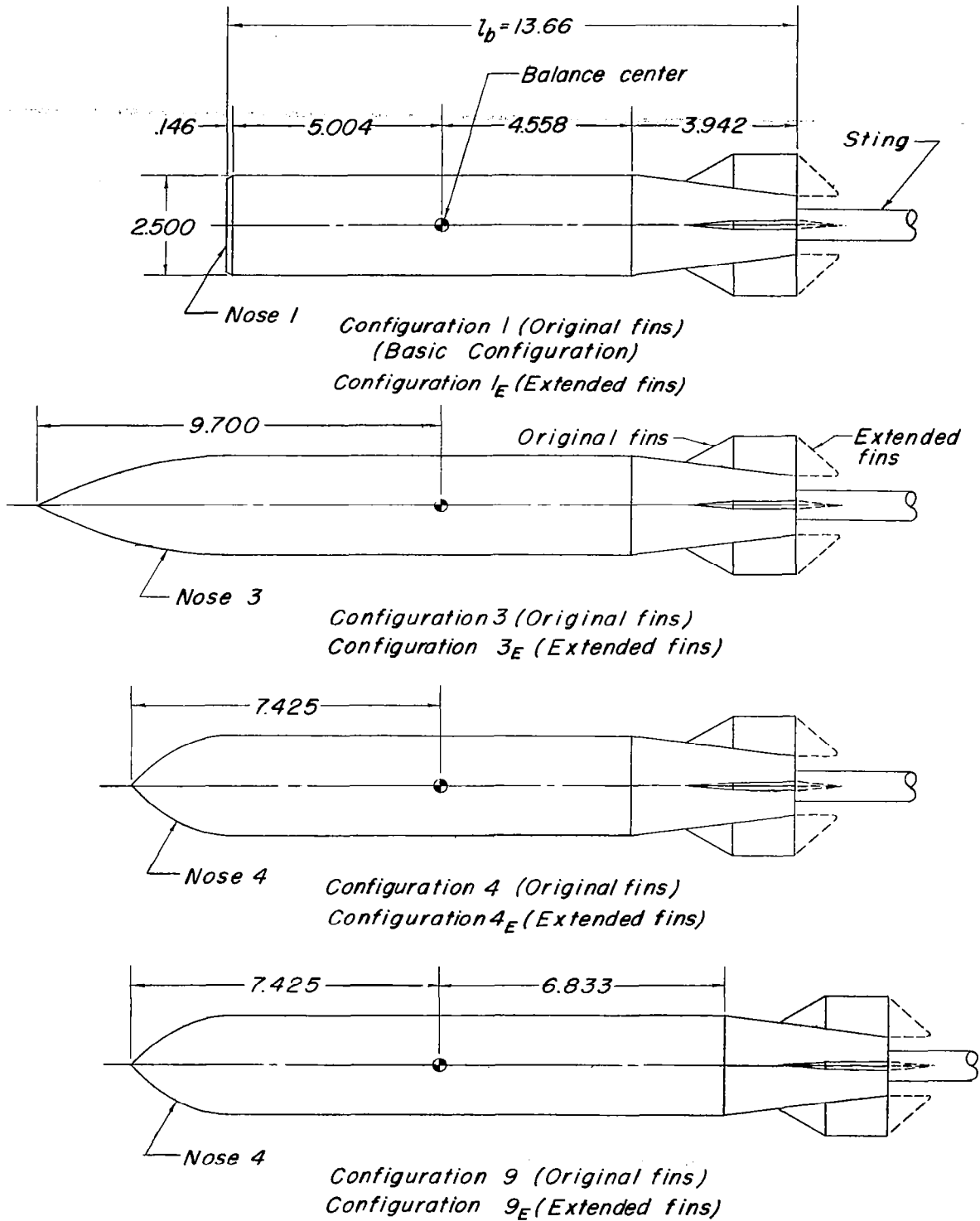
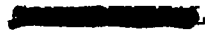
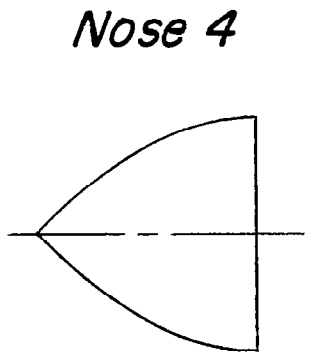
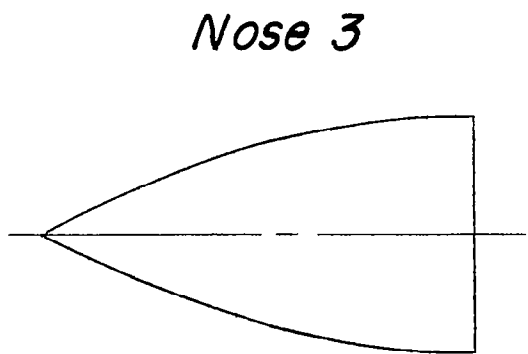
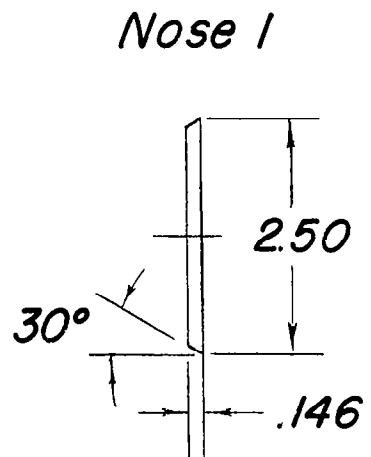


Figure 6.- Drawing of 0.1517-scale bomb configurations. All dimensions are in inches.





<i>Ordinates, inches</i>	
<i>Station</i>	<i>Radius</i>
0	0
.525	.264
1.050	.496
2.100	.880
3.148	1.115
4.197	1.243
4.550	1.250
4.696	1.250

<i>Ordinates, inches</i>	
<i>Station</i>	<i>Radius</i>
0	0
.270	.263
.540	.495
.810	.696
1.080	.866
1.620	1.112
2.160	1.233
2.275	1.240
2.421	1.250

Figure 7.- Nose profiles tested on the 0.1517-scale bomb.

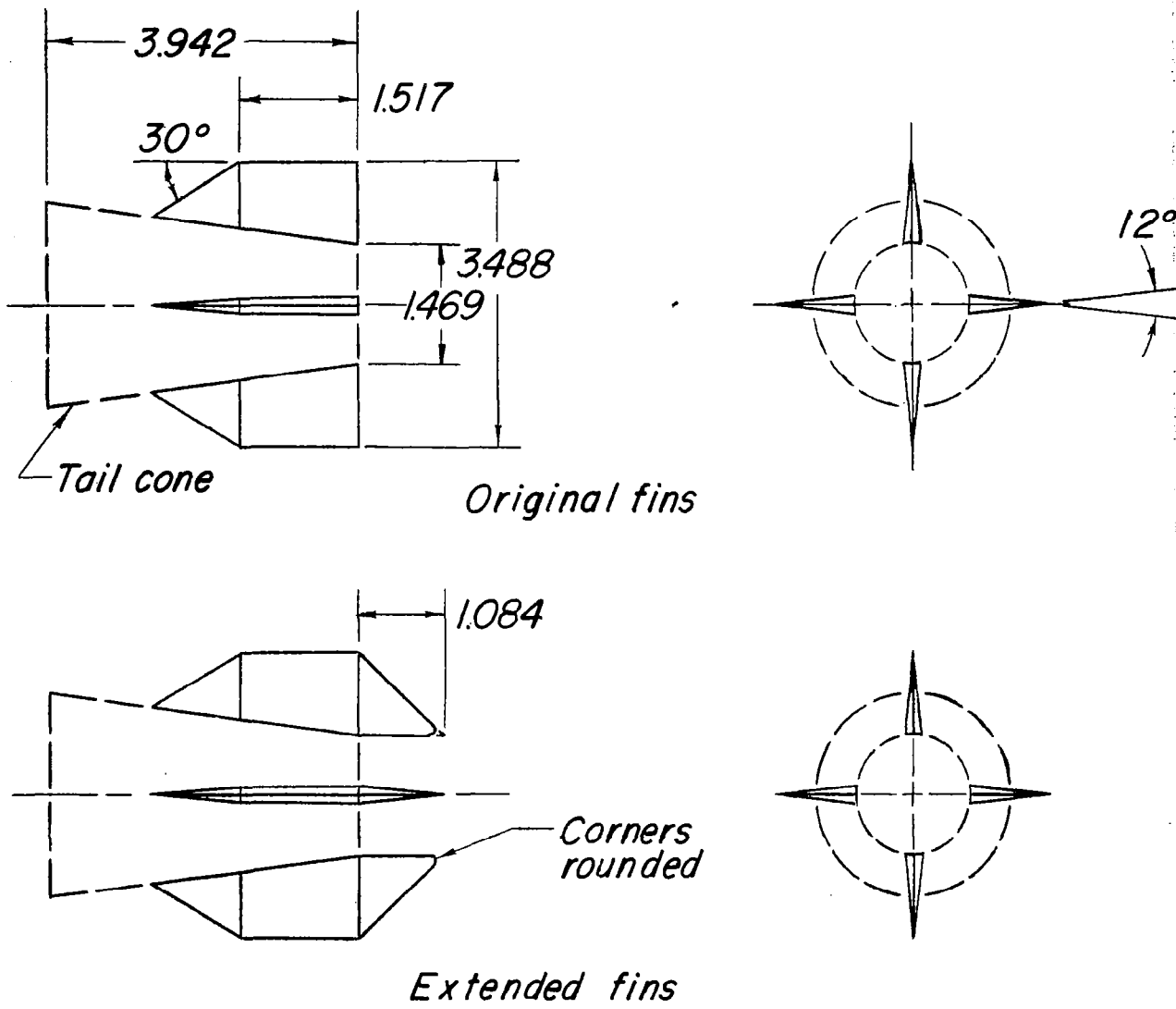


Figure 8.- Details of fins of 0.1517-scale bomb. All dimensions are in inches.

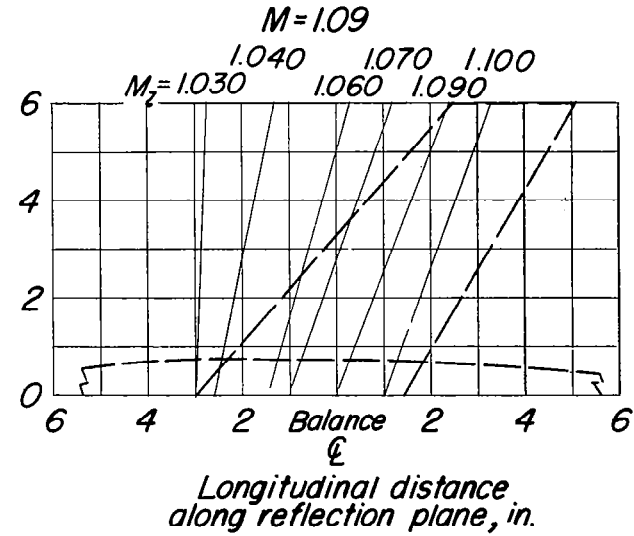
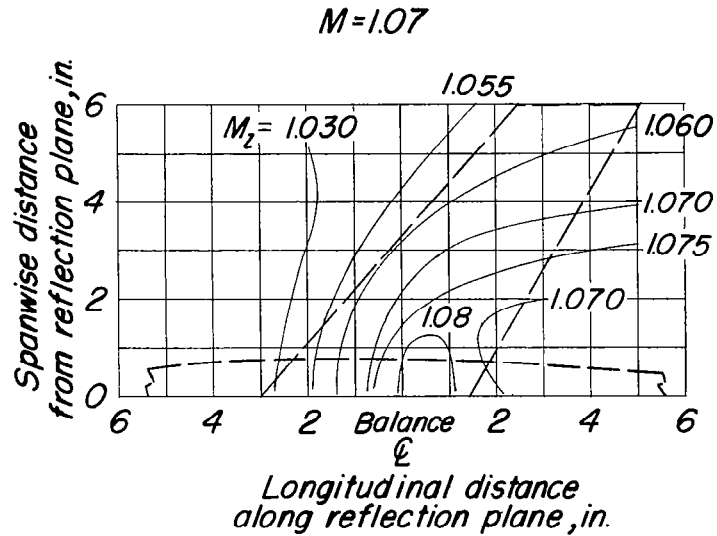
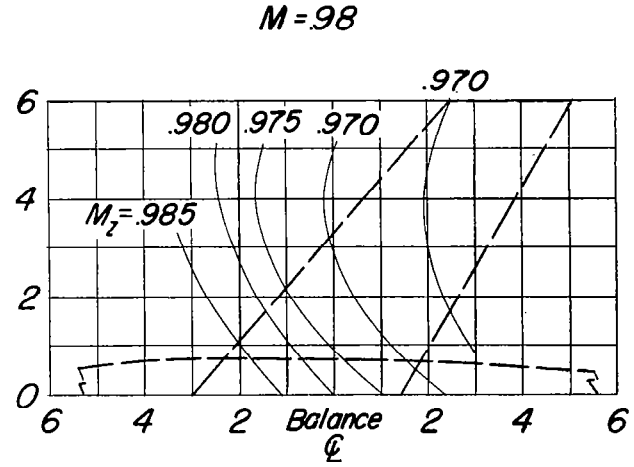
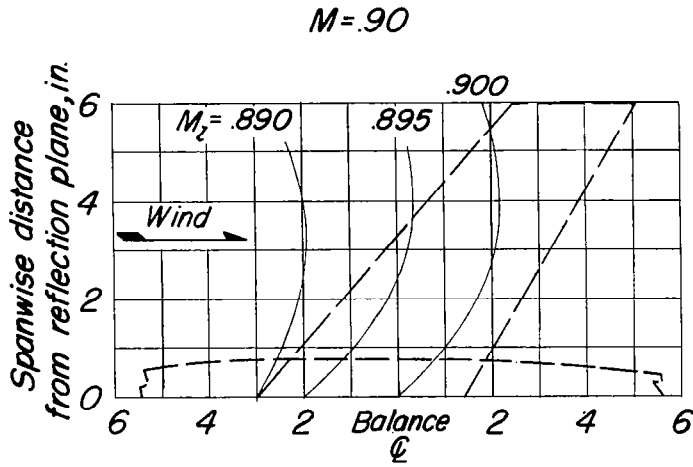


Figure 9.- Typical Mach number contours over side-wall reflection plane in region of model location.

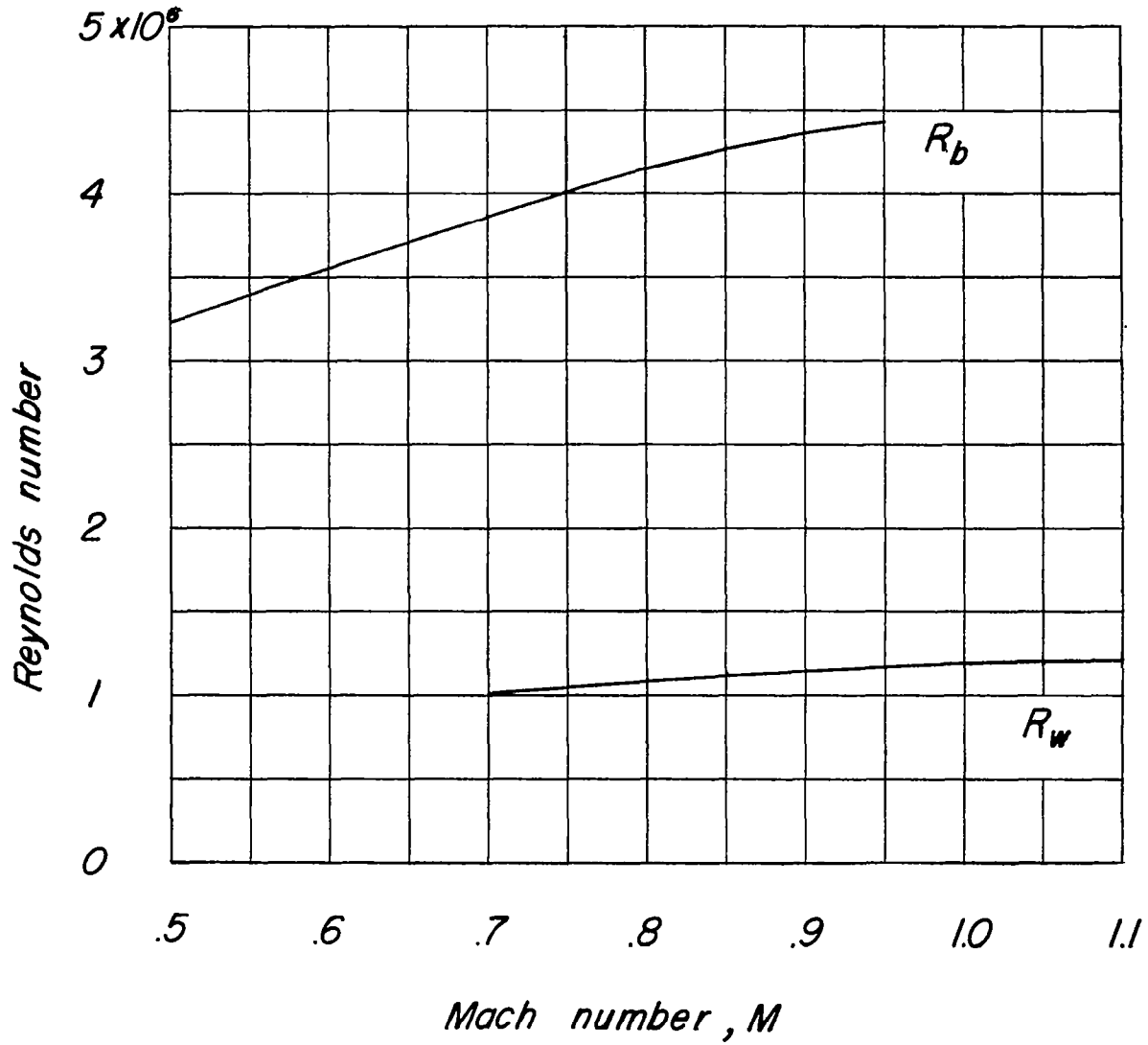
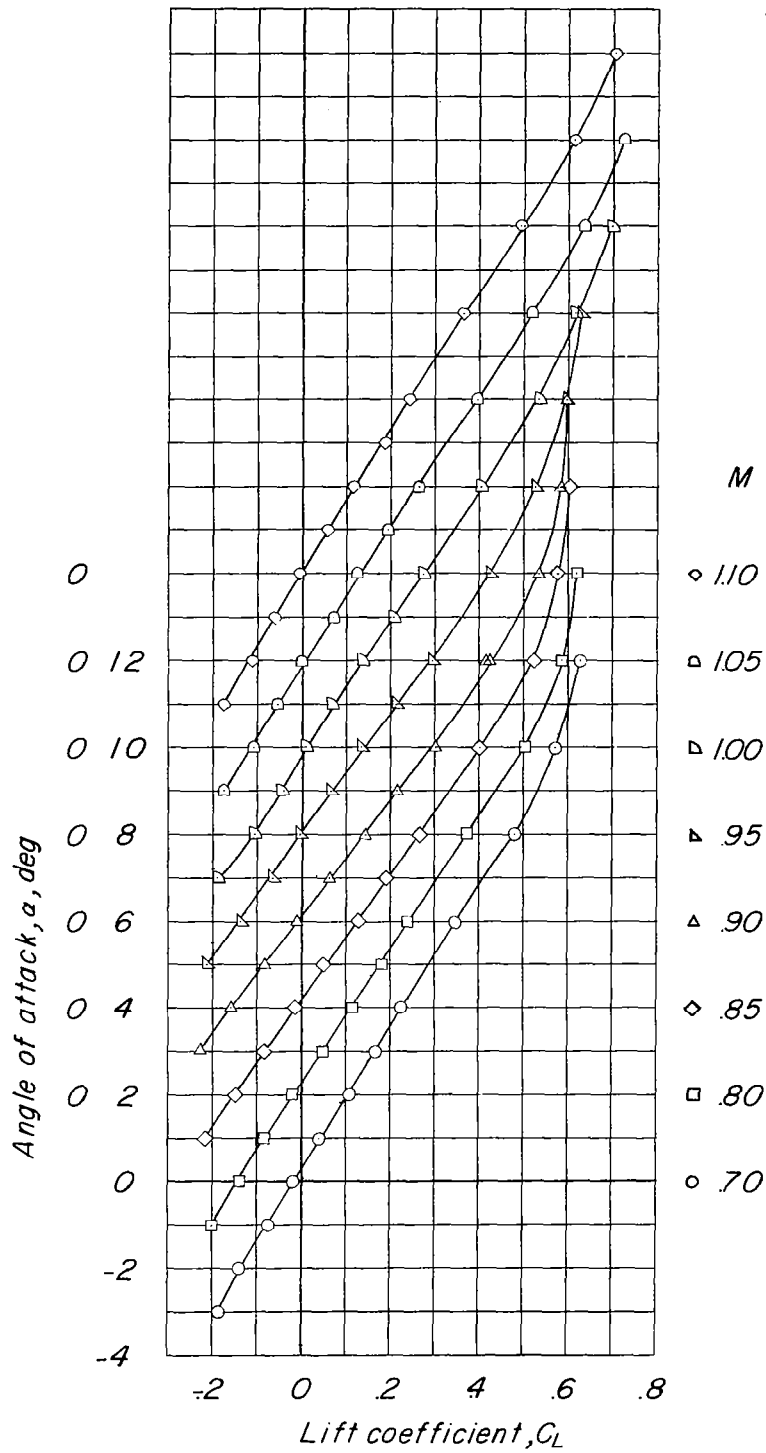
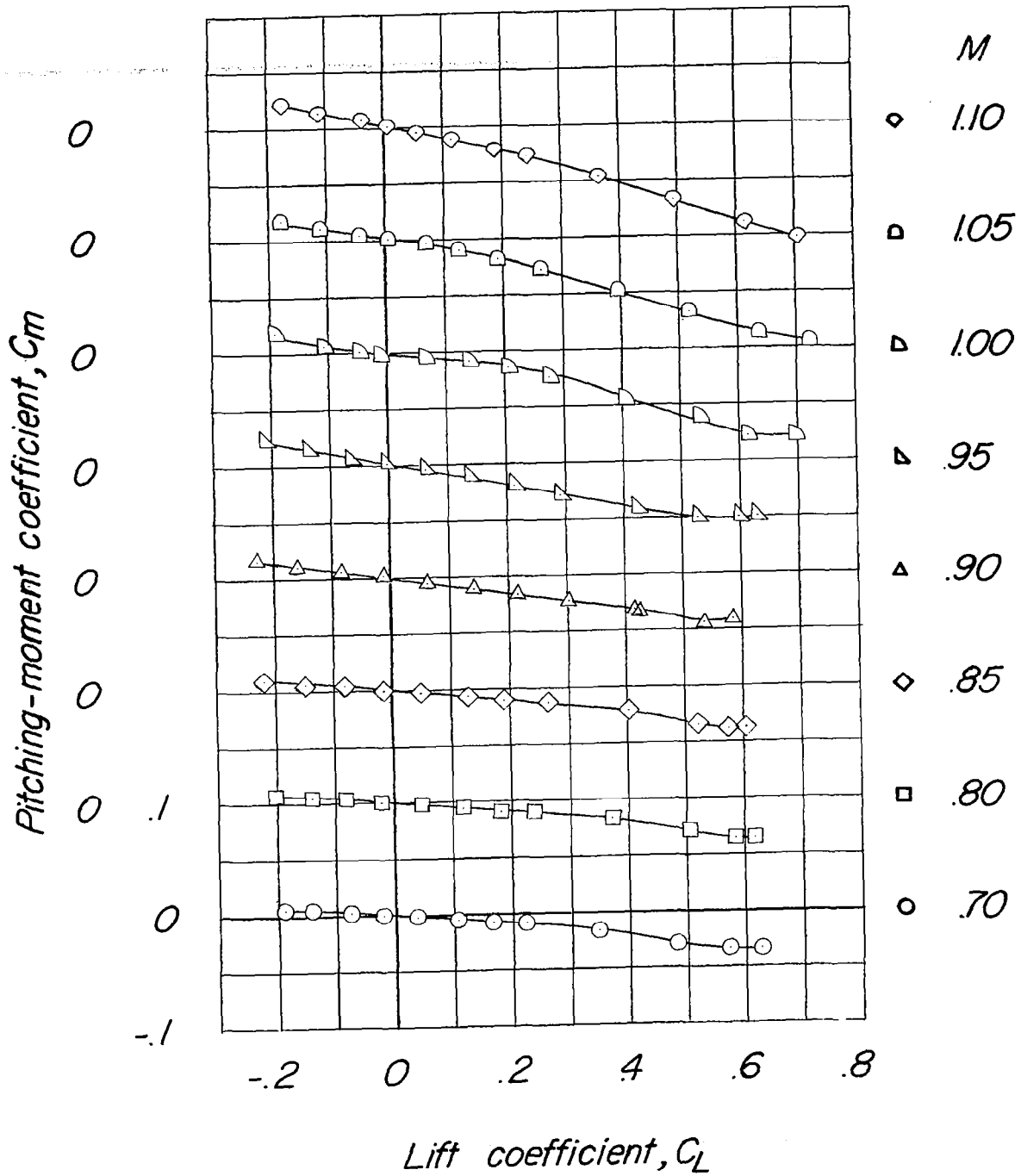


Figure 10.- Reynolds number variation with Mach number.



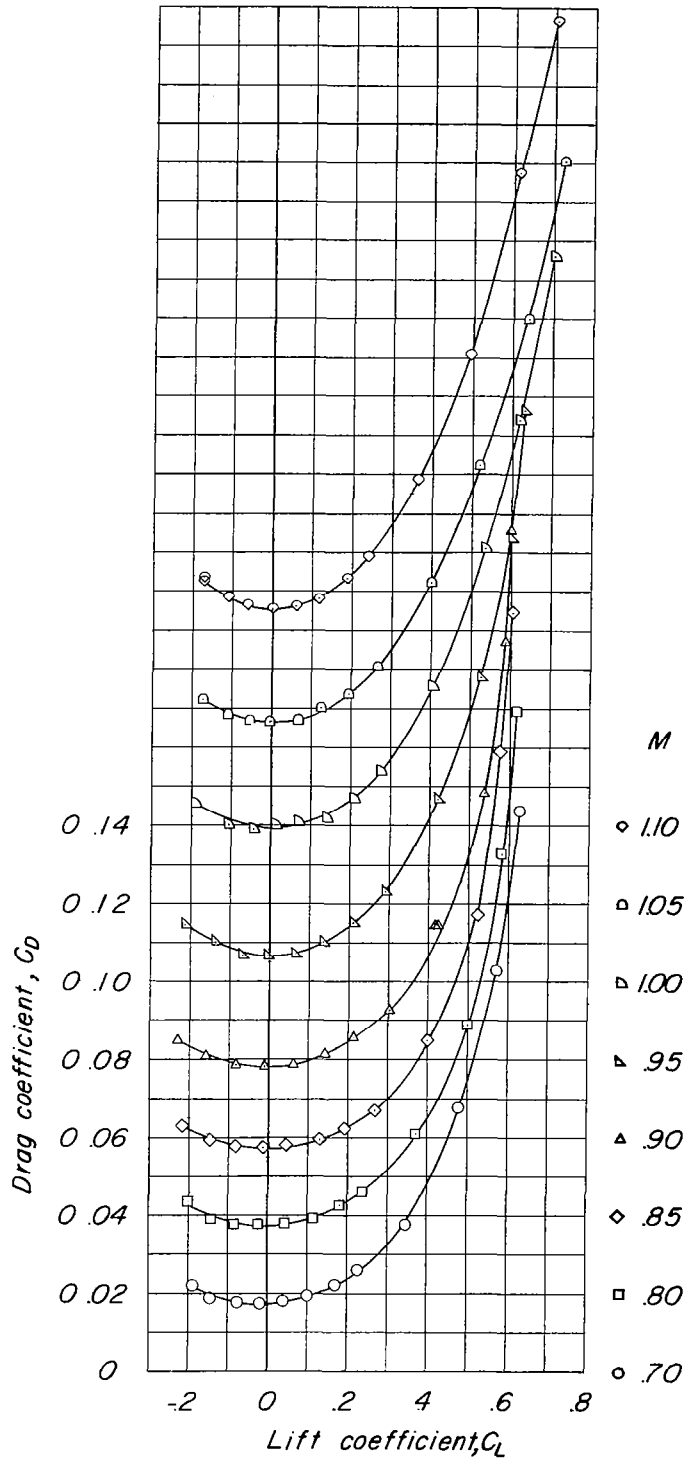
(a) α against C_L .

Figure 11.- Aerodynamic characteristics of 0.0298-scale 40° sweptback-wing-fuselage model.



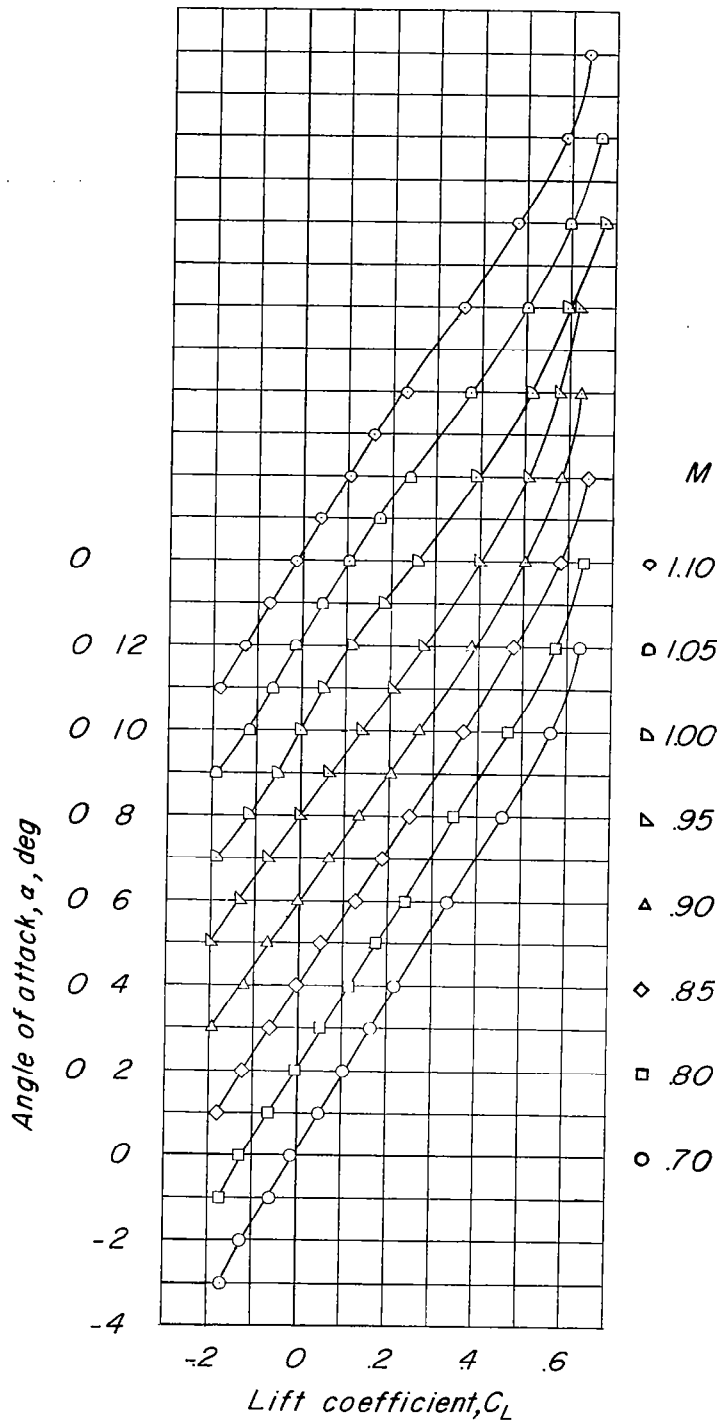
(b) C_m against C_L .

Figure 11.- Continued.



(c) C_D against C_L .

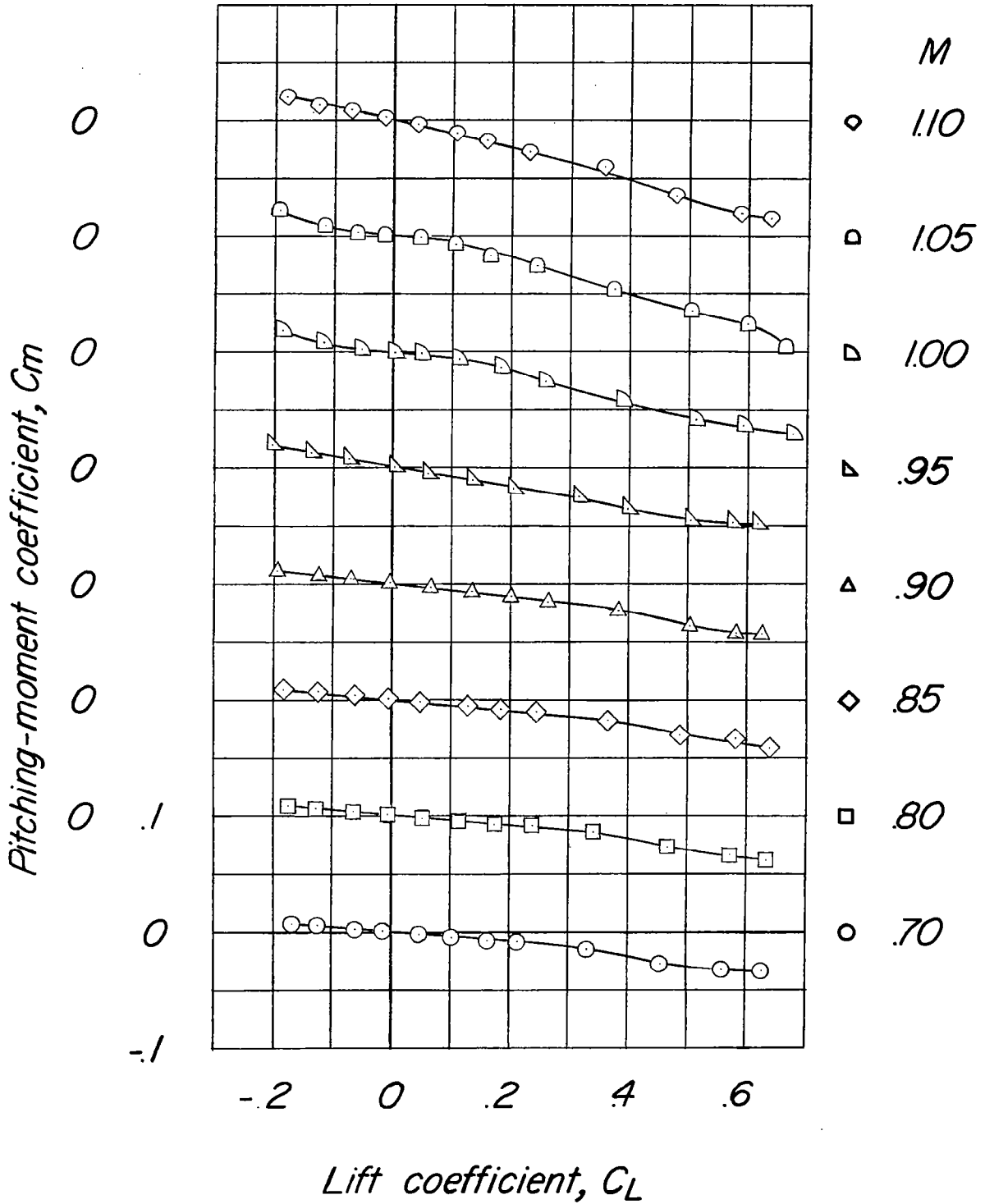
Figure 11.- Concluded.



(a) α against C_L .

Figure 12.- Aerodynamic characteristics of 0.0298-scale 40° sweptback-wing model.

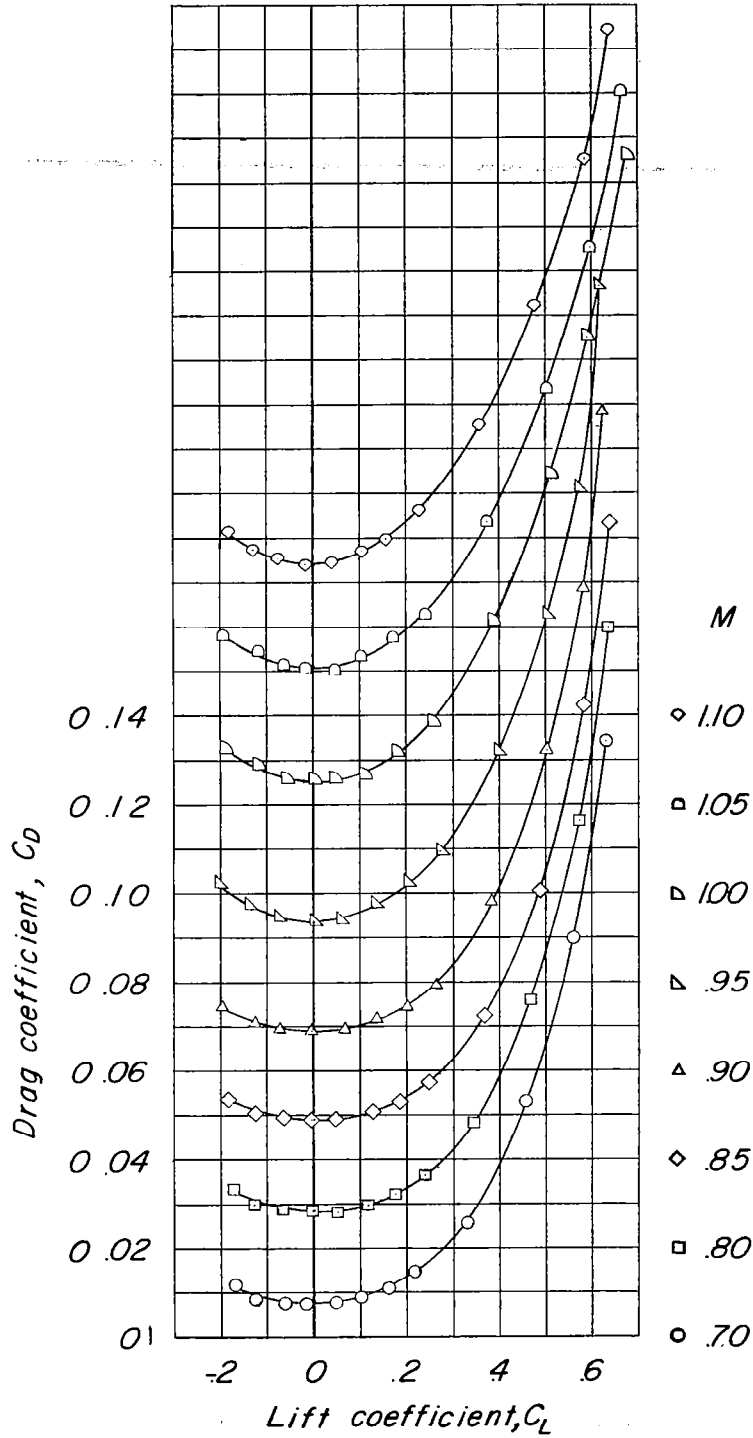
~~CONFIDENTIAL~~



(b) C_m against C_L .

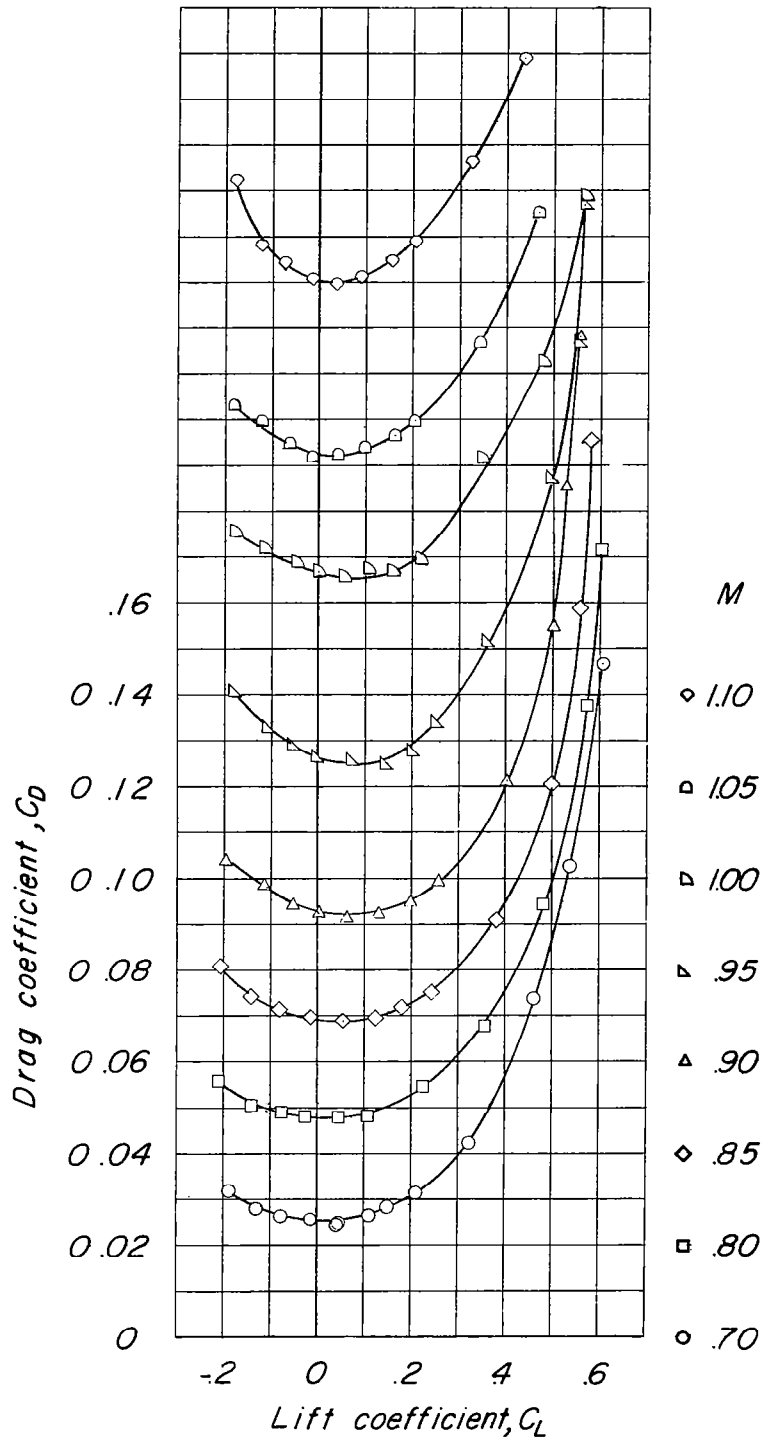
Figure 12.- Continued.

~~CONFIDENTIAL~~



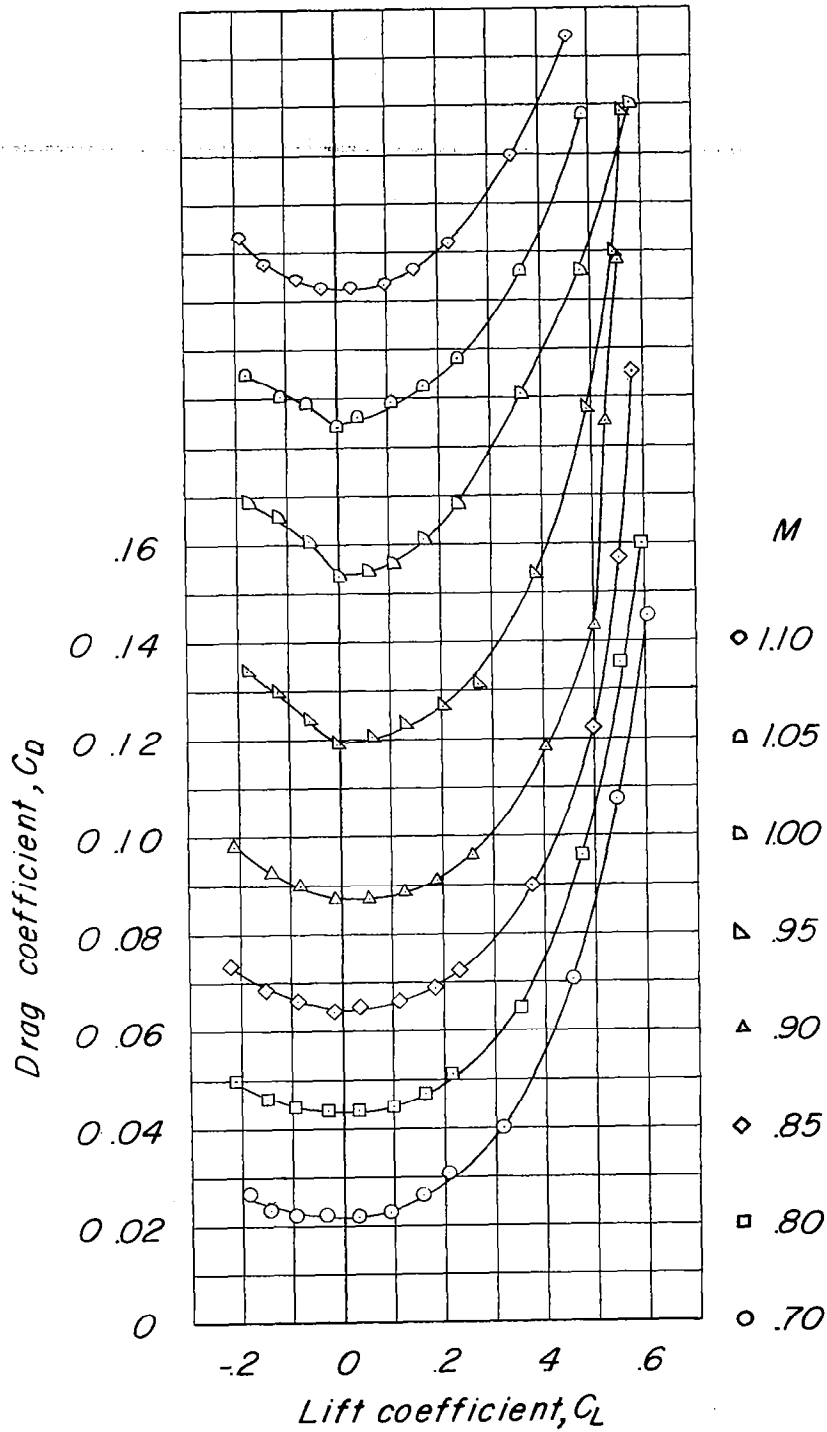
(c) C_D against C_L .

Figure 12.- Concluded.



(a) Long pylon, bomb configuration 1.

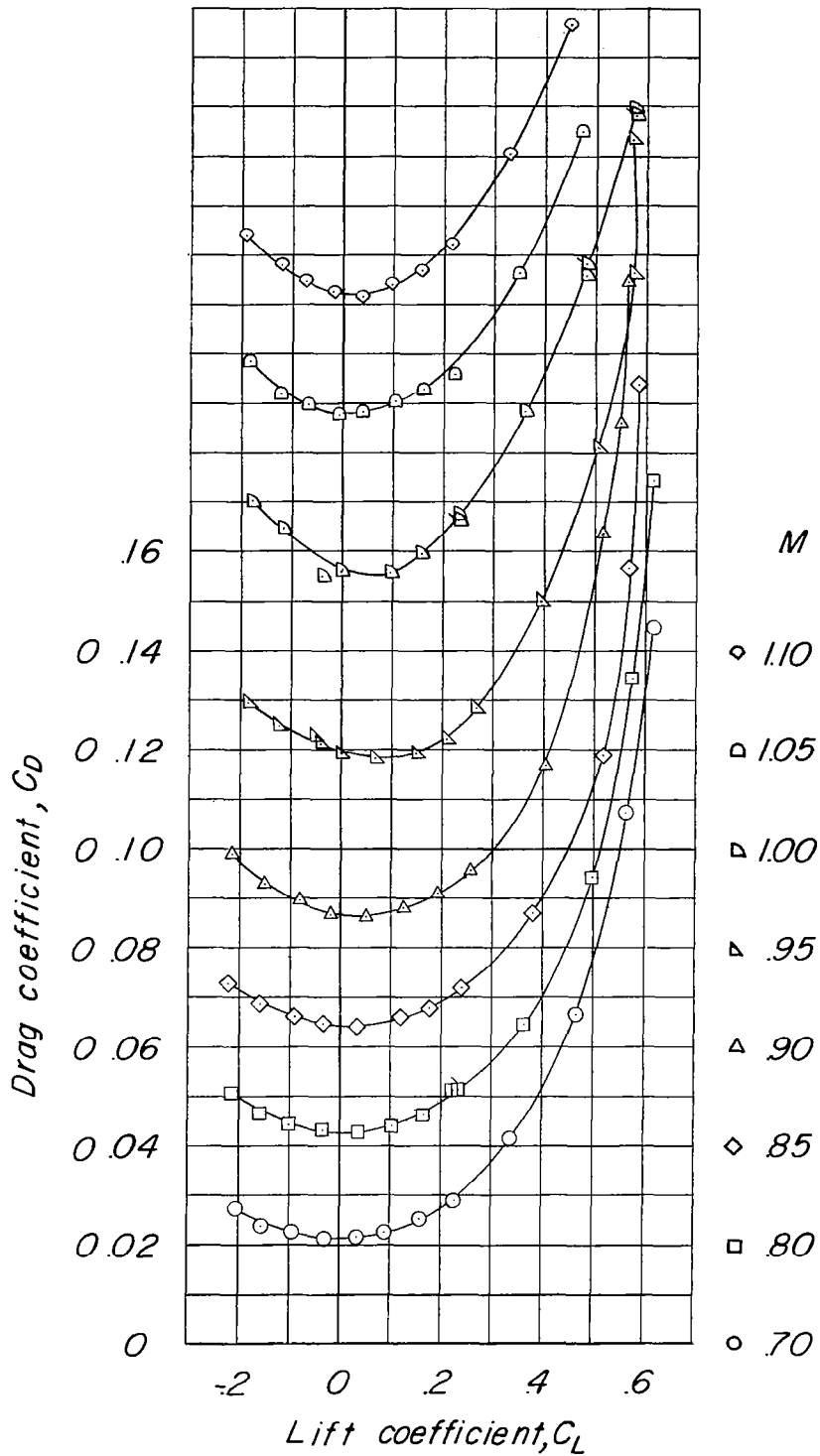
Figure 13.- Drag characteristics of 0.0298-scale 40° sweptback-wing-fuselage model with various pylon and bomb configurations.



(b) Long pylon, bomb configuration 2.

Figure 13.- Continued.

~~CONFIDENTIAL~~

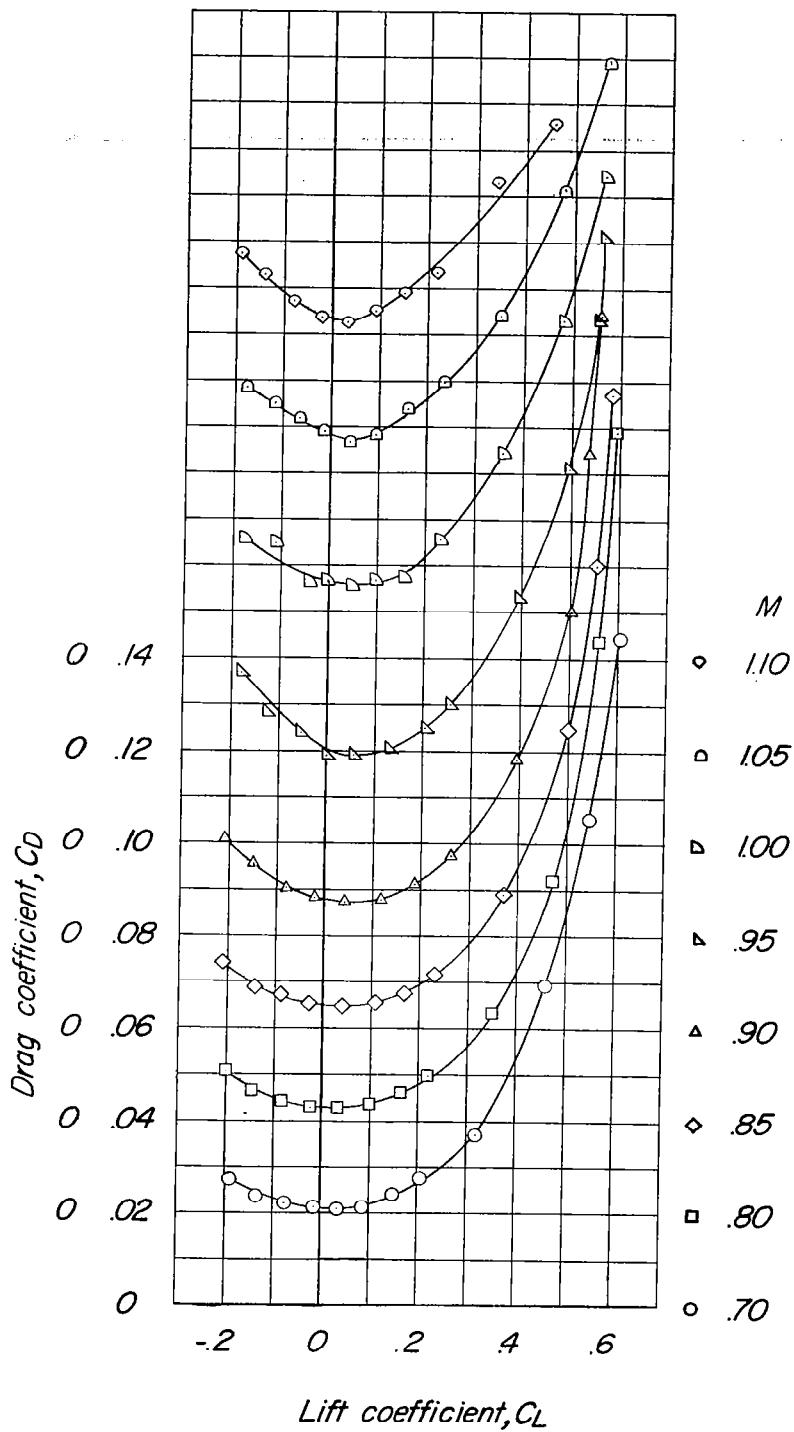


(c) Long pylon, bomb configuration 3.

Figure 13.- Continued.

~~CONFIDENTIAL~~

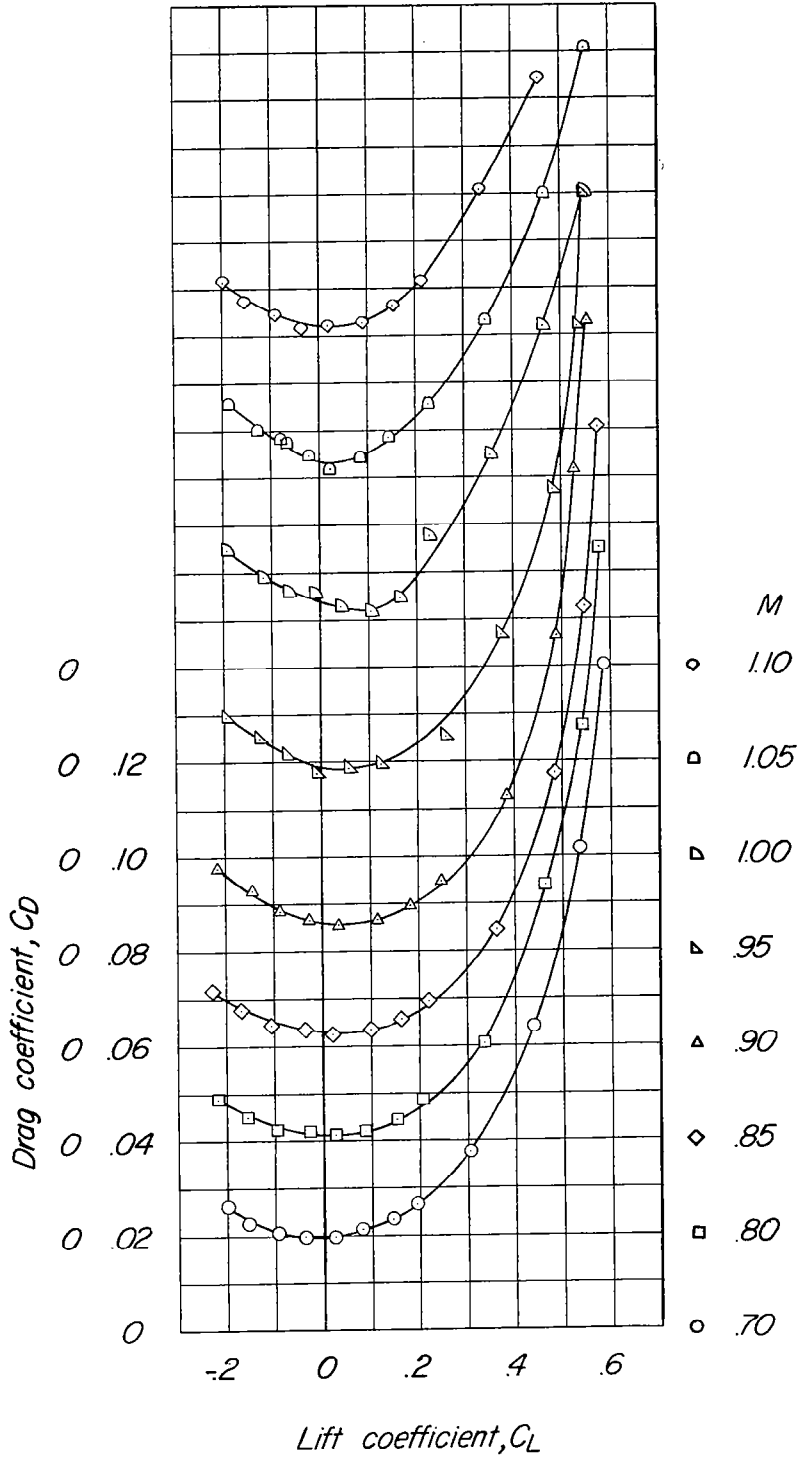
~~CONFIDENTIAL~~



(d) Long pylon, bomb configuration 4.

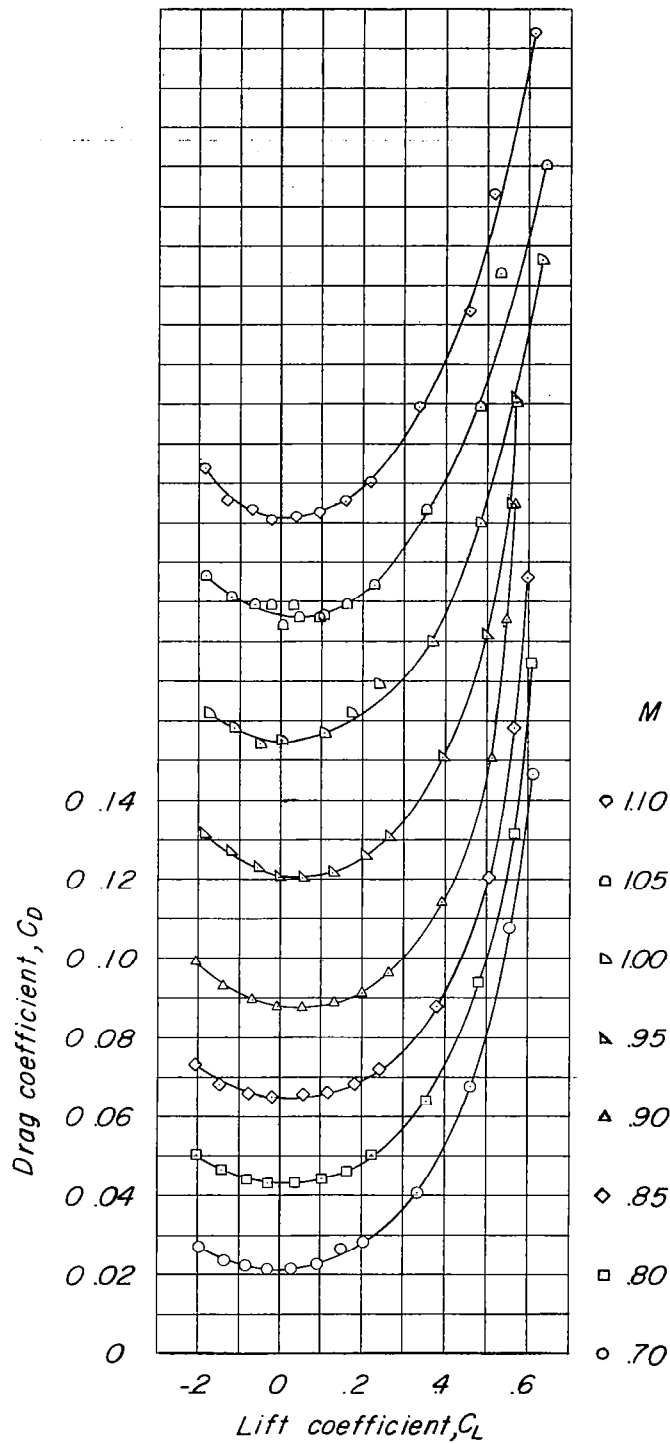
Figure 13.- Continued.

~~CONFIDENTIAL~~



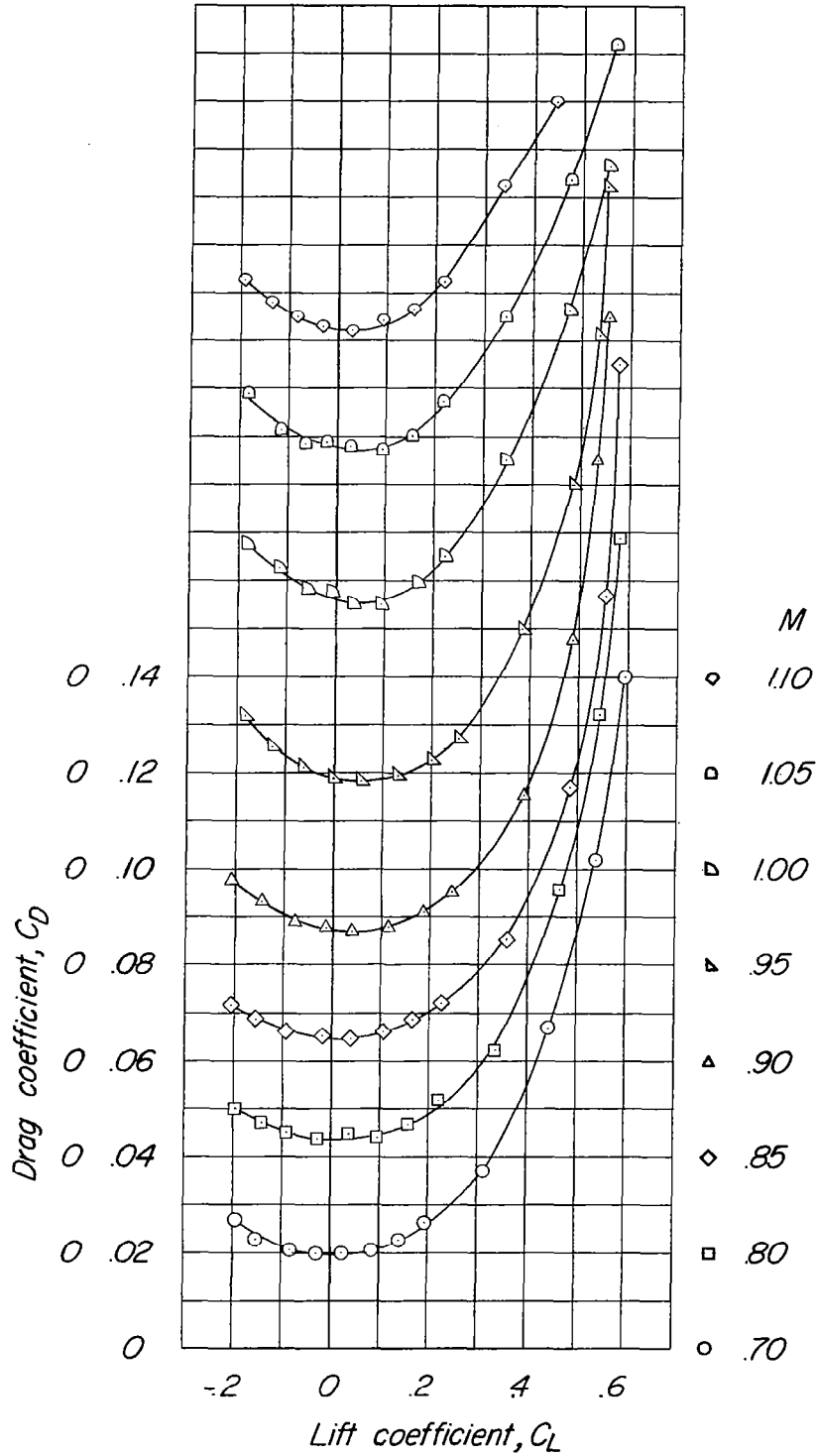
(e) Long pylon, bomb configuration 5.

Figure 13.- Continued.



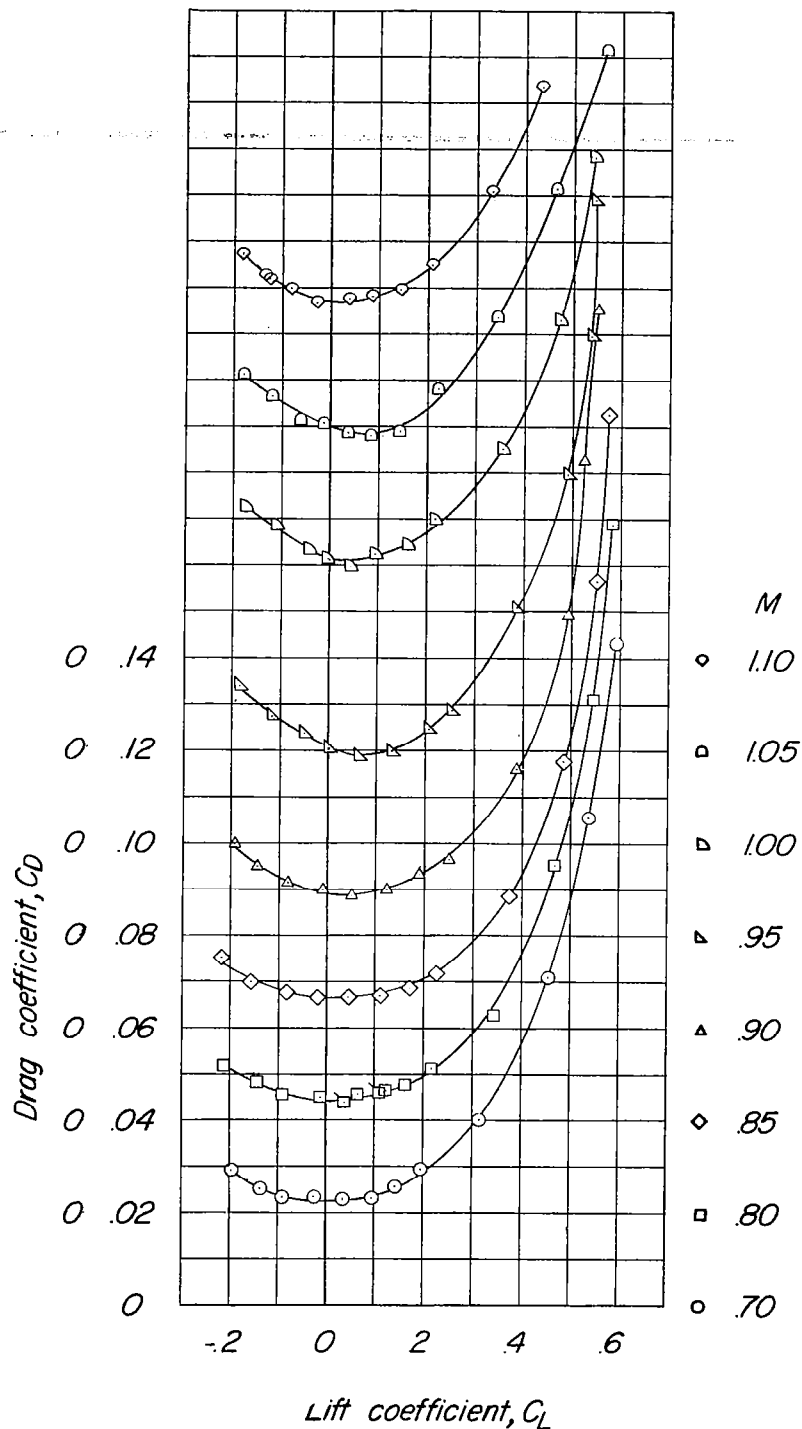
(f) Long pylon, bomb configuration 6.

Figure 13.- Continued.



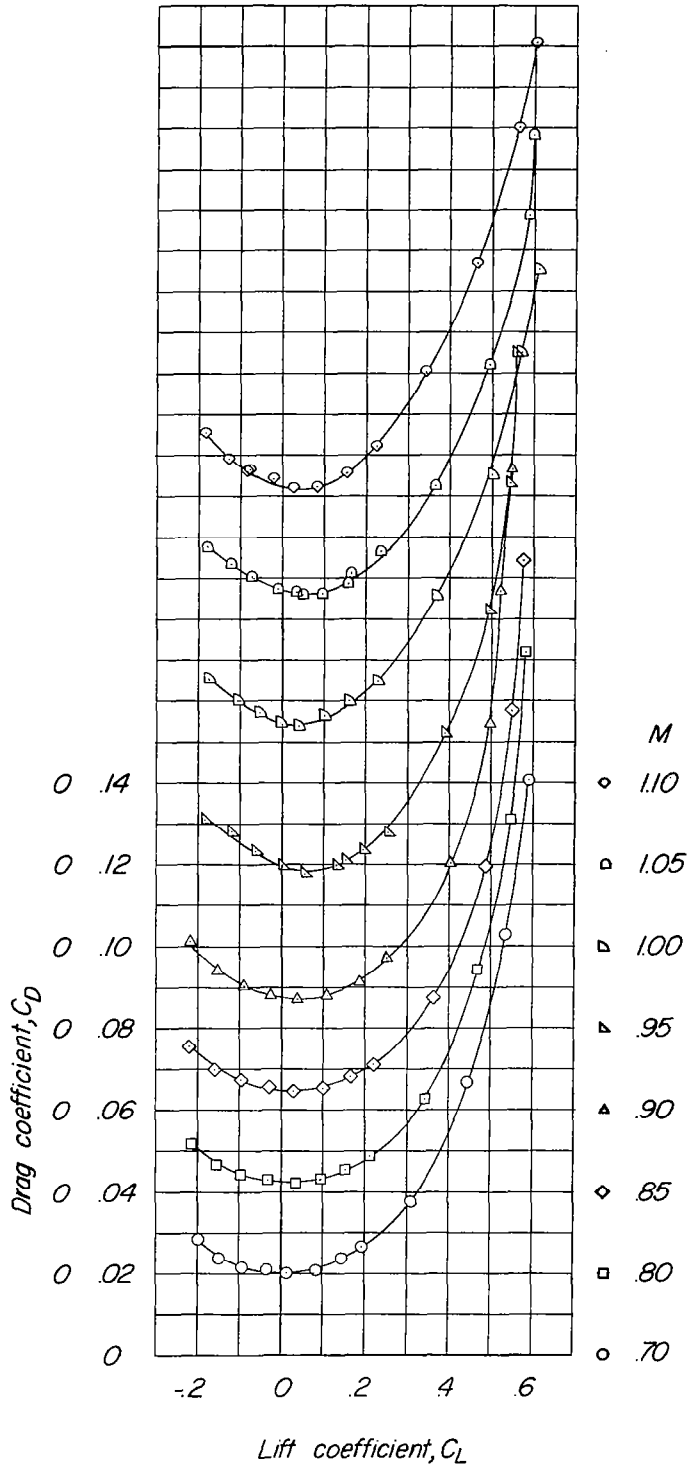
(g) Long pylon, bomb configuration 7.

Figure 13.- Continued.



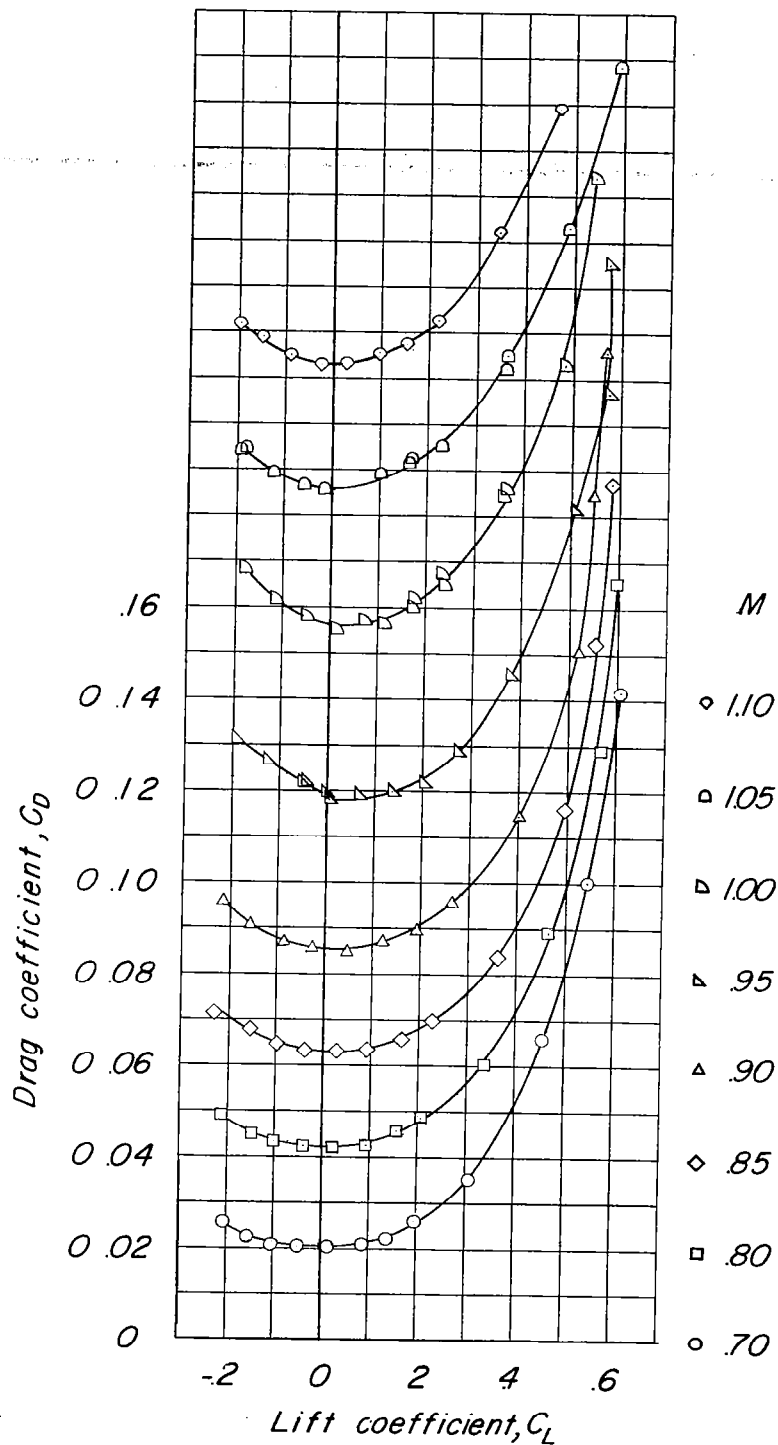
(h) Long pylon, bomb configuration 8.

Figure 13.- Continued.



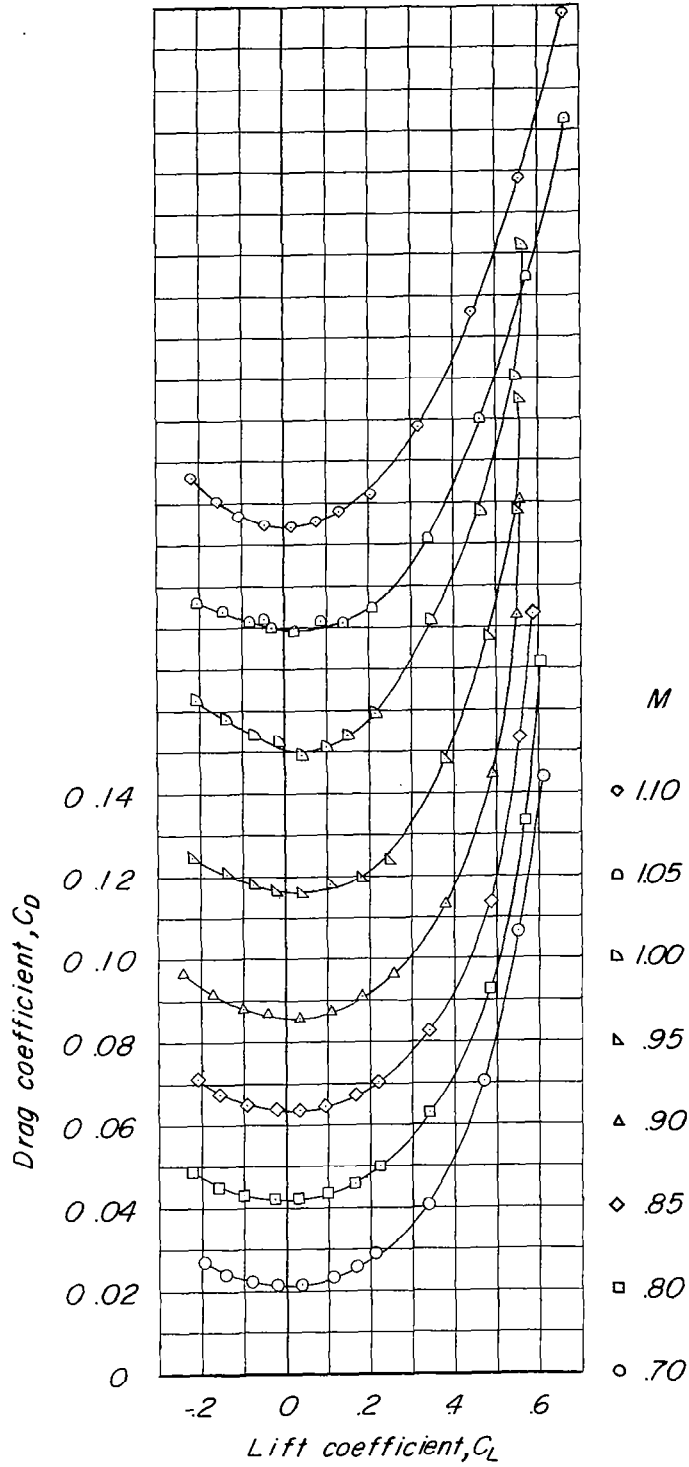
(i) Long pylon, bomb configuration 9.

Figure 13.- Continued.



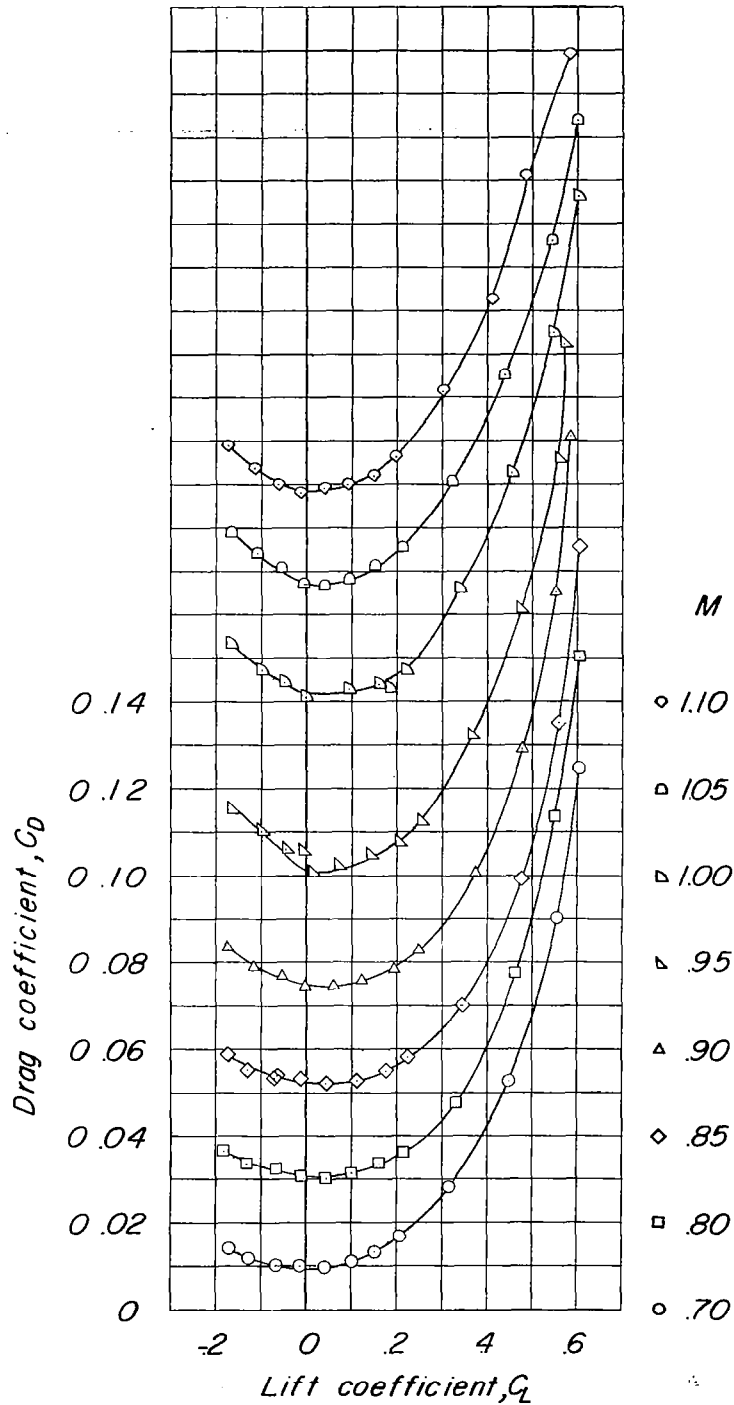
(j) Long pylon, bomb configuration β_E .

Figure 13.- Continued.



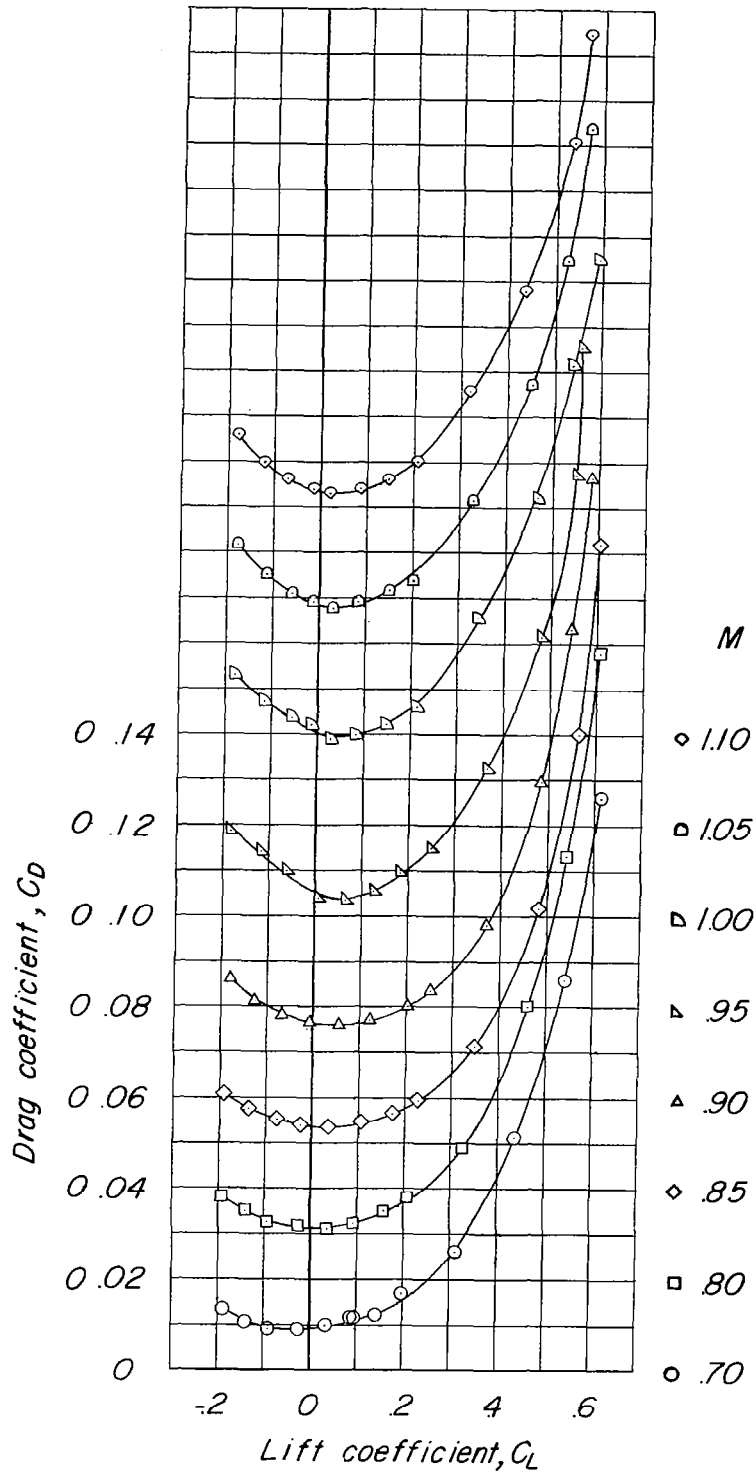
(k) Short pylon, bomb configuration 3E.

Figure 13.- Concluded.



(a) Long pylon, bomb configuration 3.

Figure 14.- Drag characteristics of 0.0298-scale 40° sweptback-wing model with long pylon and various bomb configurations.



(b) Long pylon, bomb configuration 9.

Figure 14.- Concluded.

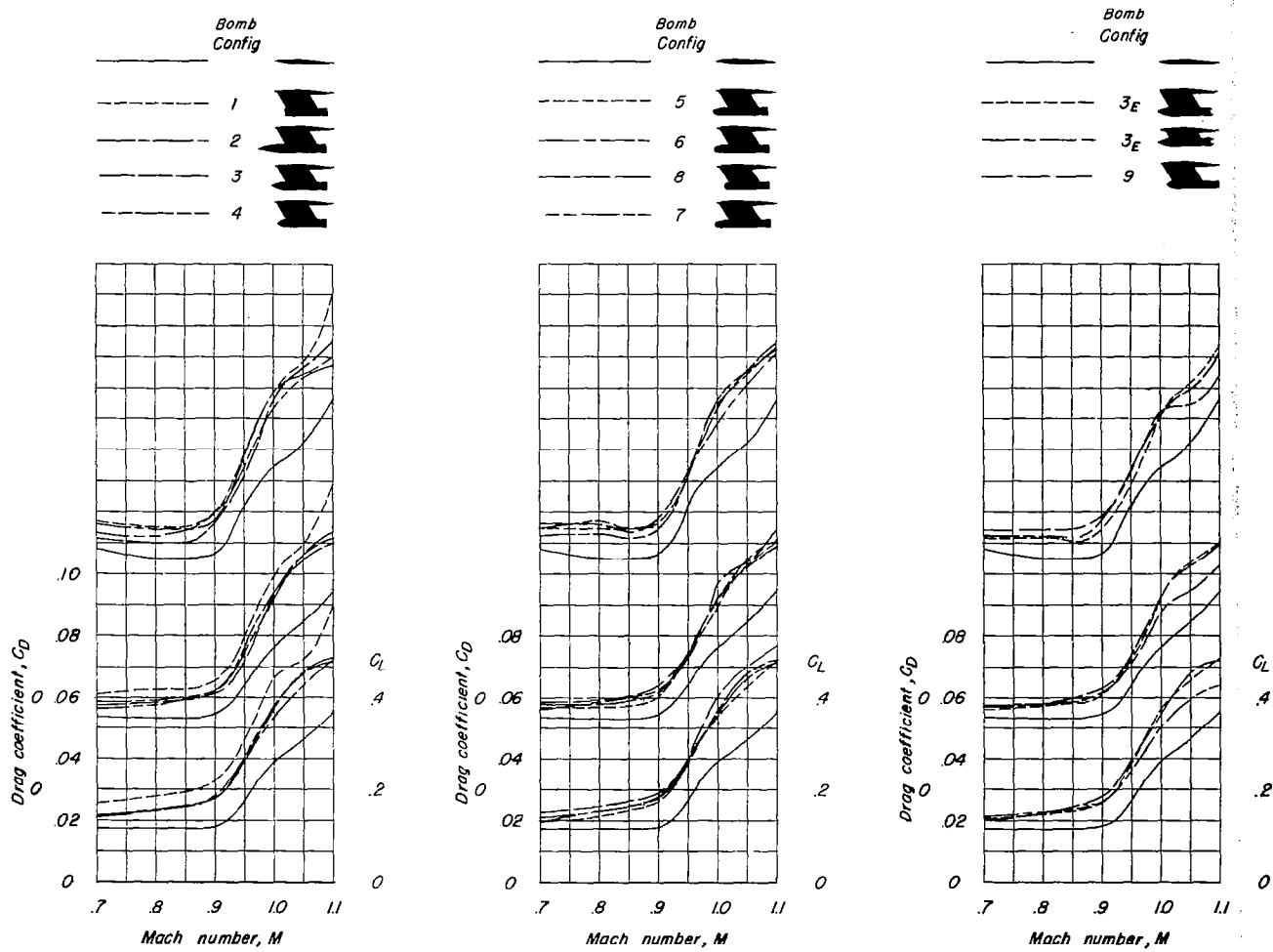


Figure 15.- Variation of drag coefficient with Mach number of a 0.0298-scale 40° sweptback-wing-fuselage model with various pylon and bomb configurations.

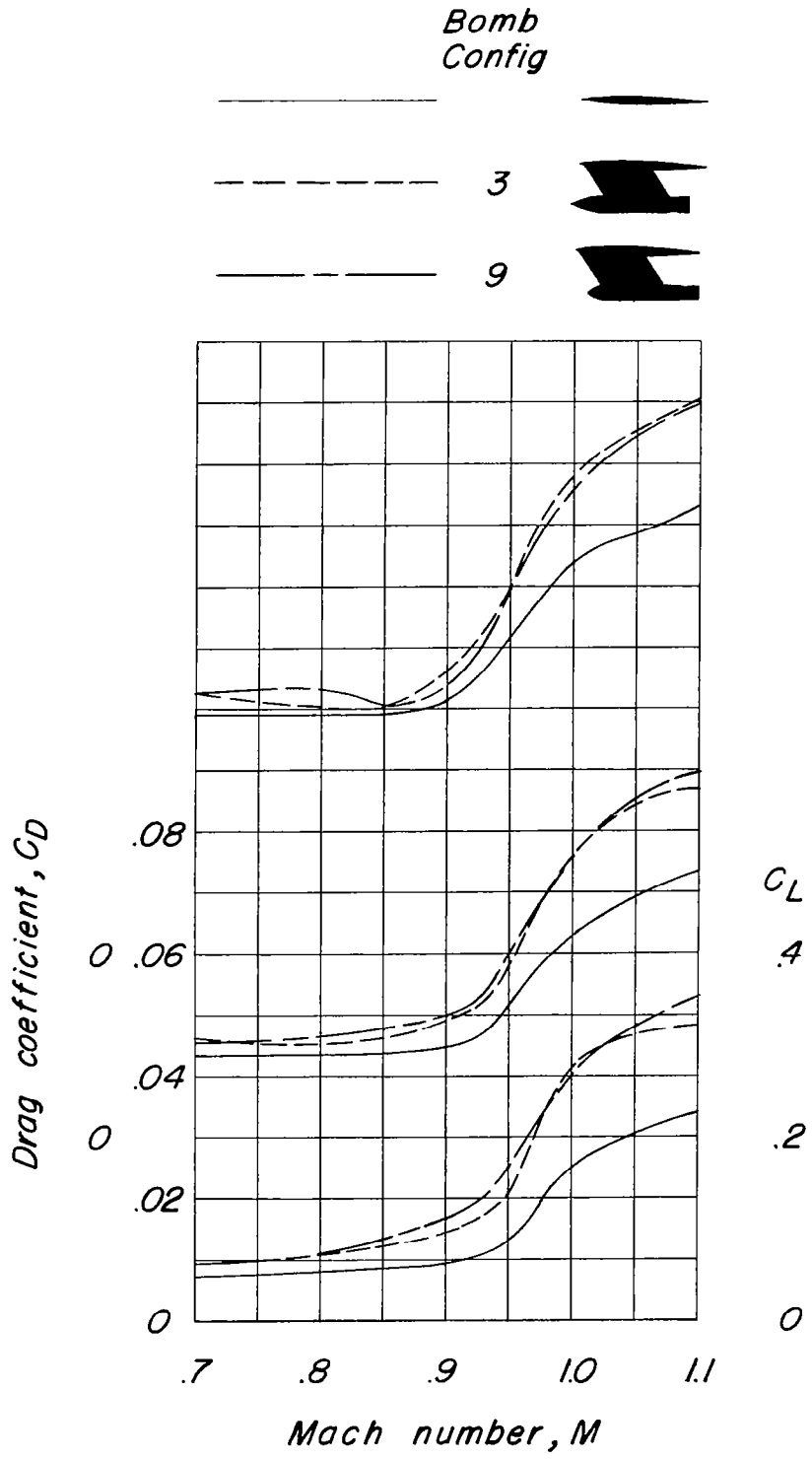


Figure 16.- Variation of drag coefficient with Mach number of a 0.0298-scale 40° sweptback-wing model with long pylon and various bomb configurations.

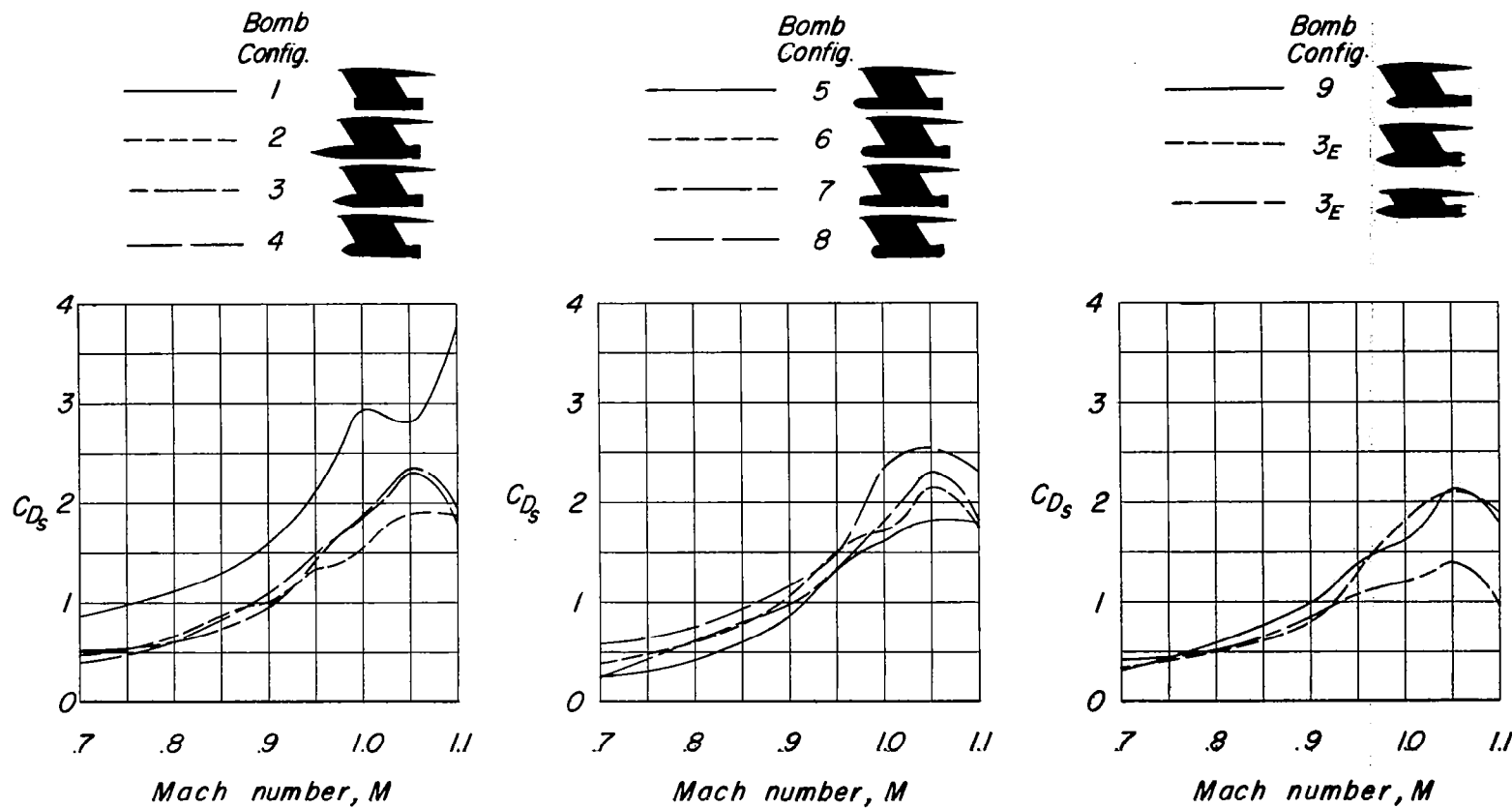


Figure 17.- Variation of bomb-plus-interference drag coefficient with Mach number. Wing-fuselage model; $C_L = 0$.

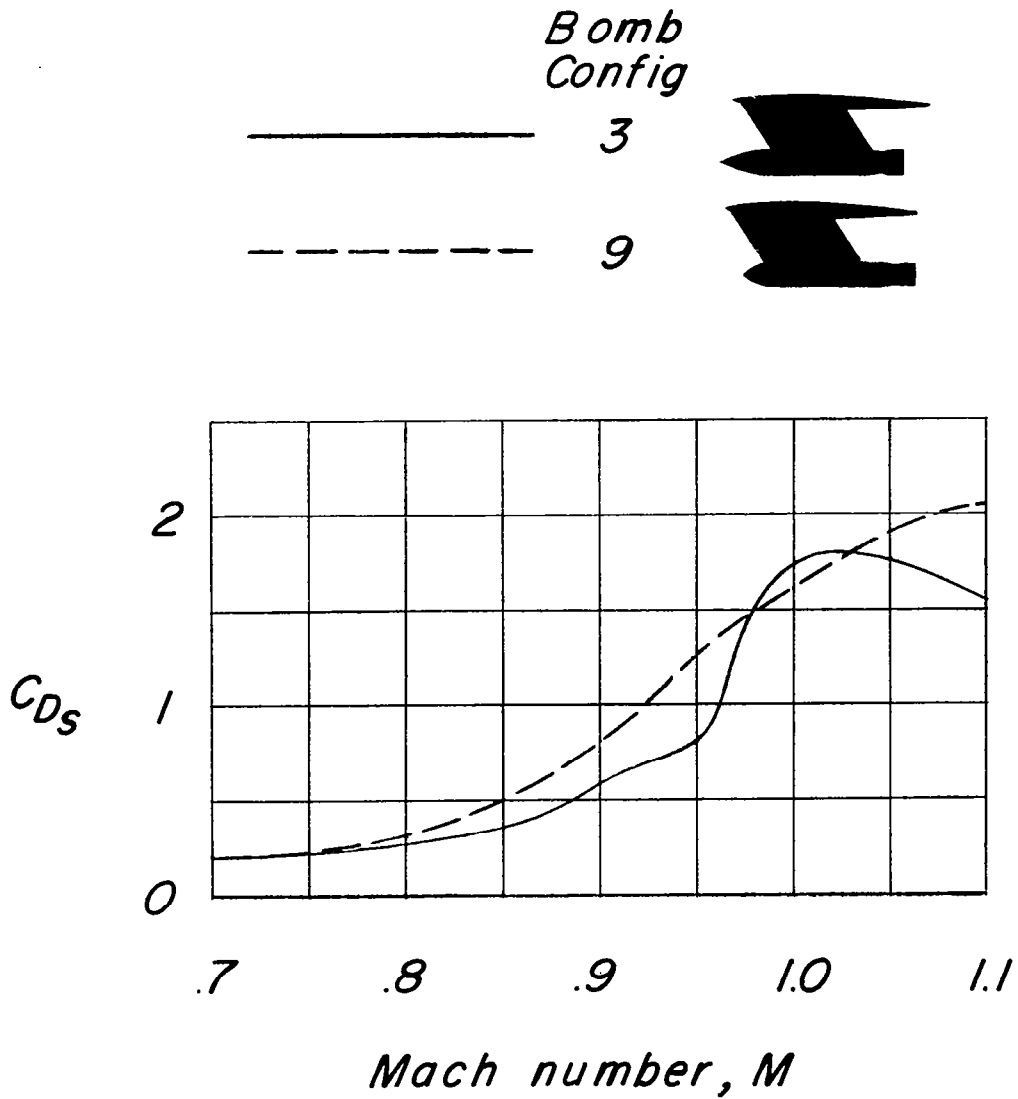


Figure 18.- Variation of bomb-plus-interference drag coefficient with Mach number. Wing alone; $C_L = 0$.

~~CONFIDENTIAL~~

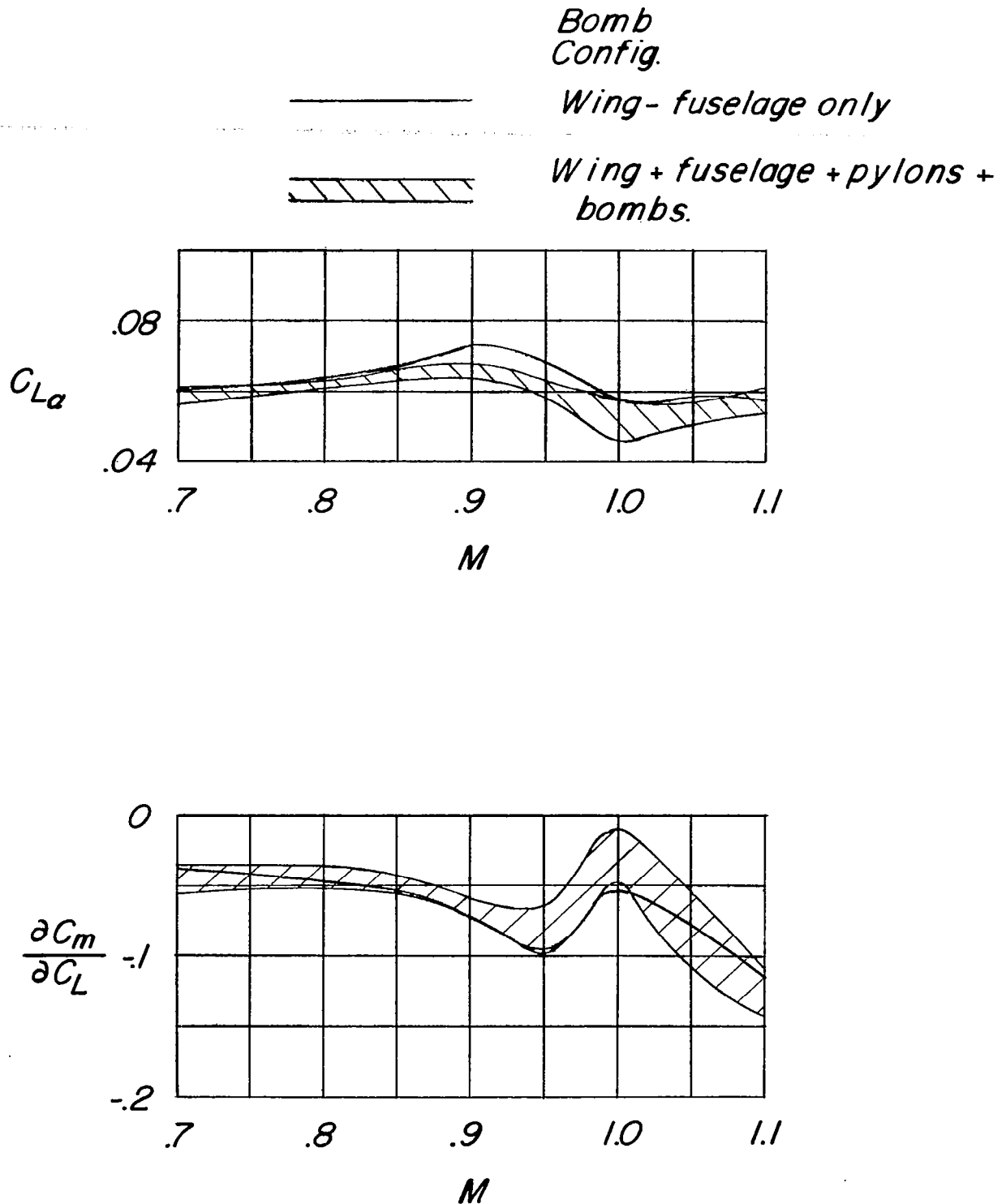


Figure 19.- Variation of lift-curve slopes and pitching-moment-curve slopes with Mach number. Wing-fuselage model.

~~CONFIDENTIAL~~

~~CONFIDENTIAL~~

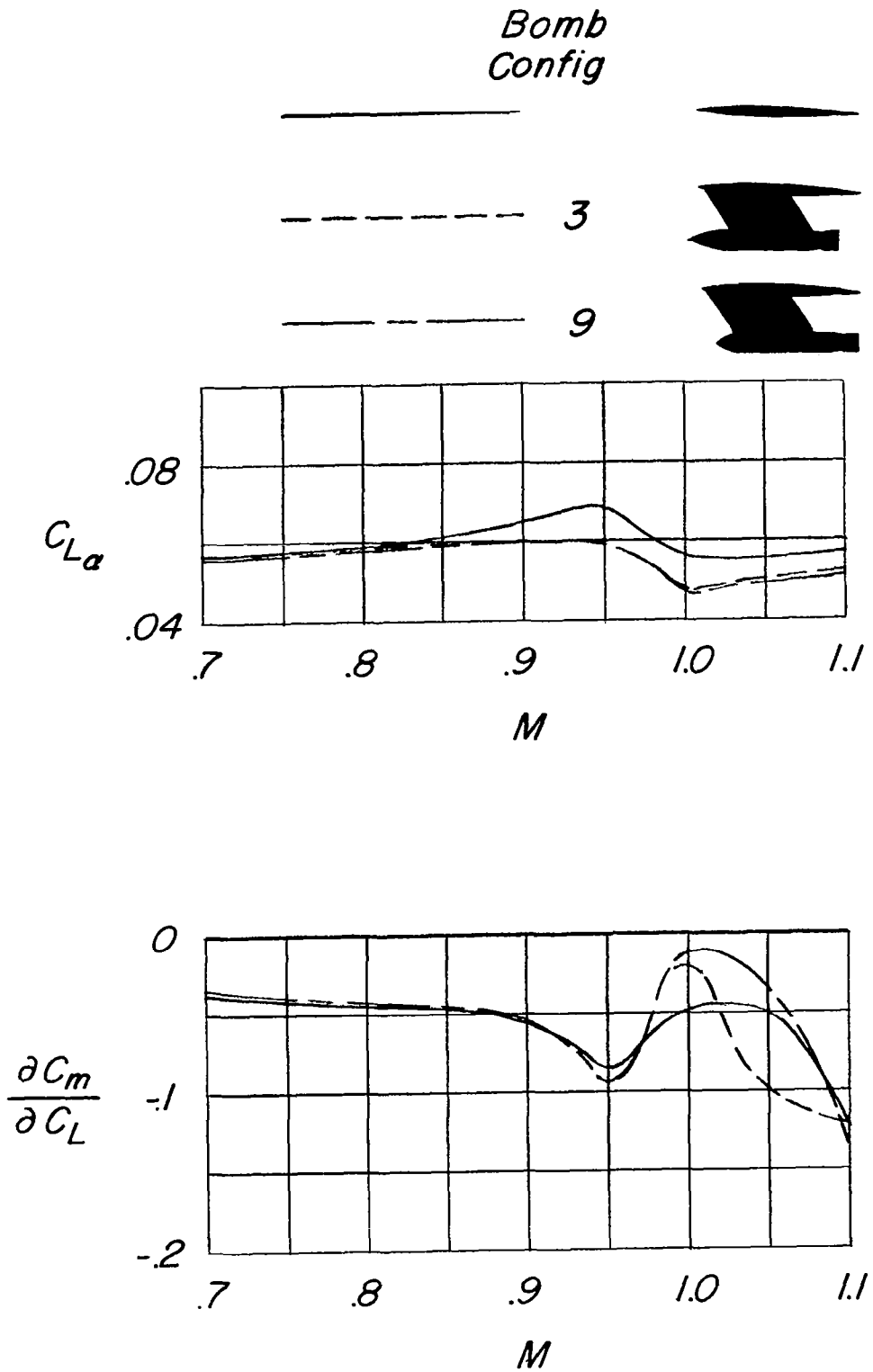
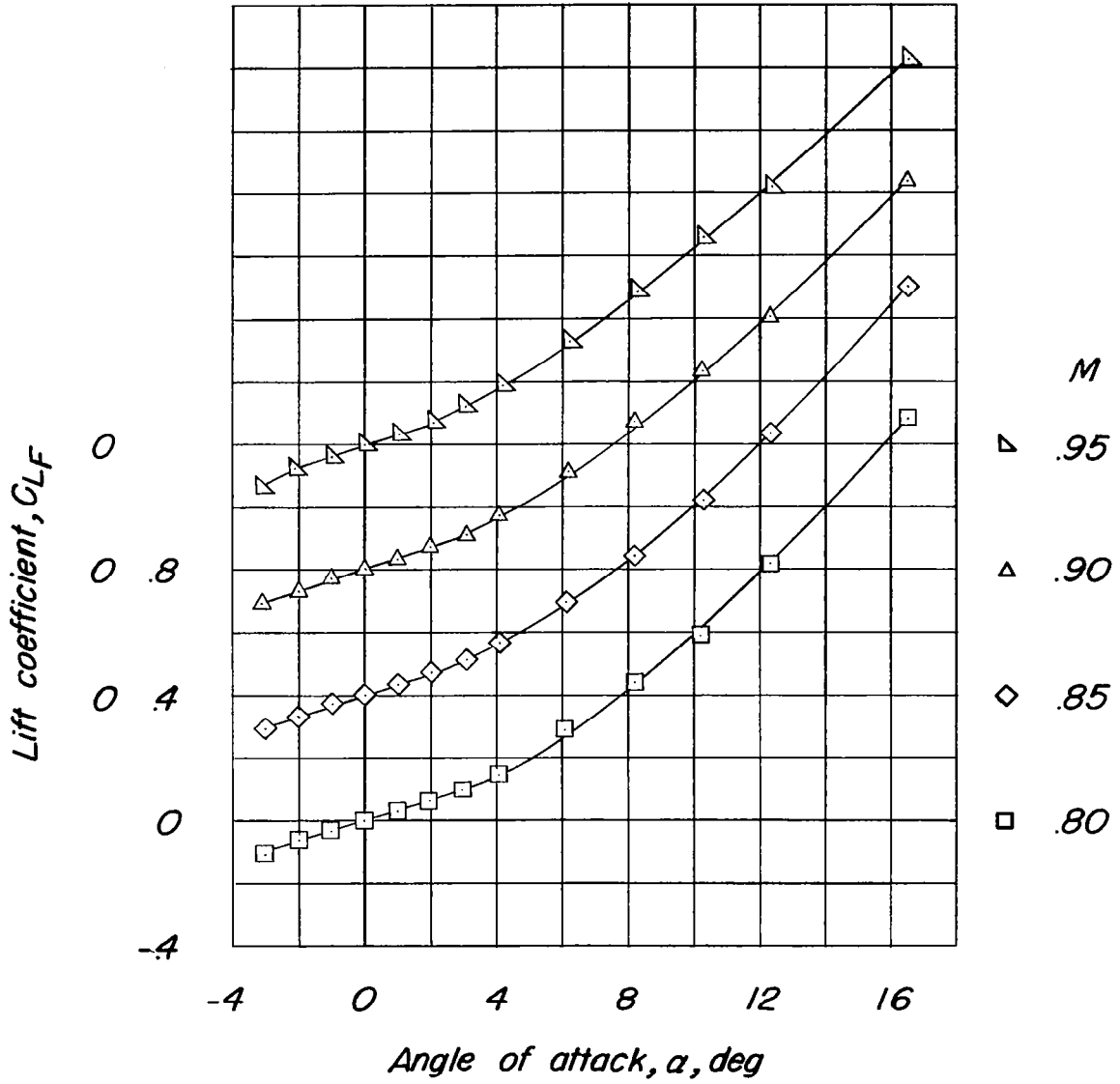


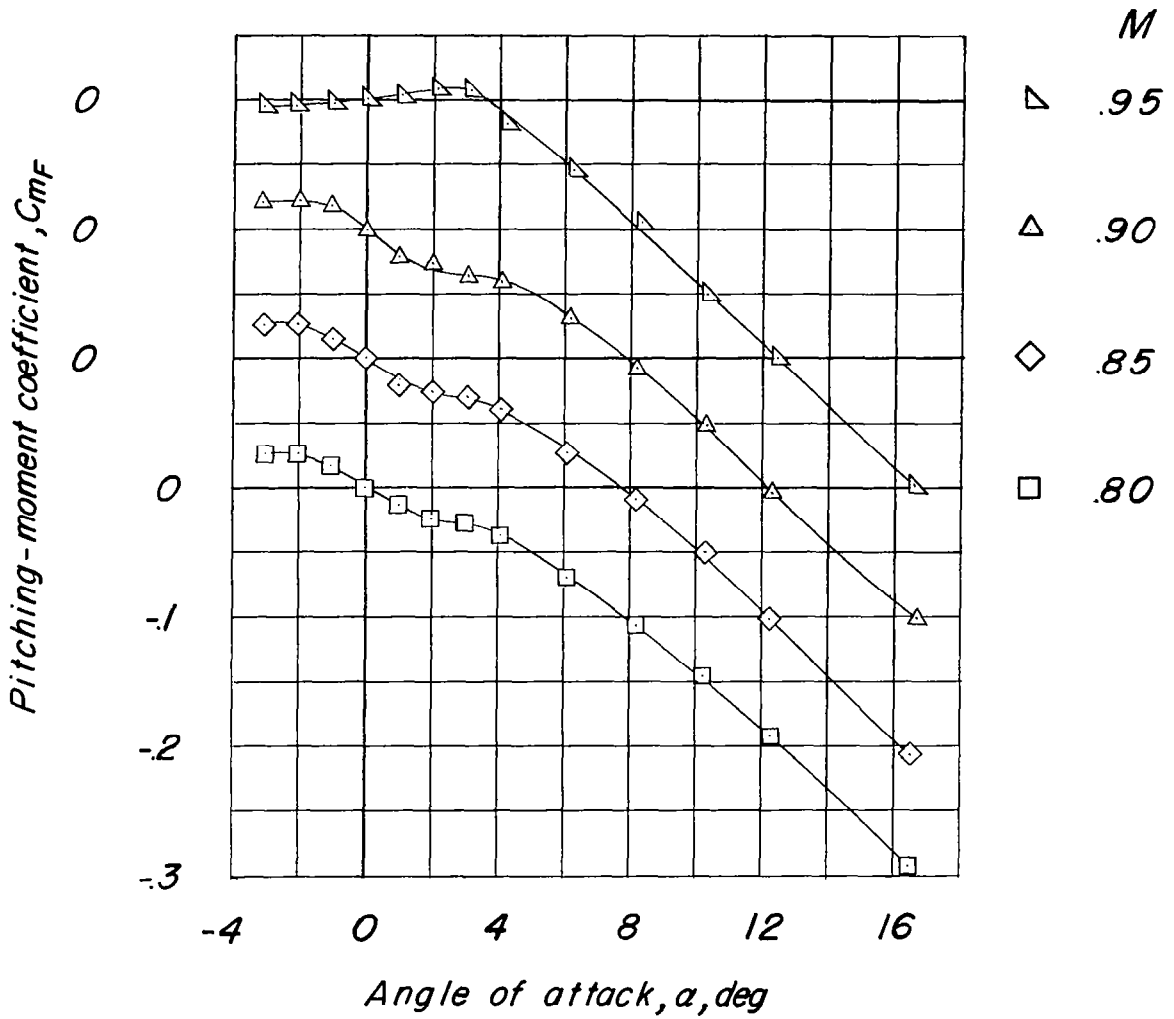
Figure 20.- Variation of lift-curve slopes and pitching-moment-curve slopes with Mach number. Wing alone.

~~CONFIDENTIAL~~



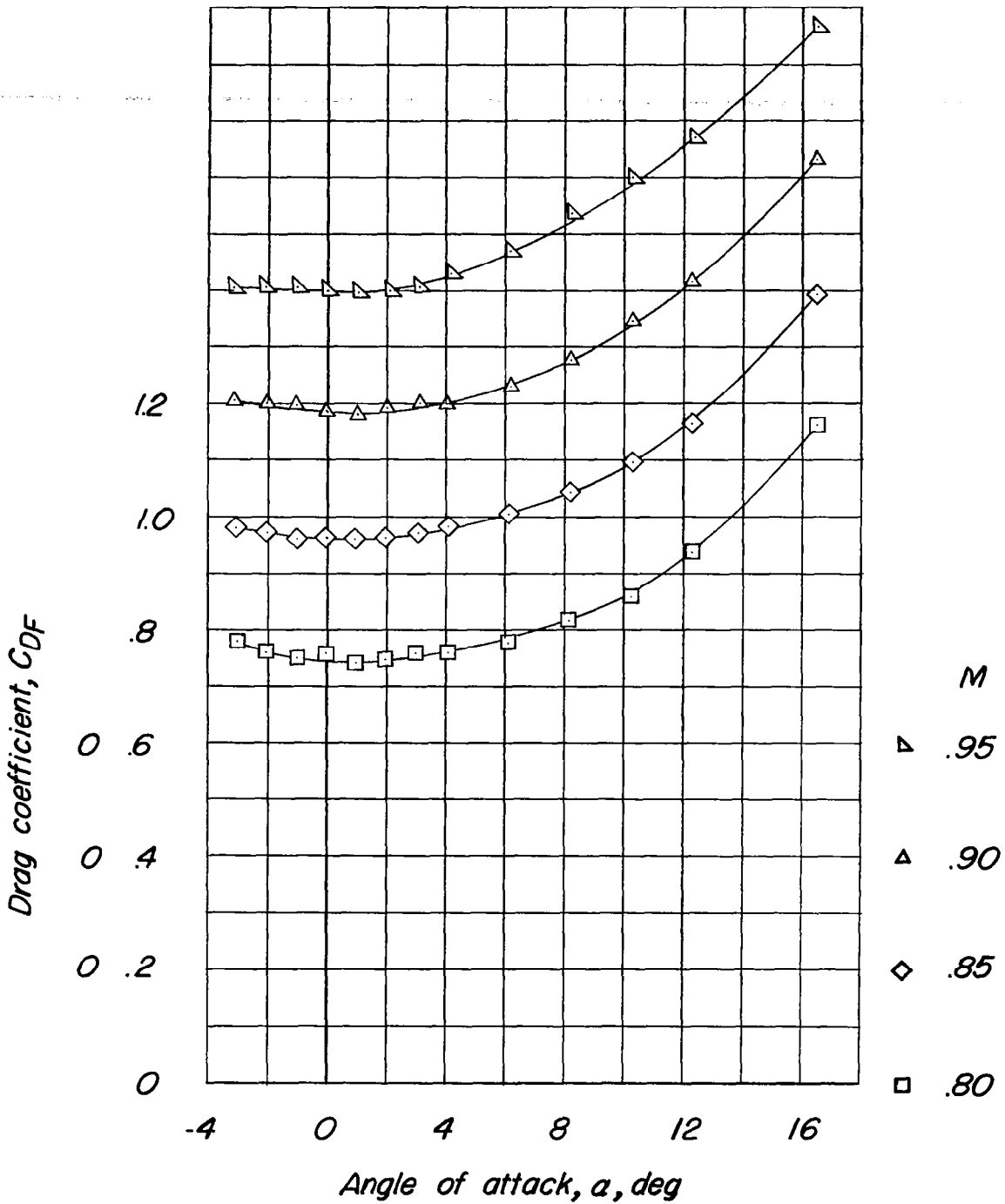
(a) Configuration 1.

Figure 21.- Aerodynamic characteristics of 0.1517-scale bomb.



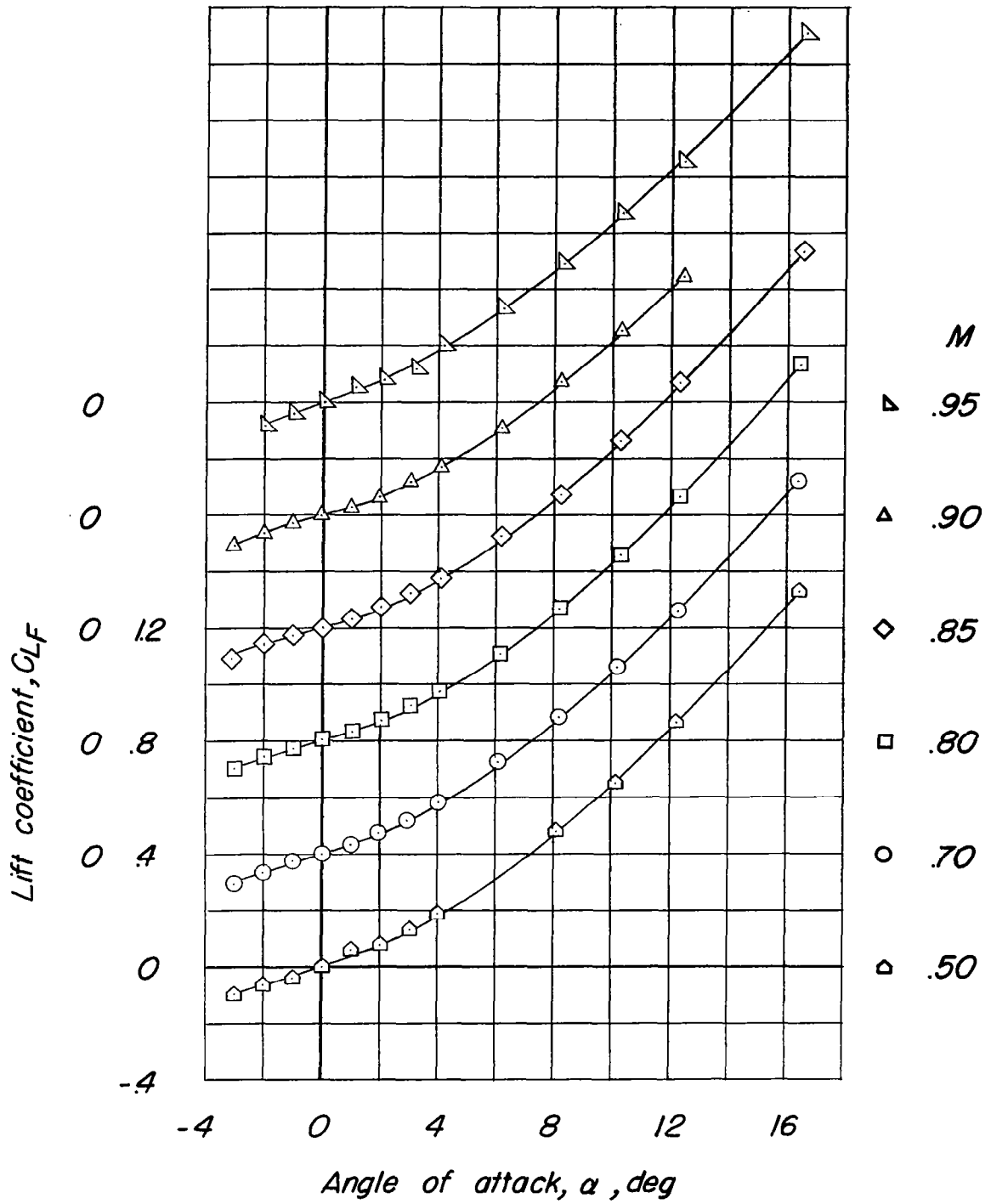
(a) Continued.

Figure 21.- Continued.



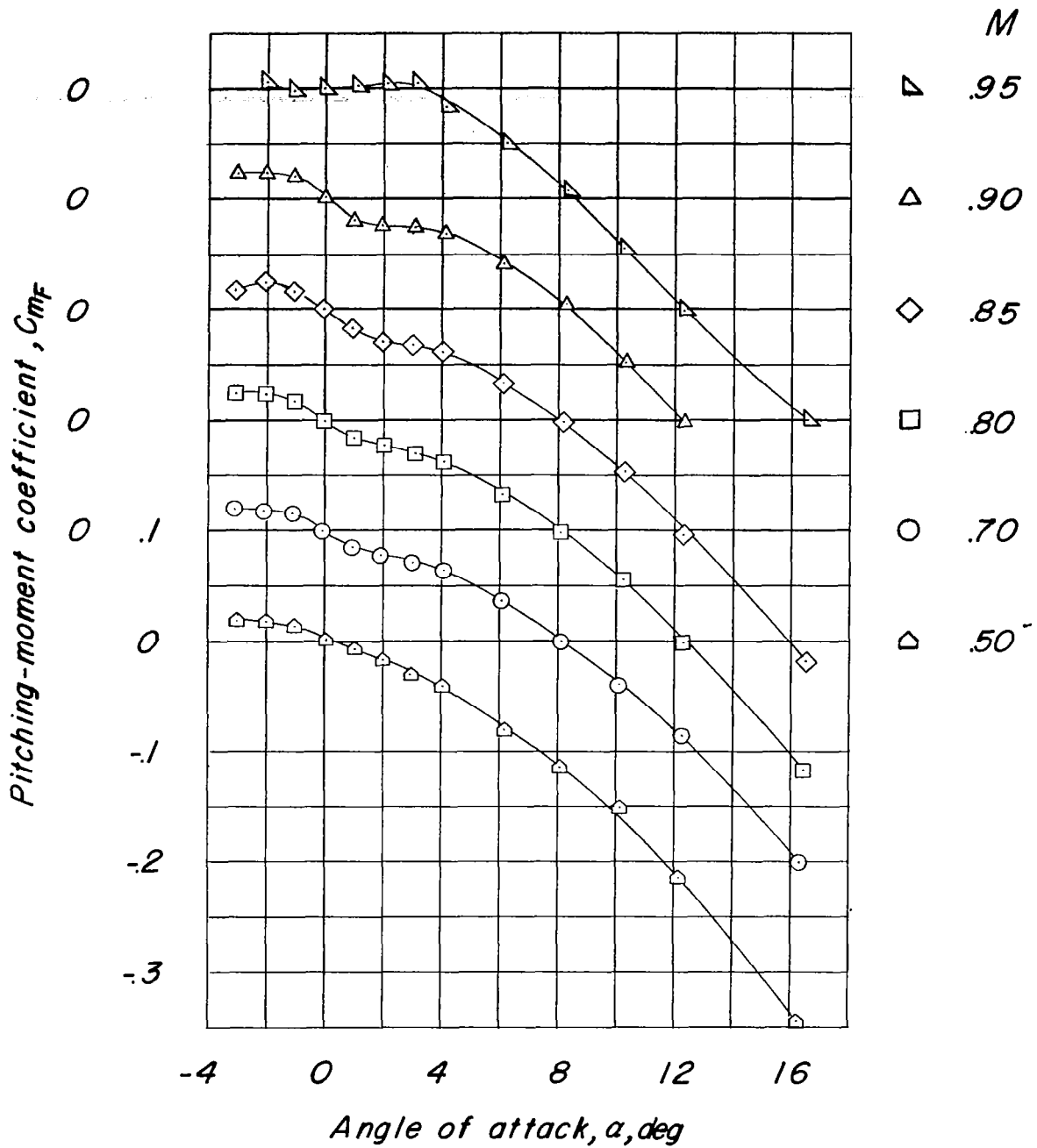
(a) Concluded.

Figure 21.- Continued.



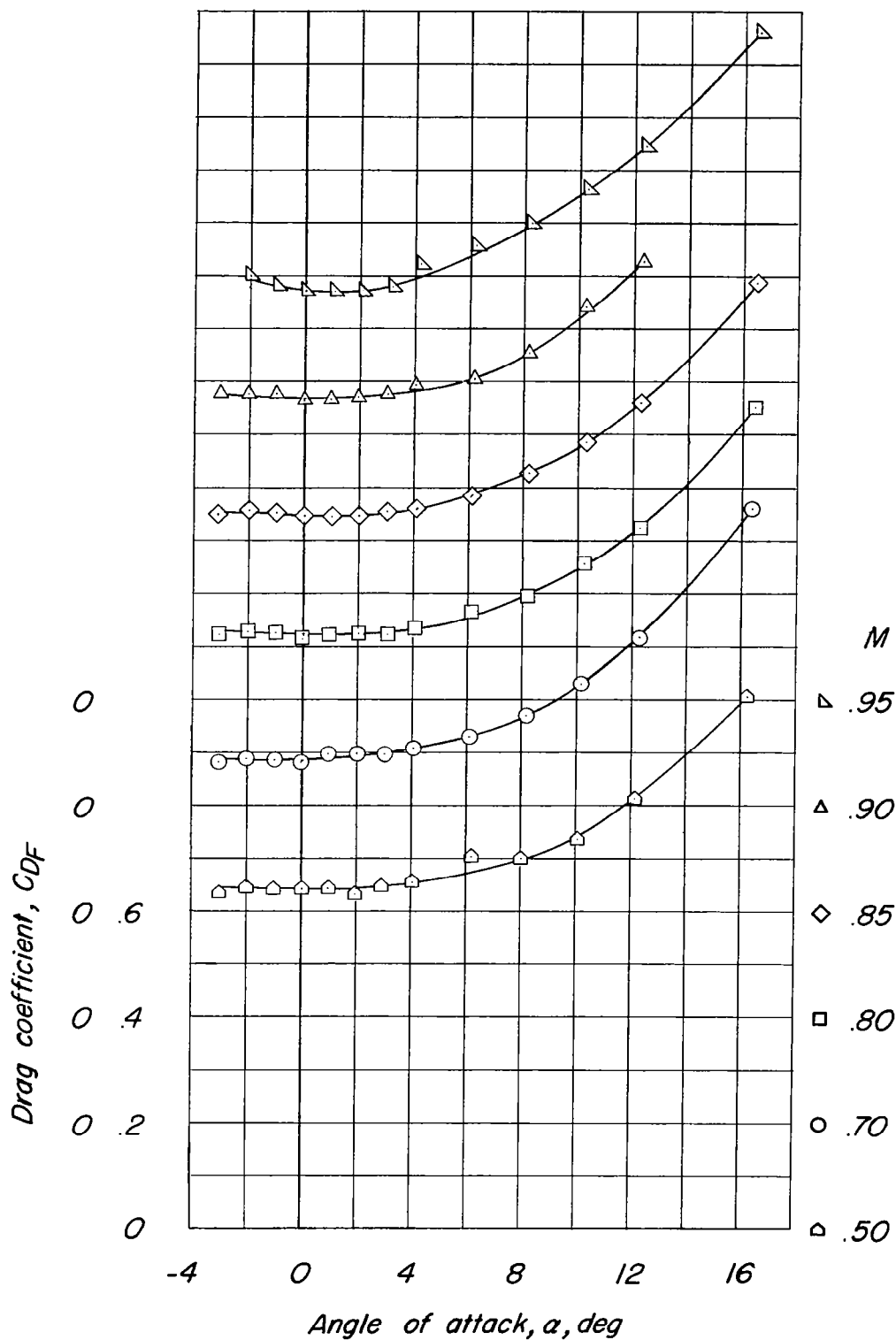
(b) Configuration 1_E.

Figure 21.- Continued.



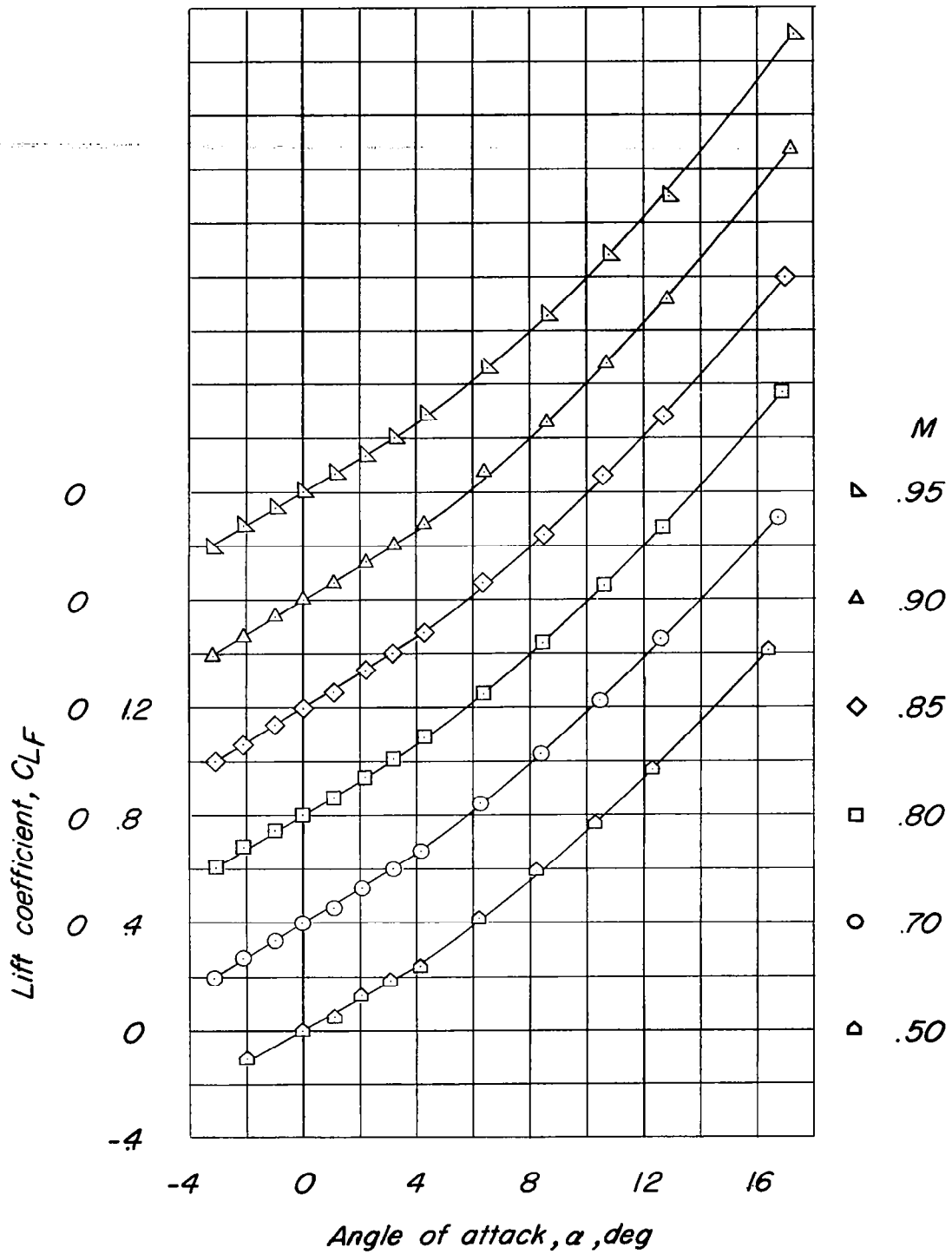
(b) Continued.

Figure 21.- Continued.



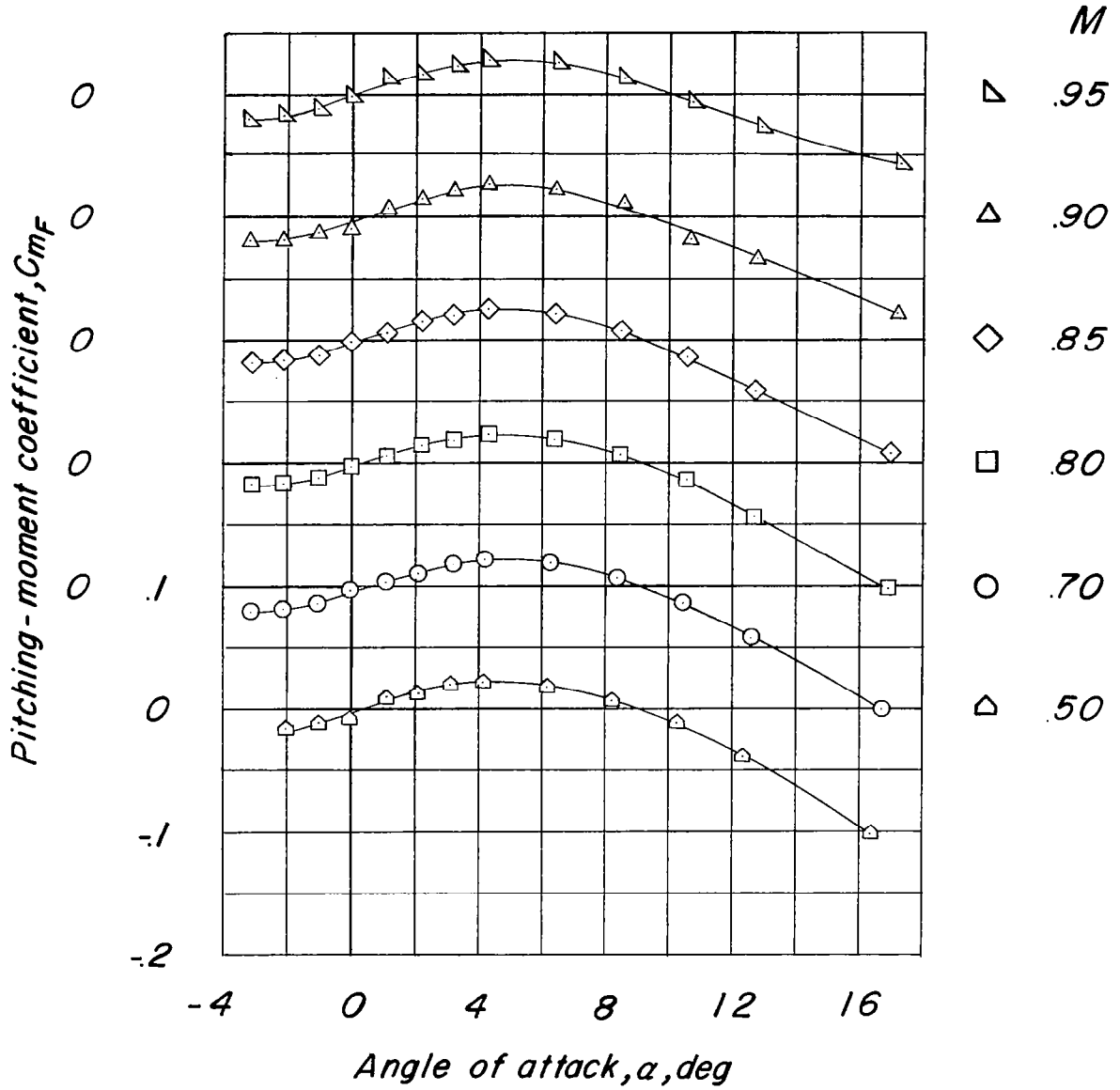
(b) Concluded.

Figure 21.- Continued.



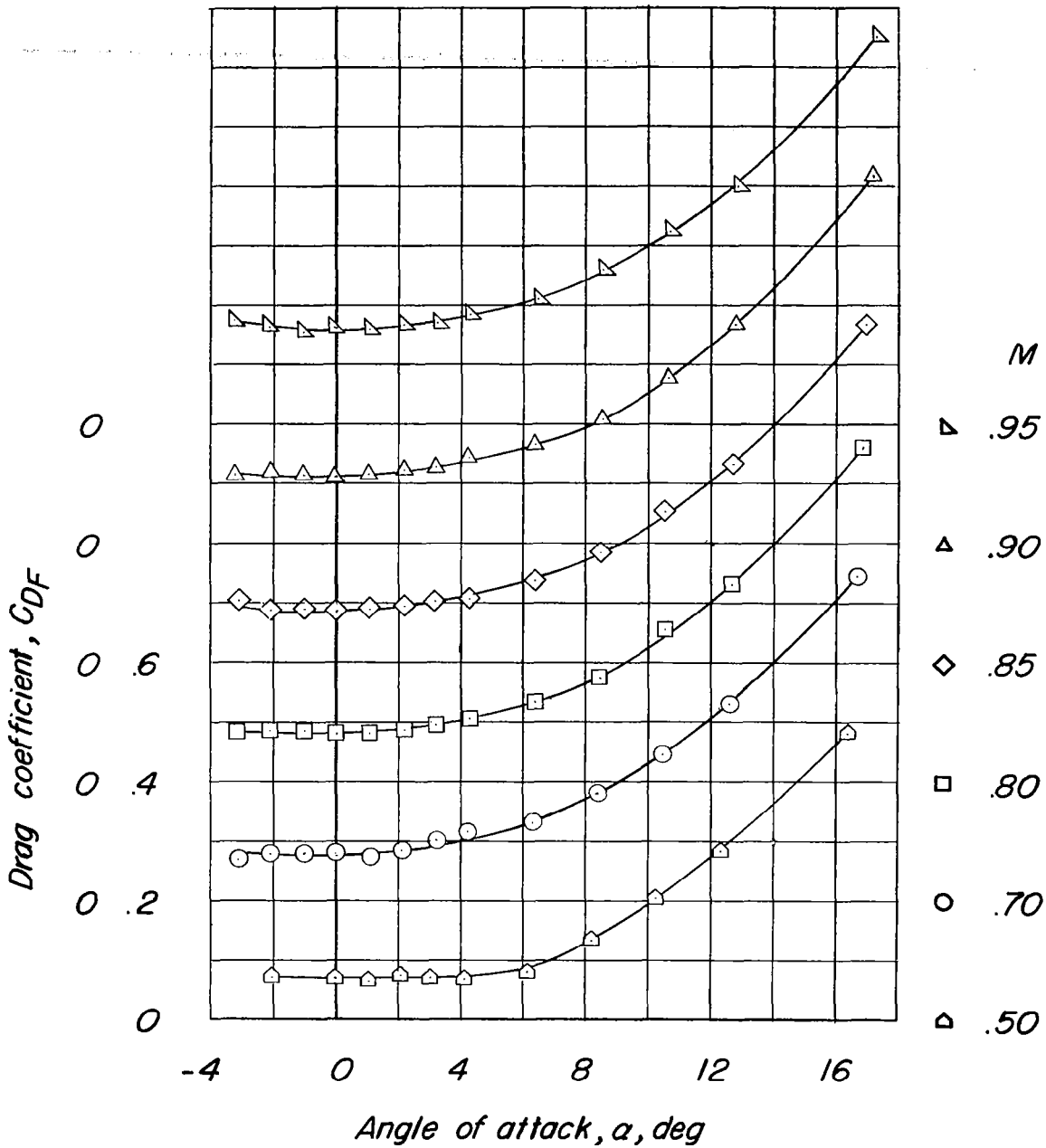
(c) Configuration 3.

Figure 21.- Continued.



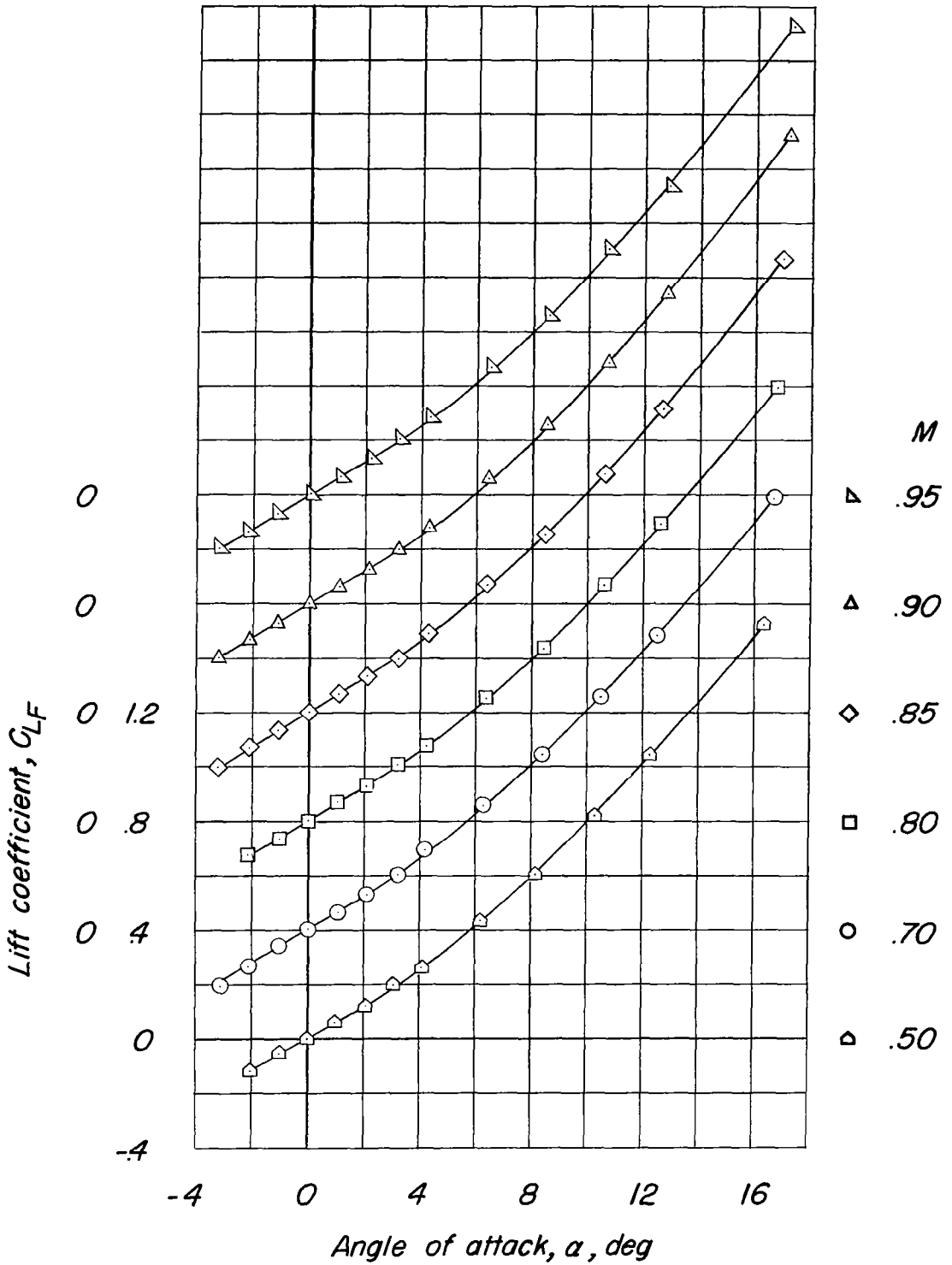
(c) Continued.

Figure 21.- Continued.



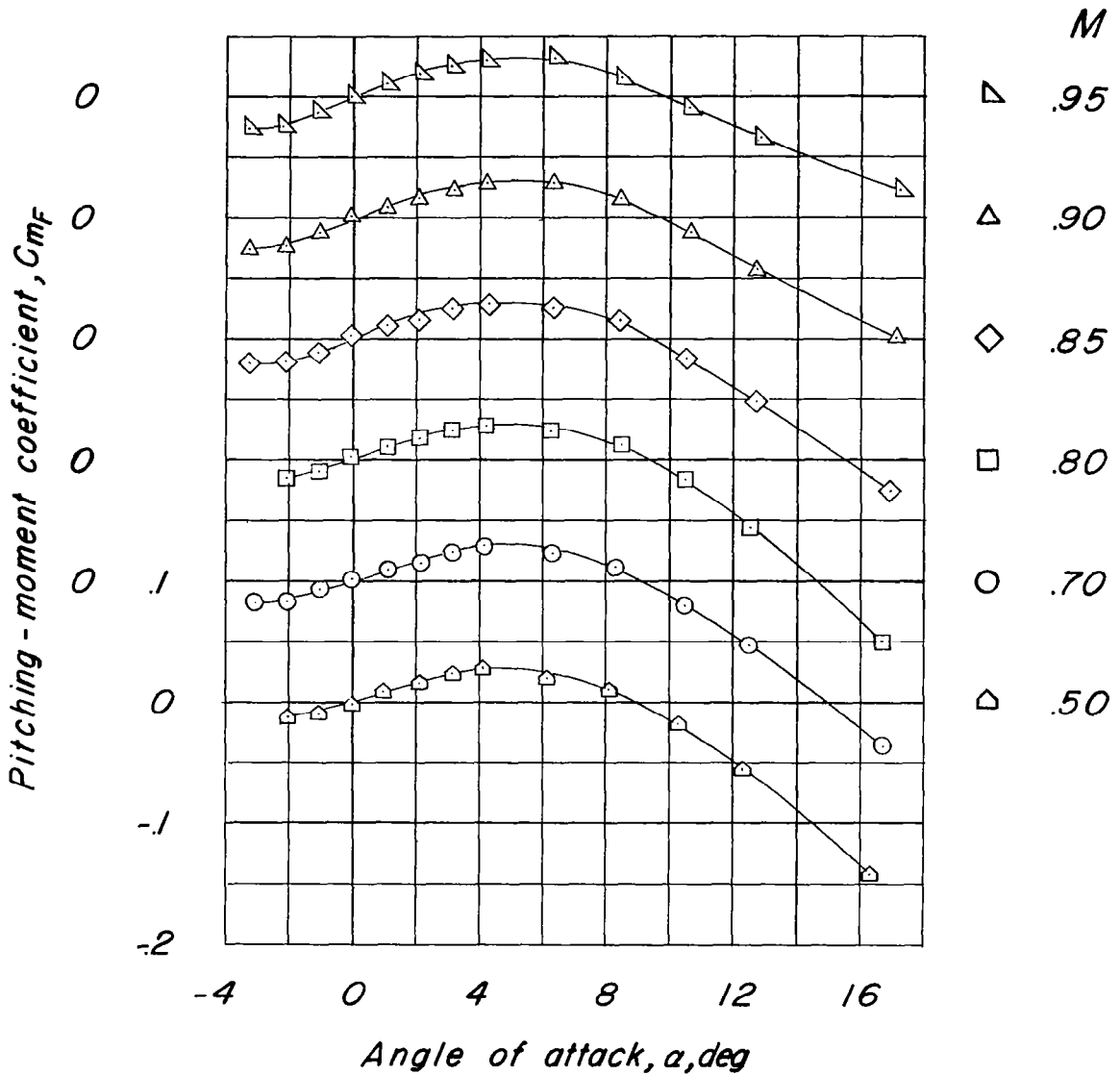
(c) Concluded.

Figure 21.- Continued.



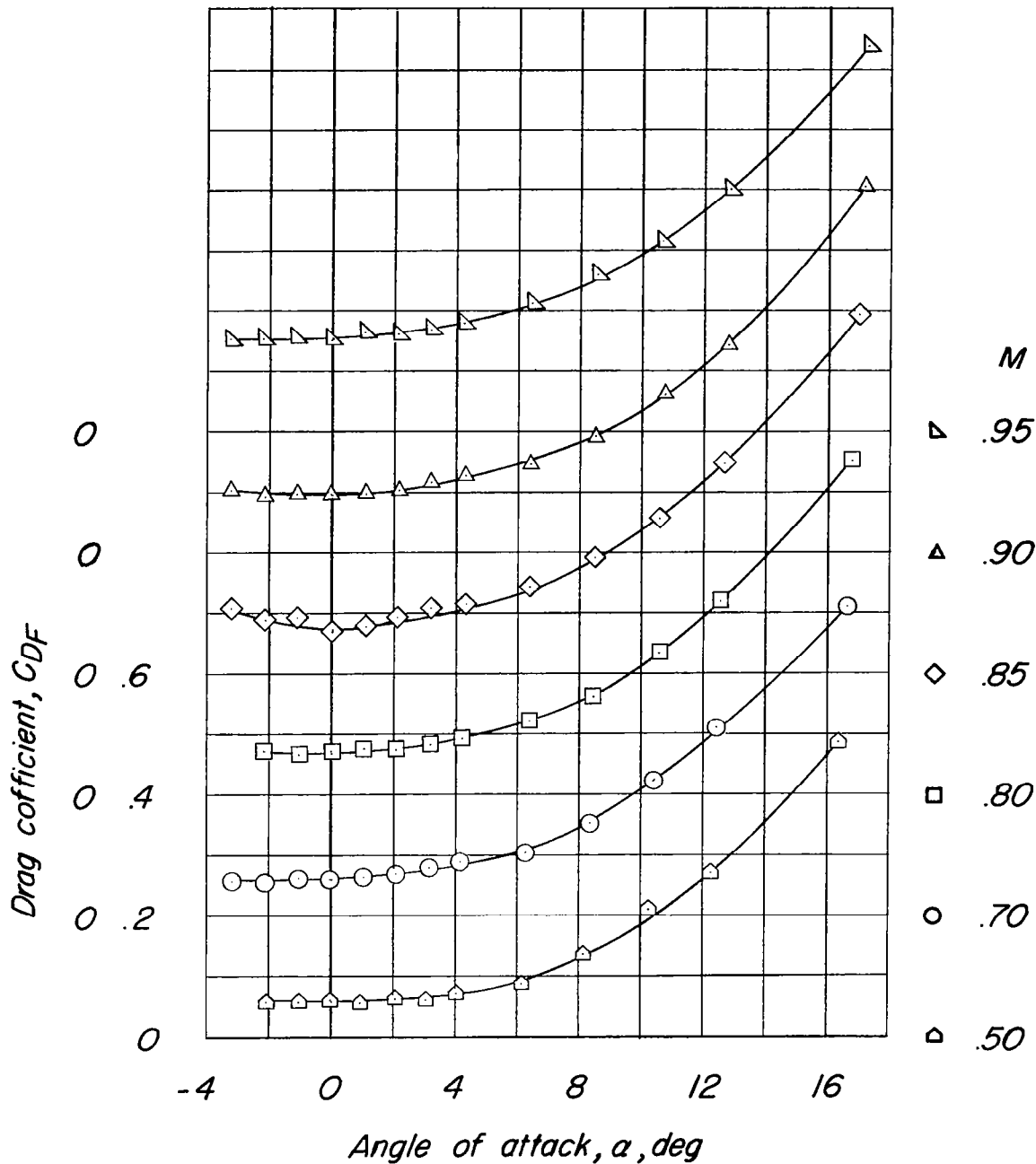
(d) Configuration 3E.

Figure 21.- Continued.



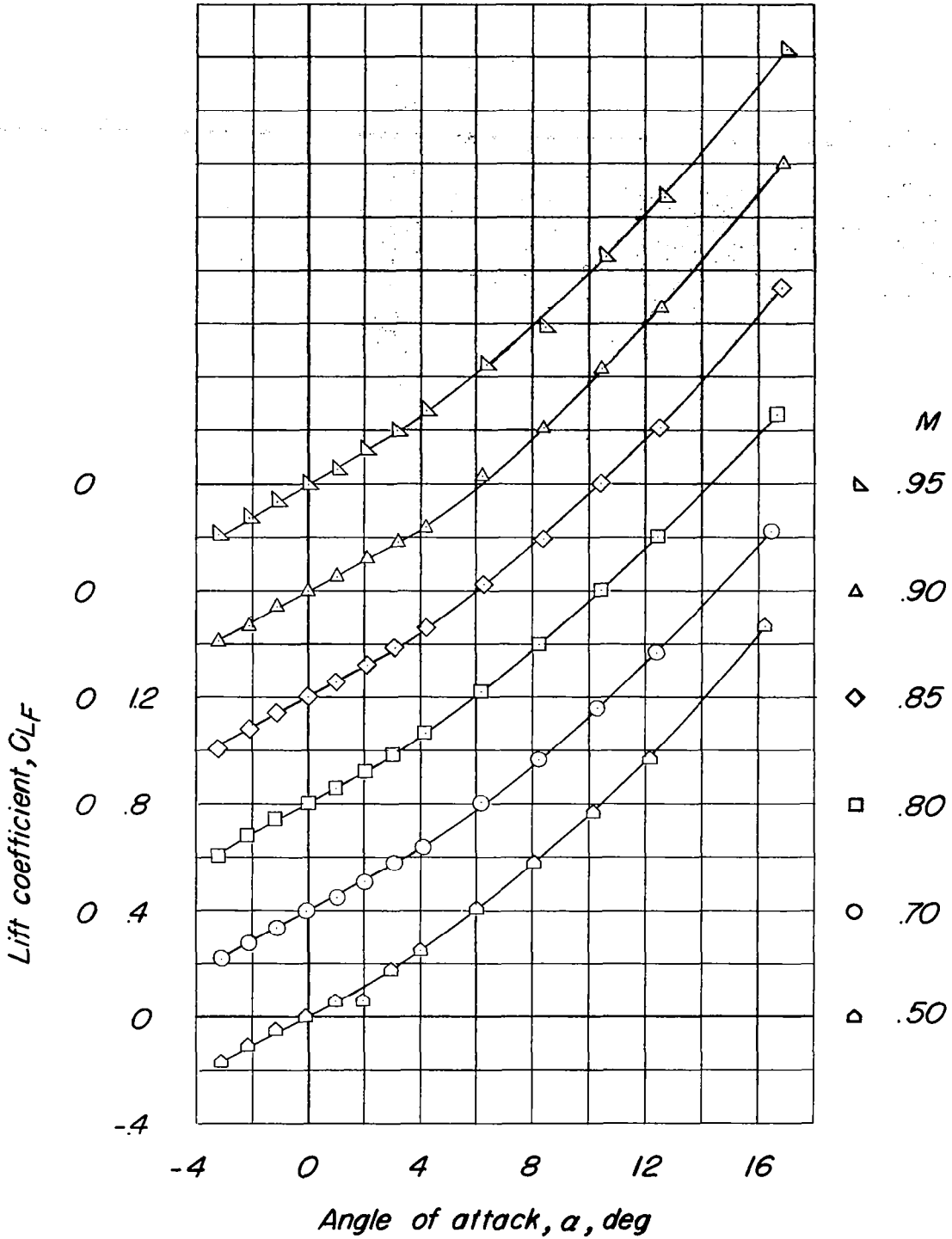
(d) Continued.

Figure 21.- Continued.



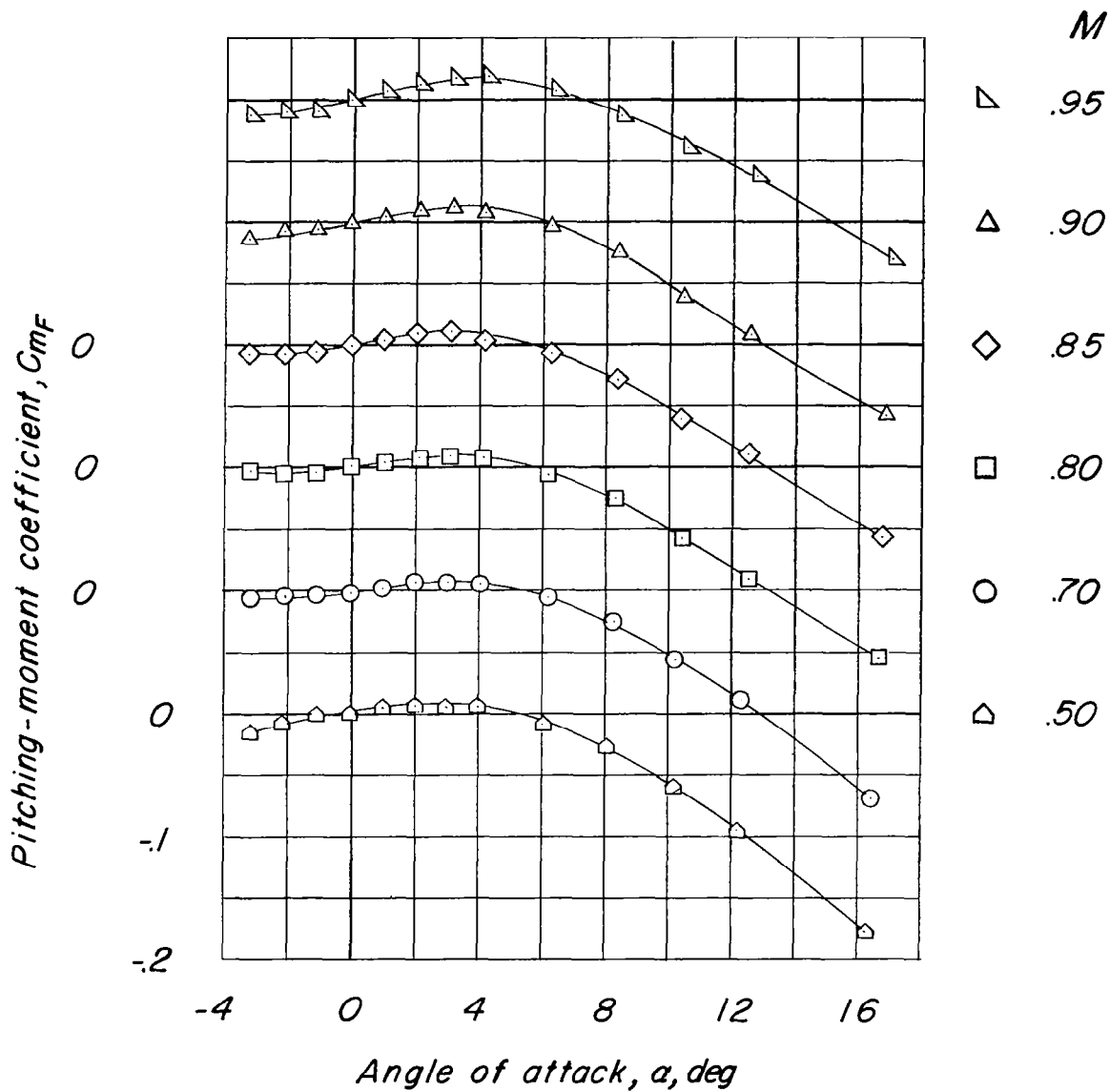
(d) Concluded.

Figure 21.- Continued.



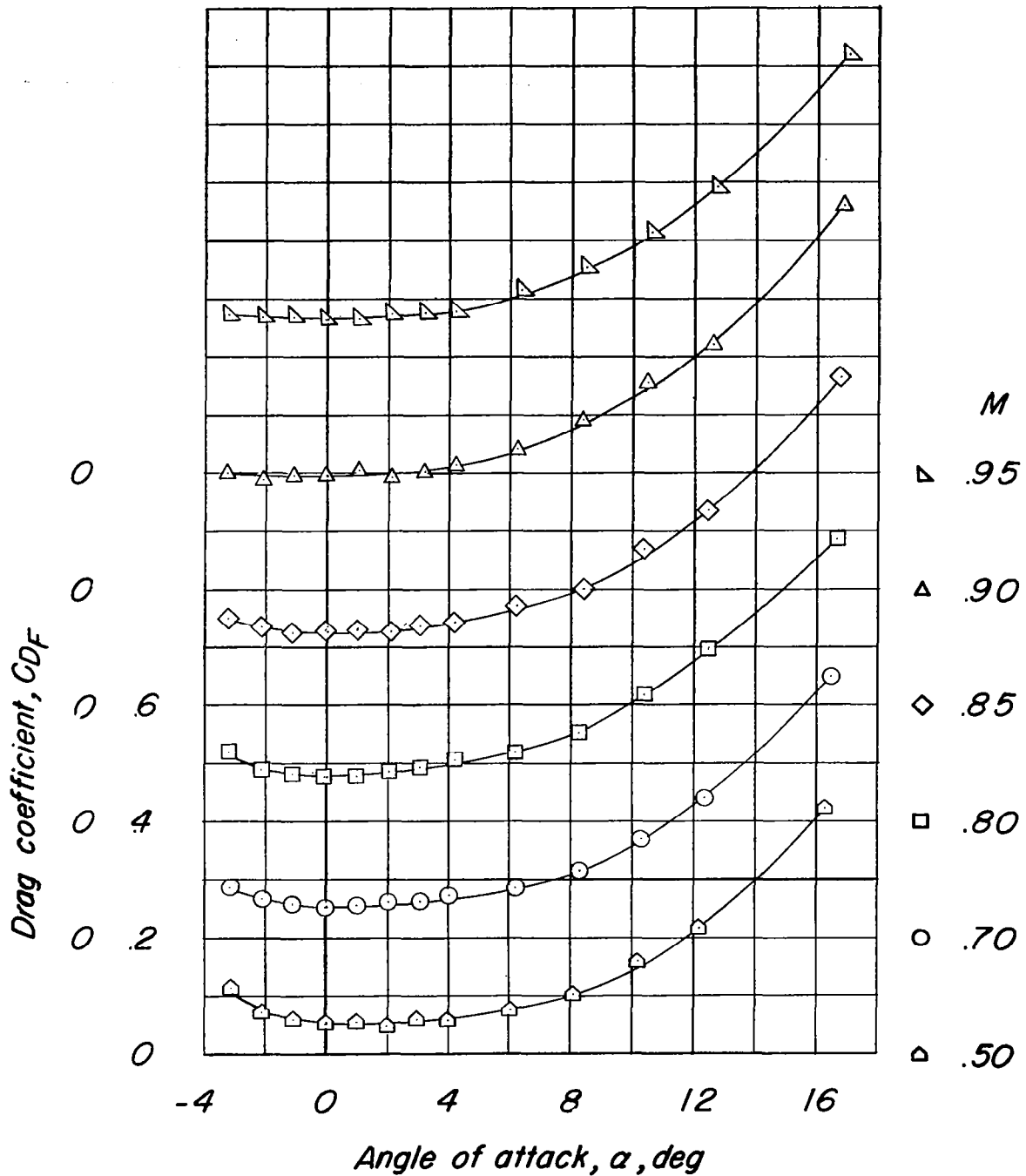
(e) Configuration 4.

Figure 21.- Continued.



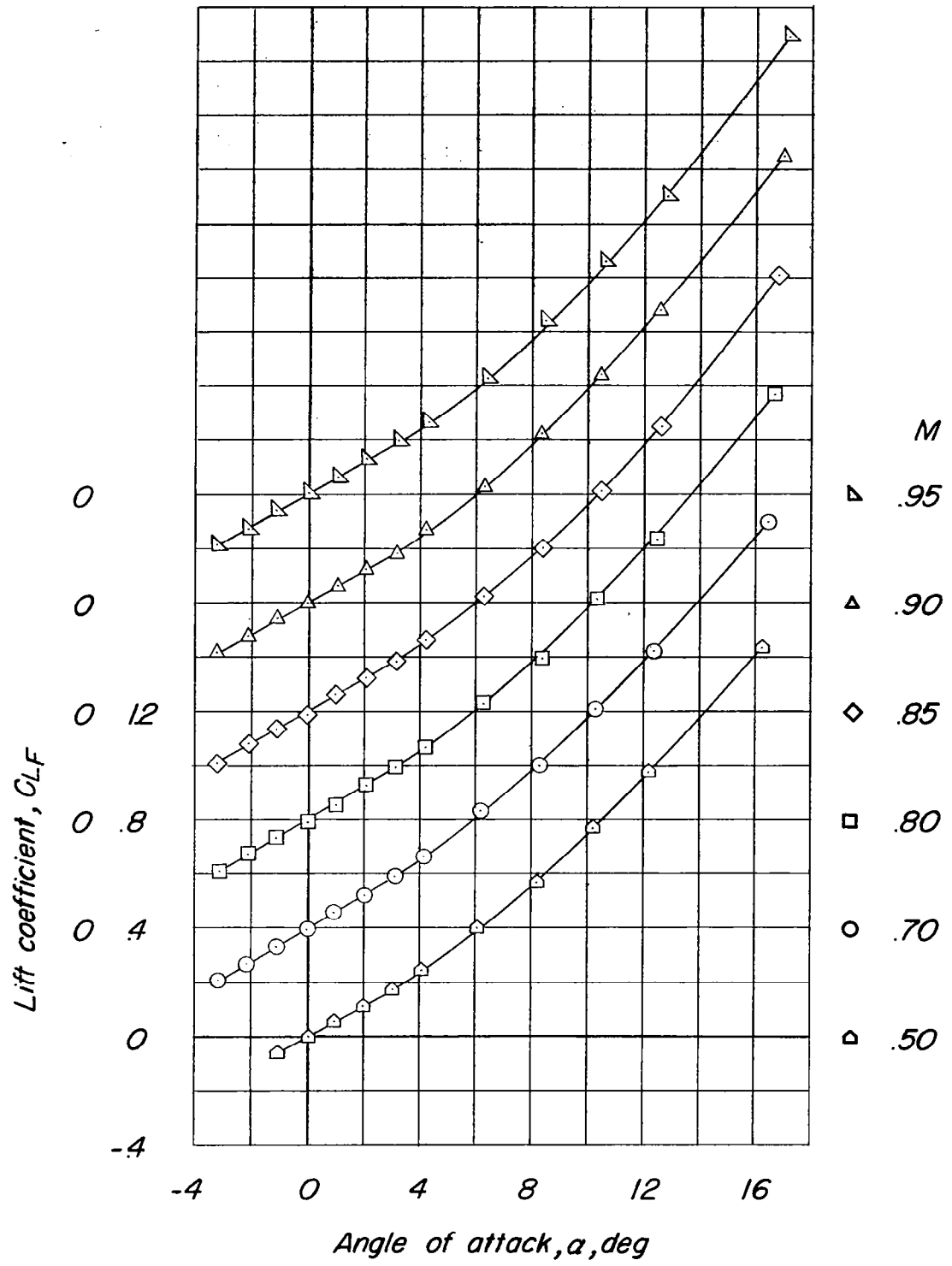
(e) Continued.

Figure 21.- Continued.



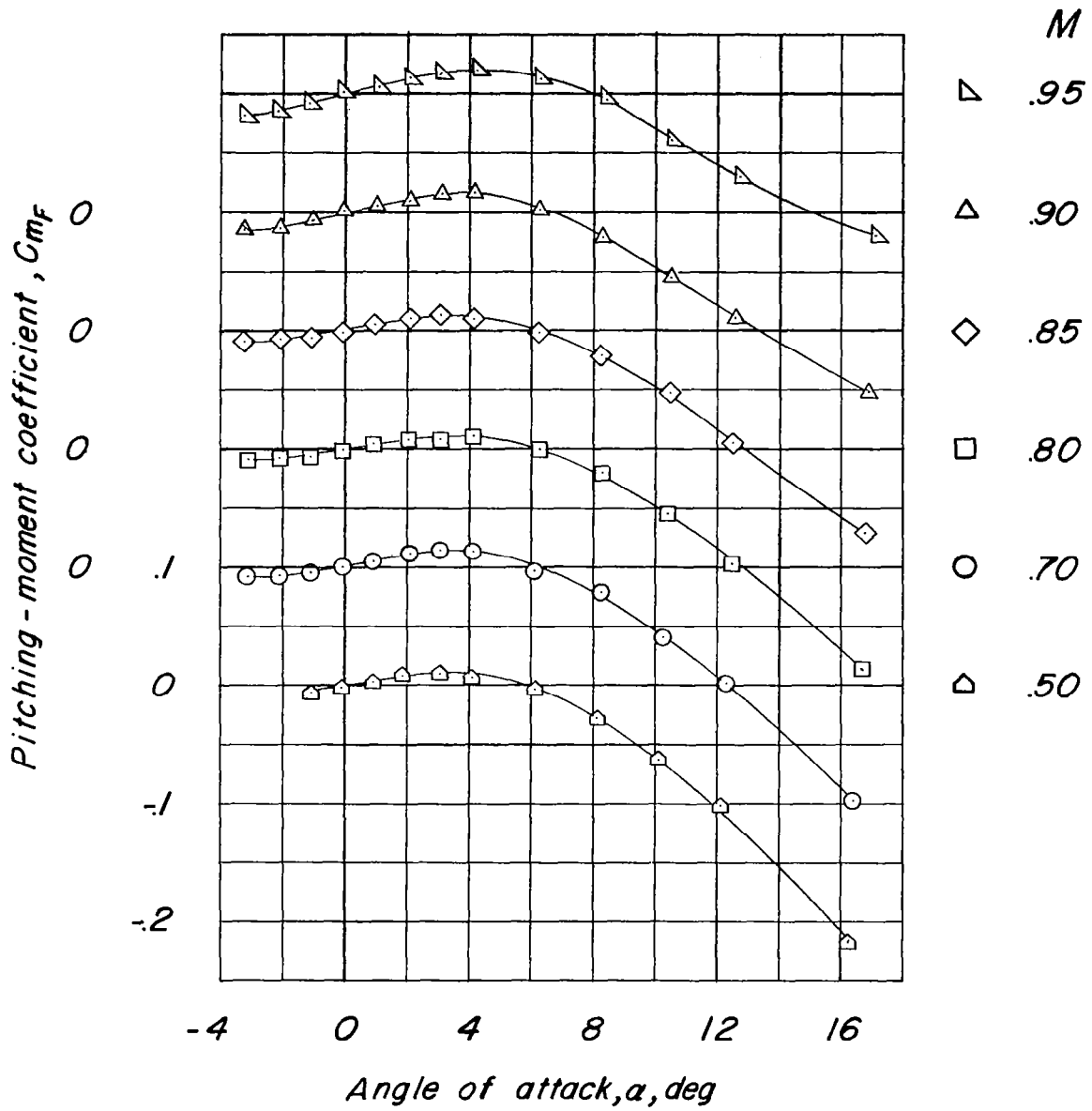
(e) Concluded.

Figure 21.- Continued.



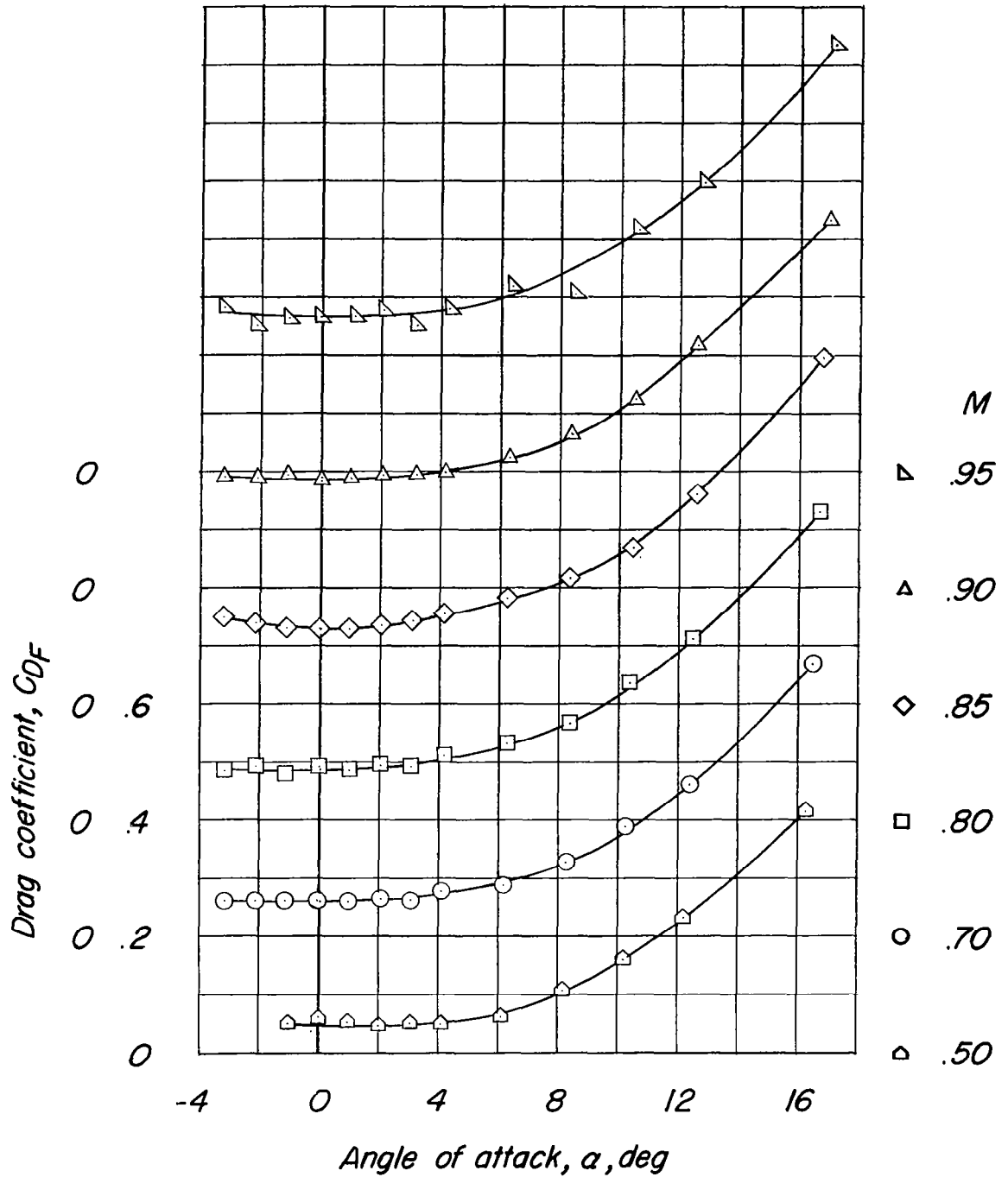
(f) Configuration 4E.

Figure 21.- Continued.



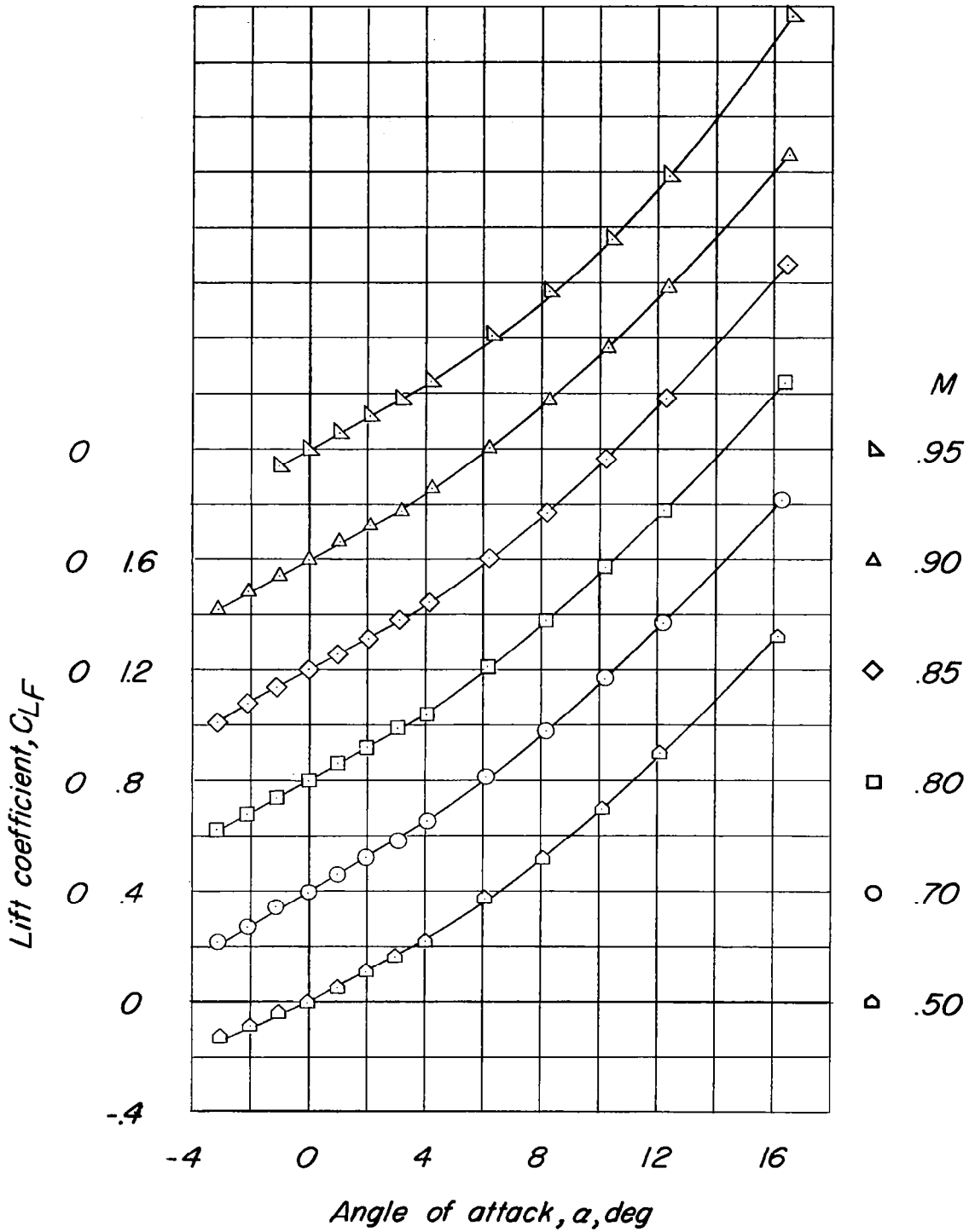
(f) Continued.

Figure 21.- Continued.



(f) Concluded.

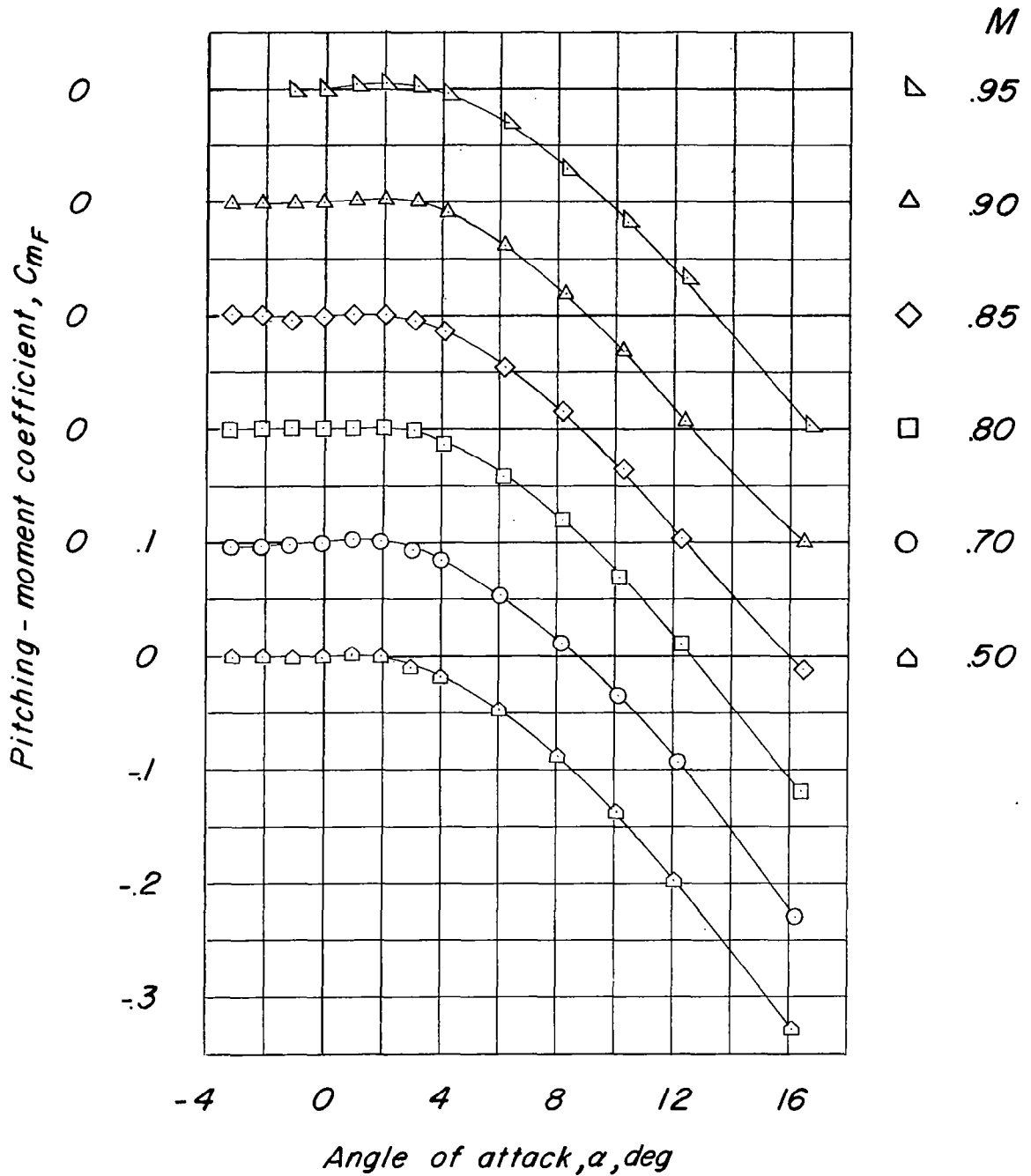
Figure 21.- Continued.



(g) Configuration 9.

Figure 21.- Continued.

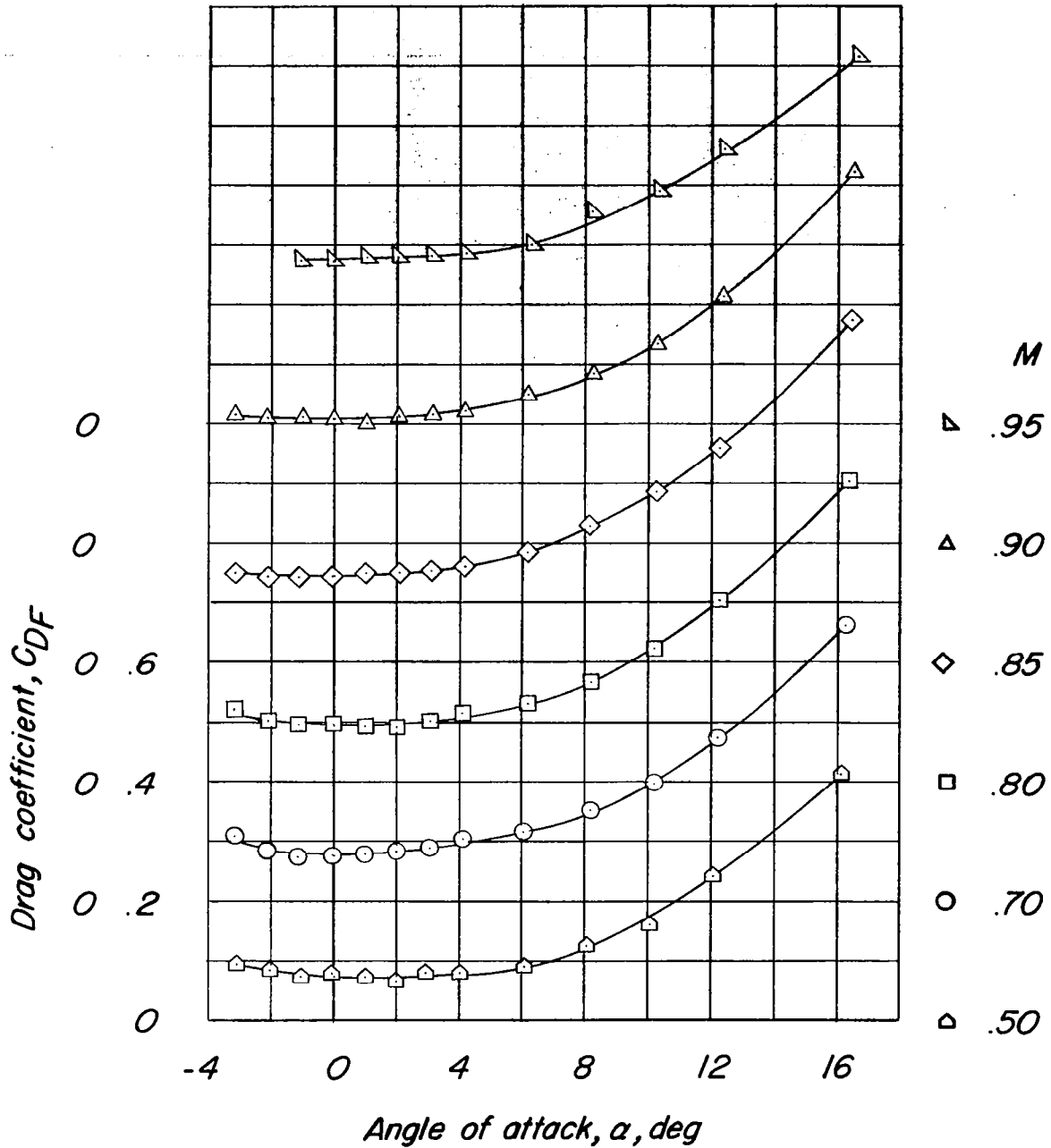
~~CONFIDENTIAL~~



(g) Continued.

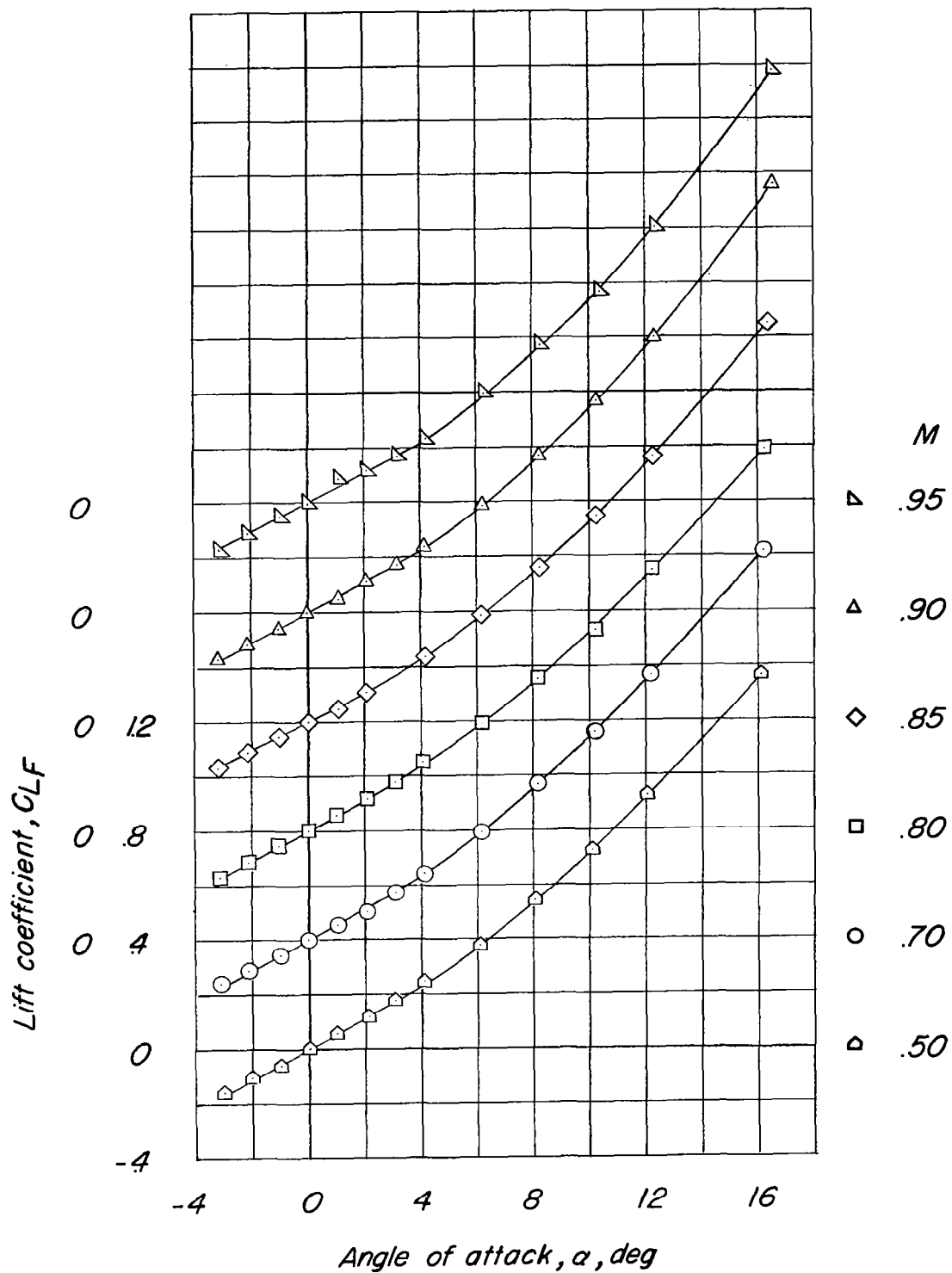
Figure 21.- Continued.

~~CONFIDENTIAL~~



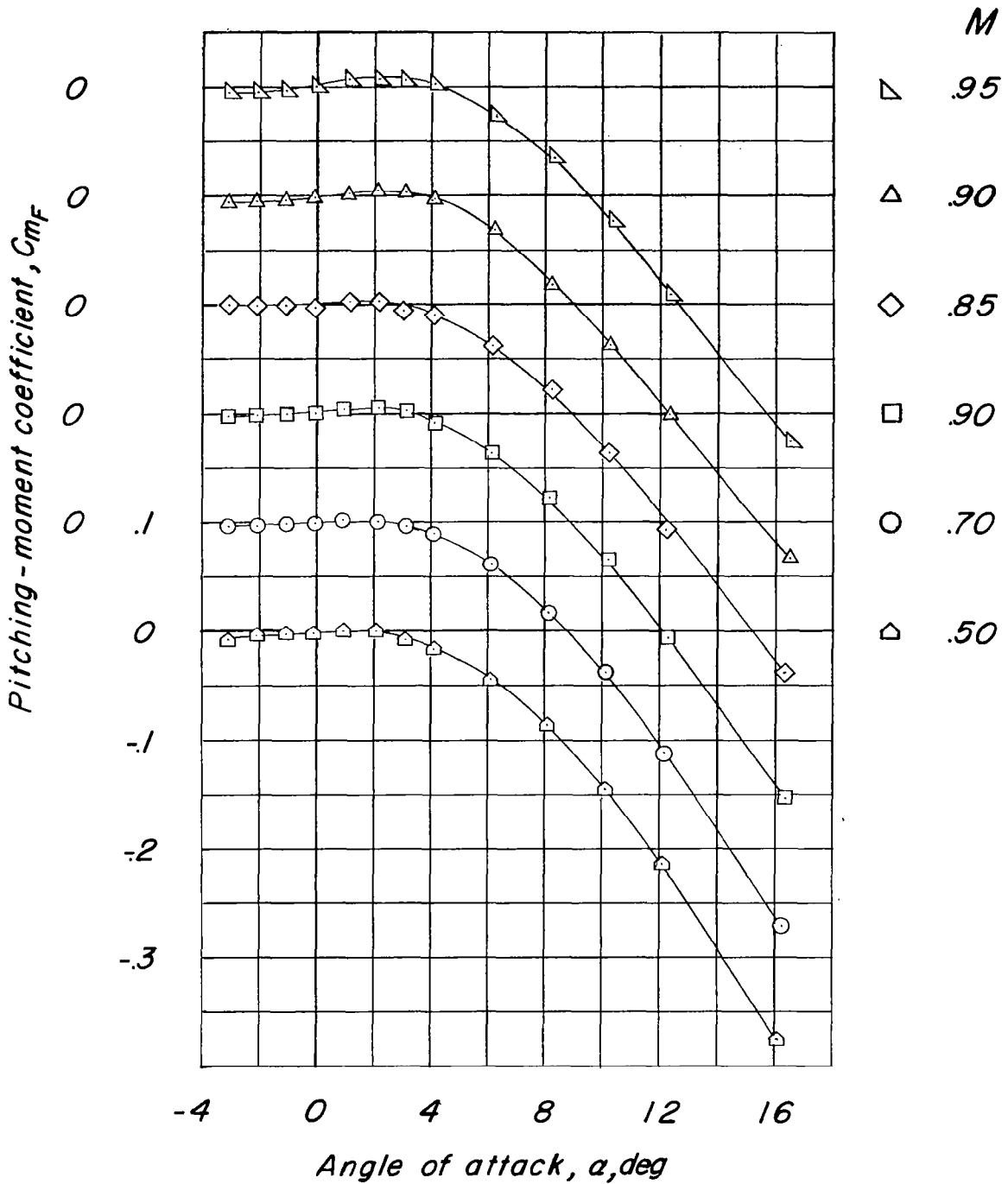
(g) Concluded.

Figure 21.- Continued.



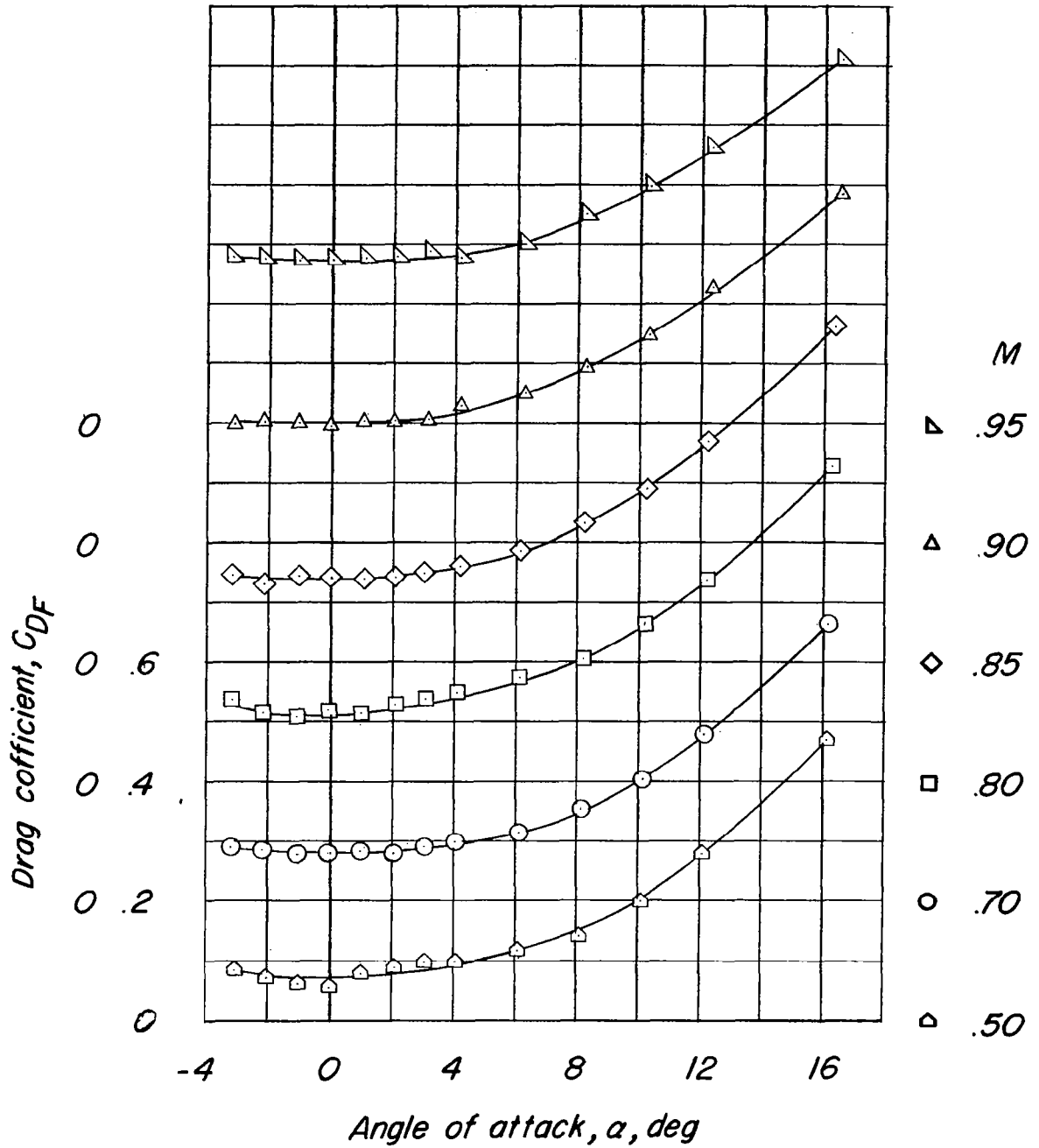
(h) Configuration 9E.

Figure 21.- Continued.



(h) Continued.

Figure 21.- Continued.



(h) Concluded.

Figure 21.- Concluded.

~~CONFIDENTIAL~~

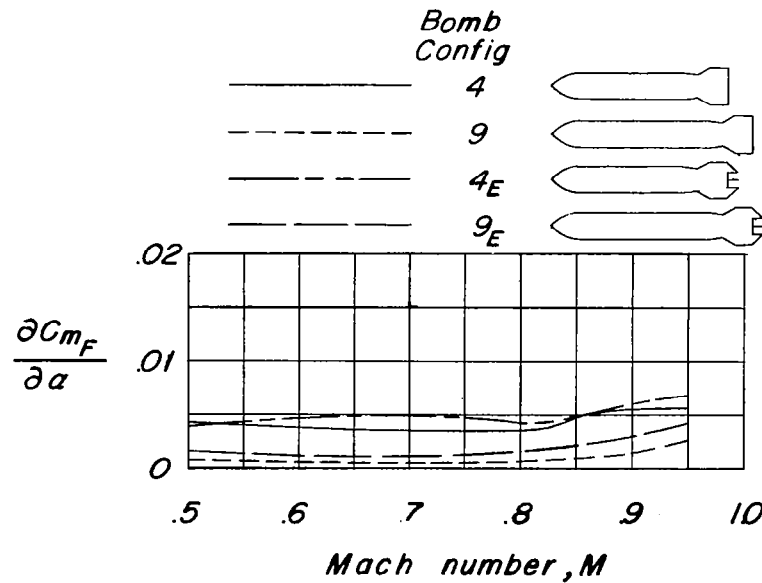
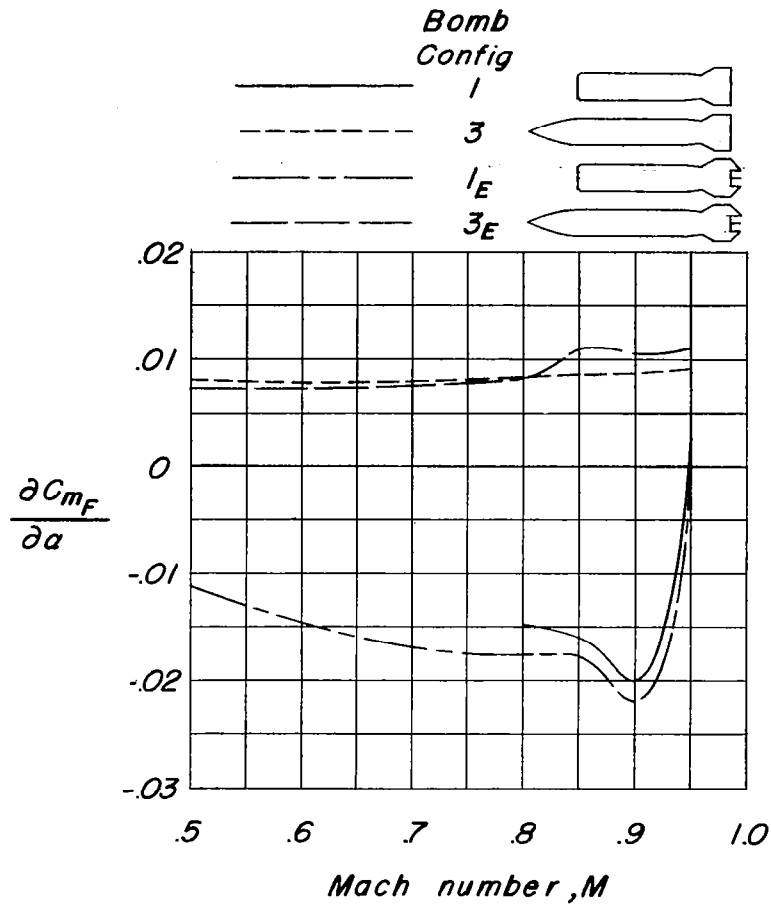


Figure 22.- Summary of pitching-moment-curve slopes of 0.1517-scale bomb configurations. $\alpha = 0^\circ$.

~~CONFIDENTIAL~~

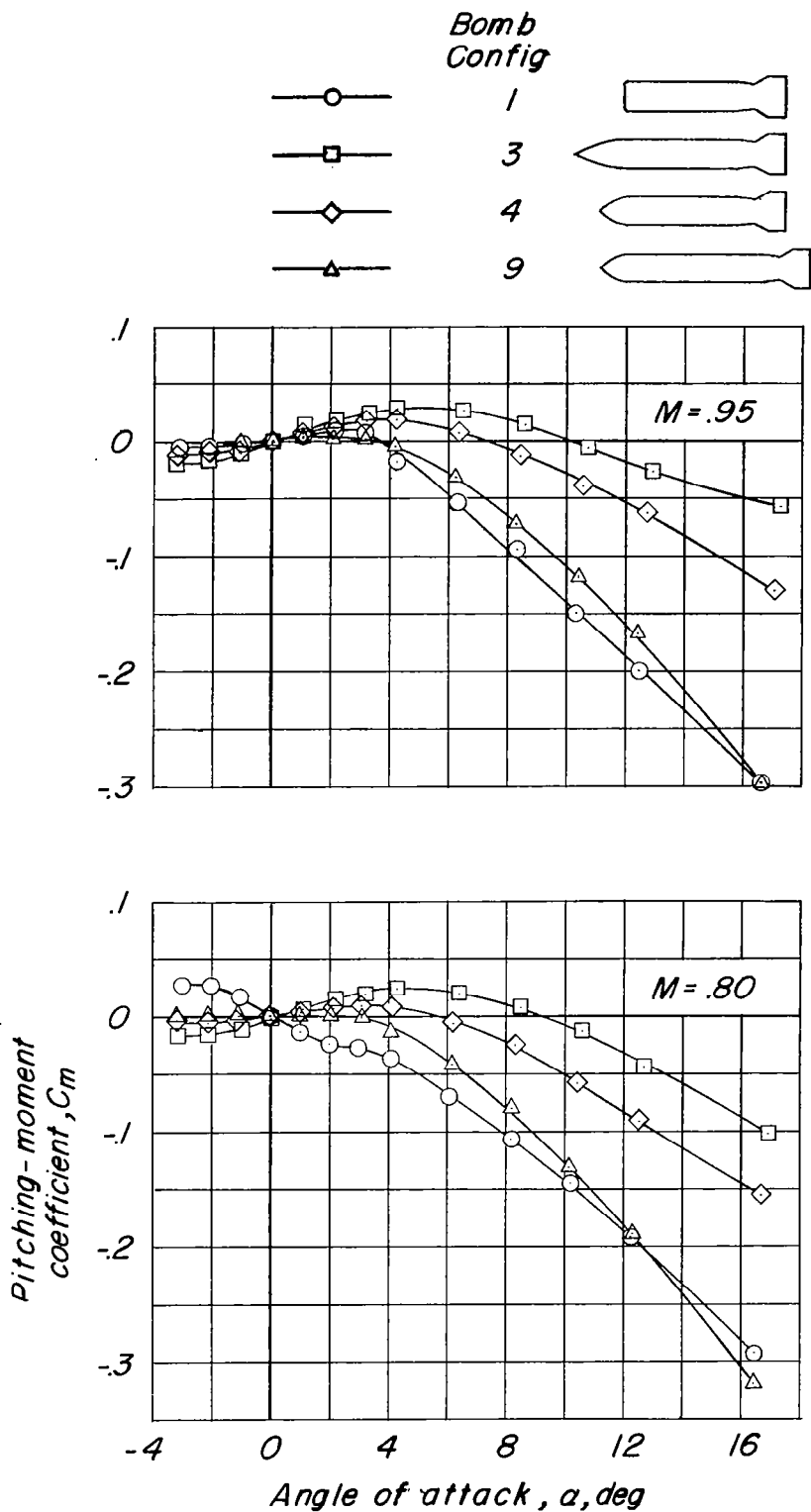


Figure 23.- Comparison of pitching-moment variation of four configurations of 0.1517-scale bomb.

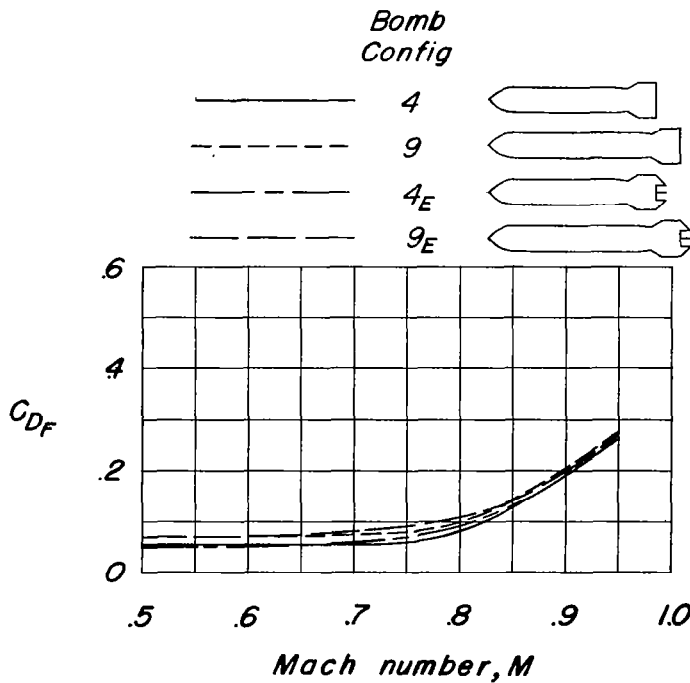
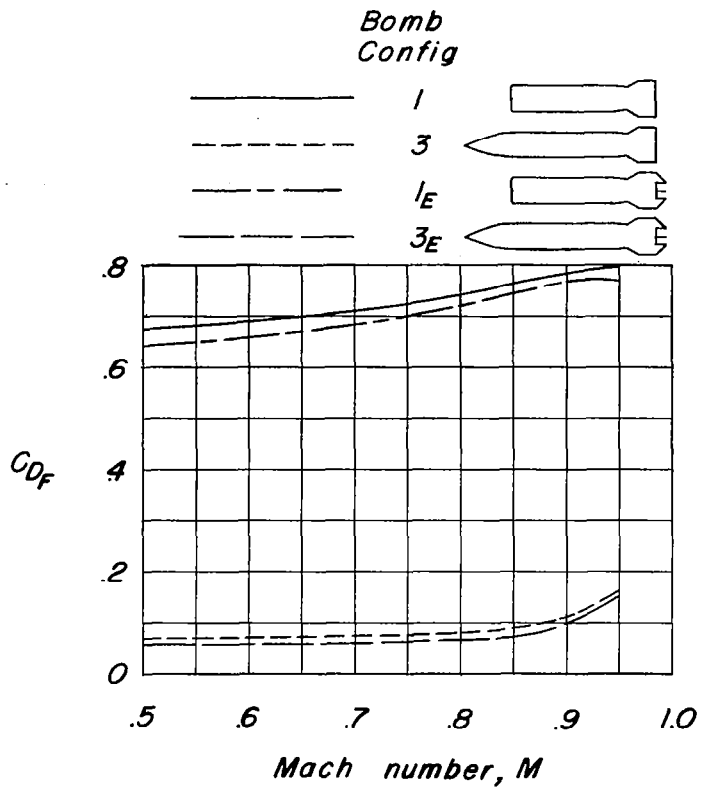


Figure 24.- Minimum drag characteristics of 0.1517-scale bomb configurations.

NASA Technical Library



3 1176 01439 0018

CONFIDENTIAL